NAVAL POSTGRADUATE SCHOOL
Monterey, California

DTIC
SELECTED
MAY 2 1 1986
D

THESIS

AN INVESTIGATION INTO THE TRIPPING BEHAVIOR OF
LONGITUDINALLY T-STIFFENED RECTANGULAR FLAT PLATES
LOADED STATICALLY AND IMPULSIVELY

by

HOWARD L. BUDWEG

March 1986

Thesis Advisor: Y.S. Shin

REPORT DOCUMENTATION PAGE

1a. REPORT SECURITY CLASSIFICATION UNCLASSIFIED	1b. RESTRICTIVE MARKINGS

2a. SECURITY CLASSIFICATION AUTHORITY	3. DISTRIBUTION/AVAILABILITY OF REPORT Approved for public release; distribution is unlimited.
2b. DECLASSIFICATION/DOWNGRADING SCHEDULE	

4. PERFORMING ORGANIZATION REPORT NUMBER(S)	5. MONITORING ORGANIZATION REPORT NUMBER(S)

6a. NAME OF PERFORMING ORGANIZATION Naval Postgraduate School	6b. OFFICE SYMBOL (If applicable) 69	7a. NAME OF MONITORING ORGANIZATION Naval Postgraduate School

6c. ADDRESS (City, State, and ZIP Code) Monterey, California 93943-5000	7b. ADDRESS (City, State, and ZIP Code) Monterey, California 93943-5000

8a. NAME OF FUNDING/SPONSORING ORGANIZATION	8b. OFFICE SYMBOL (If applicable)	9. PROCUREMENT INSTRUMENT IDENTIFICATION NUMBER

8c. ADDRESS (City, State, and ZIP Code)	10. SOURCE OF FUNDING NUMBERS			
	PROGRAM ELEMENT NO.	PROJECT NO.	TASK NO.	WORK UNIT ACCESSION NO.

11. TITLE (Include Security Classification)
AN INVESTIGATION INTO THE TRIPPING BEHAVIOR OF LONGITUDINALLY T-STIFFENED RECTANGULAR FLAT PLATES LOADED STATICALLY AND IMPULSIVELY

12. PERSONAL AUTHOR(S)
Budweg, Howard L.

13a. TYPE OF REPORT Master's Thesis	13b. TIME COVERED FROM _____ TO _____	14. DATE OF REPORT (Year, Month, Day) 1986 March	15. PAGE COUNT 101

16. SUPPLEMENTARY NOTATION

17. COSATI CODES			18. SUBJECT TERMS (Continue on reverse if necessary and identify by block number)
FIELD	GROUP	SUB-GROUP	Fluid Structure Interaction
			Stiffener Tripping
			Static/Impulsive Loads

19. ABSTRACT (Continue on reverse if necessary and identify by block number)
An experimental investigation was conducted to determine the static and dynamic responses of a specific stiffened flat plate design. The air-backed rectangular flat plates of 6061-T6 aluminum with an externally machined longitudinal narrow-flanged T-stiffener and clamped boundary conditions were subjected to static loading by water hydropump pressure and shock loading from an eight pound TNT charge detonated underwater. The dynamic test plate was instrumented to measure transient strains and free-field pressure. The static test plate was instrumented to measure transient strains, plate deflection, and pressure. Emphasis was placed upon forcing static and dynamic stiffener tripping, obtaining relevant strain and pressure data, and studying the associated plate-stiffener behavior.

20. DISTRIBUTION/AVAILABILITY OF ABSTRACT ☒ UNCLASSIFIED/UNLIMITED ☐ SAME AS RPT. ☐ DTIC USERS	21. ABSTRACT SECURITY CLASSIFICATION unclassified
22a. NAME OF RESPONSIBLE INDIVIDUAL Y.S. Shin	22b. TELEPHONE (Include Area Code) (408) 646-2568 / 22c. OFFICE SYMBOL 69 Sg

DD FORM 1473, 84 MAR
83 APR edition may be used until exhausted.
All other editions are obsolete.

An Investigation into the Tripping Behavior of
Longitudinally T-Stiffened Rectangular Flat Plates
Loaded Statically and Impulsively

by

Howard L. Budweg
Lieutenant, United States Navy
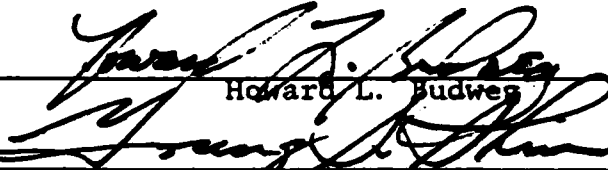B.S., University of Oregon, 1977

Submitted in partial fulfillment of the
requirements for the degree of

MASTER OF SCIENCE IN MECHANICAL ENGINEERING

from the

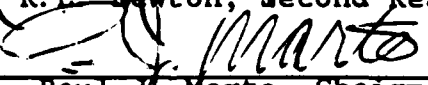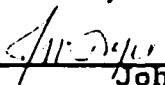NAVAL POSTGRADUATE SCHOOL
March 1986

Author: _____
Howard L. Budweg

Approved by: _____
Young S. Shin, Thesis Advisor

_____
R. E. Newton, Second Reader

_____
Paul J. Marto, Chairman,
Department of Mechanical Engineering

_____
John N. Dyer,
Dean of Science and Engineering

2

ABSTRACT

An experimental investigation was conducted to determine the static and dynamic responses of a specific stiffened flat plate design. The air-backed rectangular flat plates of 6061-T6 aluminum with an externally machined longitudinal narrow-flanged T-stiffener and clamped boundary conditions were subjected to static loading by water hydropump pressure and shock loading from an eight pound TNT charge detonated underwater. The dynamic test plate was instrumented to measure transient strains and free-field pressure. The static test plate was instrumented to measure transient strains, plate deflection, and pressure. Emphasis was placed upon forcing static and dynamic stiffener tripping, obtaining relevant strain and pressure data, and studying the associated plate-stiffener behavior.

3

QUALITY INSPECTED 3

TABLE OF CONTENTS

4

LIST OF TABLES

LIST OF FIGURES

ACKNOWLEDGEMENTS

I. INTRODUCTION

A. BACKGROUND

Military submarine hull design has concentrated on the basic structural element, a stiffener reinforced shell. The submarine shell/stiffener form is the ring stiffened cylinder. The cylinder construction, which is the least expensive and the simplest form of shell construction, takes advantage of the high strength levels in high-strength materials through the use of ring stiffeners allowing higher load bearing capacities without the cylinder becoming unstable. Additionally, high-strength material is used for its toughness (due to low temperature requirements) and resistance to high dynamic loads (e.g., depth charge attack) [Ref. 1: sect. 1.].

The submarine ring stiffened cylinder is designed with generous safety margins against overall collapse triggered by frame yielding or tripping [Ref. 1: sect. 2.1]. Tripping, a lateral-torsional buckling occuring in flexurally stiff frames which have low lateral-torsional rigidity, has been identified as a potential form of catastrophic collapse which may take place with but a single application of load. The stiffener tripping form of panel collapse is a sudden and drastic reduction in load-carrying ability, a damage mechanism which occurs through compression plastic instability affecting a large critical region of cross-section. Predictions of this prime mode of failure need to be supported by good test data that is inside the current ship design range. To date, supporting experimental data for this panel and grillage behavior is extremely scarce. Generous safety margins have been the accepted practice to avoid premature sideways tripping rather than to predict it. However, avoidance design is really an extension of design

10

based on acceptable risk, where additional strength is necessary to provide a certain level of safety against extreme conditions [Ref. 2: p. 271]. Avoidance designs may not be the answer since stiffeners (i.e., frames) may over play their part and, because of excessive rigidity, actually cause premature failure of the shell by inducing in it additional components of stress. It has been observed that the cause of ultimate collapse in the plating of a "thin-walled" shell is excessive circumferential stress rather than longitudinal stress and there may be excessive yielding of the shell at the toes of frame flanges (before collapse finally occurs) due to high circumferential stress [Ref. 3: p. 120]. The alternative approach is then: how weak may the frame rings be and still be adequate? It has been generally recognized that a stronger, more resilient type of construction is that in which frames and shell are nearly equal in strength as opposed to a hard-framed structure.

Frame dimensions are also of concern; using high web height-to-thickness ratios could lead to designs for which local stiffener tripping becomes important since excessively slender frame proportions make the frame sensitive to any tilt. Also, internal frames are equally sensitive to the effects of any tilt in bringing about tripping of frames under load. This mode of failure is usually a result of coupled flexural and torsional modes of buckling. The result in any of these cases being the same (i.e., general instability of the frame and shell in unison causing failure of the submarine hull under external pressure).

Submarine hulls require the high structural efficiency which can be achieved by reducing the excess rigidity of frames, (i.e., minimizing stress concentrations). Accordingly, if frame weight can be reduced in the process and that amount of weight used in additional thickness of the shell, the cylinder's collapse strength will effectively

11

be increased. The careful choice of ring-stiffened geometry can have a significant influence on shell performance, but there is a general lack of agreement on what the "appropriate" general collapse loads for ring-stiffened cylinders are [Ref. 4: p. 95].

B. OBJECTIVE

Submarine hull failure is a complex process involving stages of failure including initial yielding, large displacements, local instability, and finally collapse. Analysis of grillage failure and knowledge of plating behavior throughout the load range is necessary, both statically and dynamically. It is therefore of considerable importance to be able to predict the safe buckling behavior through general and reliable methods of analysis which provide necessary correlations between sea loads and their effects on a structure. According to A.E. Mansour [Ref. 5: p. 42], no satisfactory analysis method exists for inelastic tripping of stiffeners welded to continuous plating or for the prediction of the inelastic collapse strength. Therefore, it is more than a matter of being able to predict stresses, but the way in which the stresses are used to anticipate failure.

This investigation and analysis will follow the guideline that in many physical problems, resort to experiment is often the shortest cut to a decision as to which analyses need be made and what effects are important in those analyses [Ref. 6: p. 332]. Employing this guideline, data obtained on a specific model design of a longitudinally narrow-flanged T-stiffened rectangular flat plate under static and dynamic (i.e., underwater charge detonation) conditions, will be investigated and analyzed.

II. STRUCTURE BEHAVIOR

A. STATIC TRIPPING PHENOMENA

Tripping (or compound failure), as shown in Figure 2.1 , will be discussed here qualitatively in terms of a rectangular flat plate stiffened by a T-stiffener. Generally speaking, stiffener bending stress arises from the reaction of a plating-stiffener combination to a loading (i.e. water pressure) normal to the plating, while the plating itself acts as one flange of this system. In the case of a ship hull, the shell plating performs functions of contouring and sealing in addition to sharing the load carrying requirement with the stiffeners, (ring stiffeners in the case of submarines) [Ref. 7: p. 104].

The web of the T-stiffener can be considered a plate restrained against rotation (hinged) along one edge, free and elastically supported by the flange on the other one (the restraining effect of the web on the flange being small). Also, the flange can be thought of as a plate simply supported by the web along one side and free on the other [Ref. 8: p. 342]. In an actual structure, a stiffener welded to one side of a plate results in a considerable increase in the flexural rigidity of the stiffener since the adjacent zones of the plate take part in the bending of the deflected stiffener, that is, the stiffeners not only carry a portion of the load but subdivide the plate into smaller panels, thus increasing the critical stress at which the plate will buckle [Ref. 8: p. 381]. Additionally, there occurs an incompatibility of the buckling patterns (as favored by the web and the flange) which tends to make the buckling load higher than it would be for either the web or the flange of the stiffener alone [Ref. 9: p. 2]. Therefore, such combinations are able to support ultimate loads well above the load for local buckling of the plate.

13

rotation out of
vertical plane
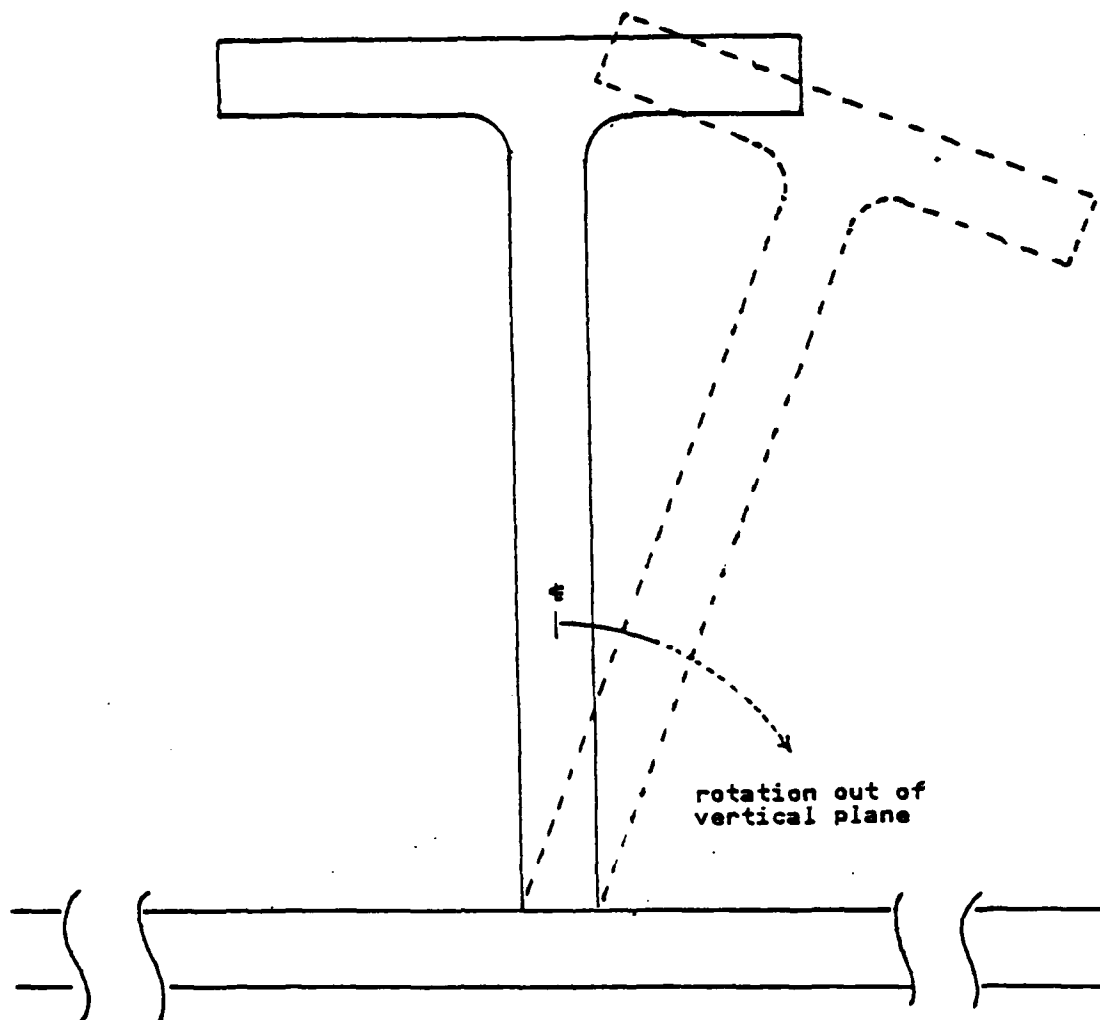
Figure 2.1   Stiffener Tripping.

14

Even though there is a substantial restraining effect of the plate on the stiffener and of the stiffener on the plate, there are also plate-stiffener destabilizing influences on each other. The fact that the plate prevents the stiffener from moving laterally in any other way except by rotation around the toe of the web, dictates the form of failure called tripping. This mode of failure involves the twisting of the stiffener about its line of attachment to the plating, a coupled displacement combination of sideways flexure and stiffener rotation. For example, as the load orthogonal to the plate increases, the effectiveness of the plate decreases until at some limiting stress the stiffener-plate combination fails and as the plate buckles, the rotational constraint provided by the plate at the line of attachment of the stiffener changes, thus increasing the stiffener's sensitivity to tripping. Once the stiffener starts lateral torsional buckling, any increase in deformation will cause an unloading which is triggered by yielding after considerable deformation. [Ref. 2: p. 732]

There is the possibility that under extreme conditions a submarine hull ring stiffener may trip. If such deformations were to become large, the support furnished by the ring to the cylinder hull would be impaired and there would be a redistribution of pressure resistance to adjacent rings resulting in a rapid deterioration in the general capacity of the shell to resist pressure.

B. DYNAMIC RESPONSE

Under static loading, stresses and strains are generally distributed throughout the entire body and every part of the body has an opportunity to particicpate. However, under impulsive loading, transient and highly localized stresses and strains exist in the rapidly changing stress system. This dynamic phenomenon involves interactions between inertial, hydrodynamic, and elastic forces which can arise as a

15

consequence of the detonation of an explosive charge. The structural response to a plane step shock wave has attracted considerable interest since steep-fronted shock waves are characteristic of underwater explosions and have similar properties [Ref. 10: p. 319].

The large amount of energy that is transmitted to a structure (when it is dynamically loaded) distributes itself within the metal and much of the absorbed energy is observed in the form of macroscopic and microscopic inelastic deformations. It has been noted that the critical value of the equivalent static pressure in dynamic loading is considerably higher than the static buckling pressure. The critical load is so high that buckling is plastically initiated (i.e., an unstable behavior called dynamic plastic buckling) [Ref. 11: p. 6]. This is a consequence of two uniquely dynamic effects. First, the shape of the structure impulsively loaded and constraints imposed upon it frequently determine both the location and the amount of plastic flow that will take place. Secondly, the intense transient stress disturbances and the extremely high pressures and rapid loading rates of impulsive loads markedly influence the mechanical properties of the metal being loaded: the hardness increases, the tensile strength goes up, and yield and plastic flow characteristics are altered. Metal behavior is strongly contingent upon stress level, behaving at the highest extremes of pressures as a fluid and at lowest stresses as an elastic body. That is, metal possesses rigidity when elastic, but at very high stress levels it completely loses its rigidity and acts as a fluid. [Refs. 12,13: p. 146,121]

III. EXPERIMENT AND MODEL DESIGN

A. BASIC MODEL

The intention of this investigation and the several preceding it [Refs. 14,15,16] has been to use one basic flat plate model and vary the stiffener types and plate thicknesses so that the underwater explosion shock (undex) response of these different geometries could be studied. But, due to several equipment failures, stiffener design geometries which showed no instability, and strain gage over-ranging, there was not a significant amount of dynamic tripping information compiled. However, each attempt was an invaluable step in the process of developing the proper model and the necessary experimental expertise.

It was clear that the model should be redesigned since no obvious tripping behavior was demonstrated in any of the previous four underwater shock tests. Also, as a preventive measure against equipment failure and strain gage over-ranging, a static test was performed (on a model of the same geometry as the redesigned test panel) to field test the same type of strain gages and same equipment used in the undex test.

The new test panel was designed after closely examining the physical deformations of each of the previous undex test panels. The objective was to combine the greatest plate deflection with the most sensitive stiffener. The model plate thickness used in the Rentz investigation [Ref. 14: p. 75] exhibited the most favorable plate deformation, while the rectangular stiffener behavior in the Langan investigation [Ref. 16: p. 51] gave the most promise of showing instability. Based on this, the model established was a 0.1875 inch thick test panel, 18 inches in length by 12 inches in width, machined out of the center of a 6061-T6

17

aluminum blank measuring 27 inches by 33 inches and two inches thick. One free-standing longitudinal narrow-flanged T-stiffener (vice a rectangular stiffener) was machined as an integral part of the plate. The T-stiffener web slenderness ratio (i.e., web height divided by its thickness) was also increased to enhance the stiffener's sensitivity to plate deflection. Additionally, to avoid the stiffener end tensile fractures observed in previous tests, the T-stiffener ends were detached from the boundaries of the cavity as shown in Figure 3.1 .

B. STATIC TEST

In order to verify the reliability (under more controlled conditions) of all the electronic equipment, cabling, and strain gage type (and attachment) that would be used for the underwater shock test, a static test was performed. The static test also was expected to provide valuable insight into the behavior of the redesigned test panel and the opportunity of comparing the static and the dynamic responses of a specific plate-stiffener geometry.

The experimental procedure was intentionally kept as simple as possible with the desire to collect only strain and deflection data as the stiffened plate (i.e., test panel) was deformed by increasing water pressure from zero psi to 350 psi. This pressure range was selected to cause approximately a four plate thickness deflection (deflection predictions calculated using the finite element/finite central difference computer code, EPSA, Elasto Plastic Shell Analysis) [Ref. 14: p. 24]. It was expected that this amount of deflection would produce tripping behavior in the stiffener. The test configuration was as shown in Figure 3.2 .

The stongback used to enclose the test panel cavity, see Figure 3.3, was machined from a one inch thick high strength

18

−TEST PANEL−
top view
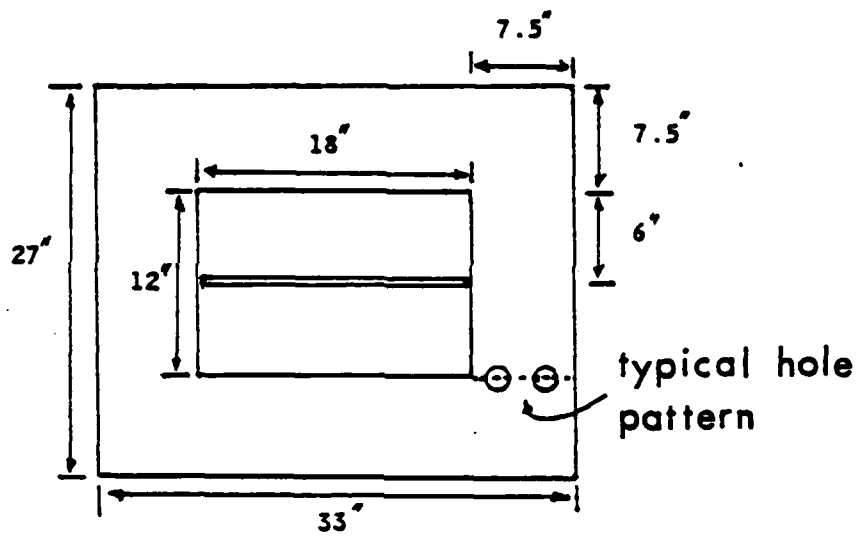
stiffener side view   stiffener end view
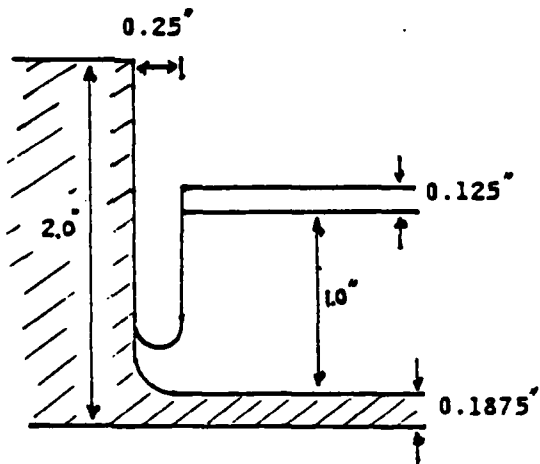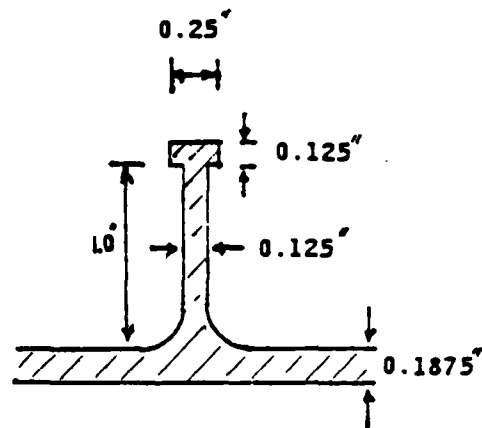
Figure 3.1   Test Panel With Longitudinal
Narrow-flanged T-stiffener.

19

steel sheet and was drilled and tapped for standard three-
quarter inch pipe fittings for a low point filling connec-
tion and a high point vent. Between the inlet valve and
strongback there was installed a zero to 400 psig Ashcroft
pressure gage and the high point vent was fitted with a
standard three-quarter inch gate valve. To provide an
adequate pressure seal, the strongback and test panel mating
surfaces were coated with a Permatex high pressure sealant
and separated by a precut one-eighth inch thick cork gasket.
The test panel and strongback were then secured together by
28, one inch in diameter, A325 high strength structural
steel bolts and torqued to 500 ft-lbs. The test medium was
potable water and was used to gradually fill the test panel
cavity and purge it of all air. The source of applied pres-
sure was a manually operated, single piston, reciprocating
hydropump rated for 1000 psi. A check valve and gate valve
arrangement was used to regulate the pressure in 25 psi
increments from zero psi to 350 psi. Several minutes (2 to
3 minutes) were needed at each increment to allow deflection
readings to be obtained. The strain measurements were
recorded continuously on a magnetic tape recorder. Strain
gage arrangement and details of the electronic instrumenta-
tion will be discussed in the underwater shock test section.

C. UNDERWATER SHOCK TEST

1. Undex Experiment Design

It is well known that the shock wave loading of a
body by an underwater explosion is complicated considerably
by the secondary effects of the explosion phenomena.
Therefore, as in previous studies [Refs. 14,15,16: p.
27,18,16], by using the correct test configuration and
sample time window, the data sampling can essentially be
limited to the response of the test panel to the incident
shock wave emanating from the charge. Consequently, the
secondary effects from bulk cavitation, cavitation closure,

20
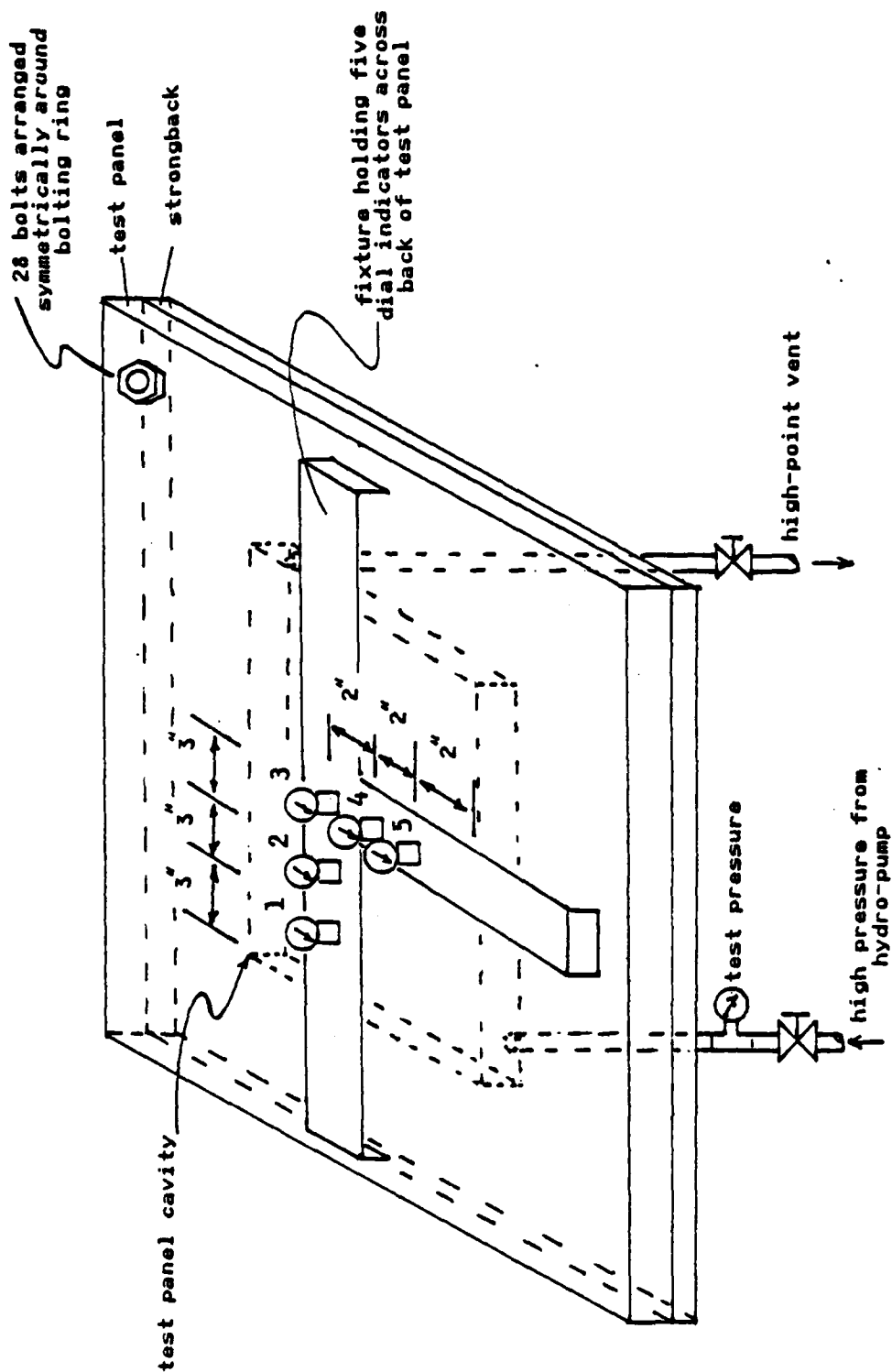
Figure 3.2   Static Test Configuration.
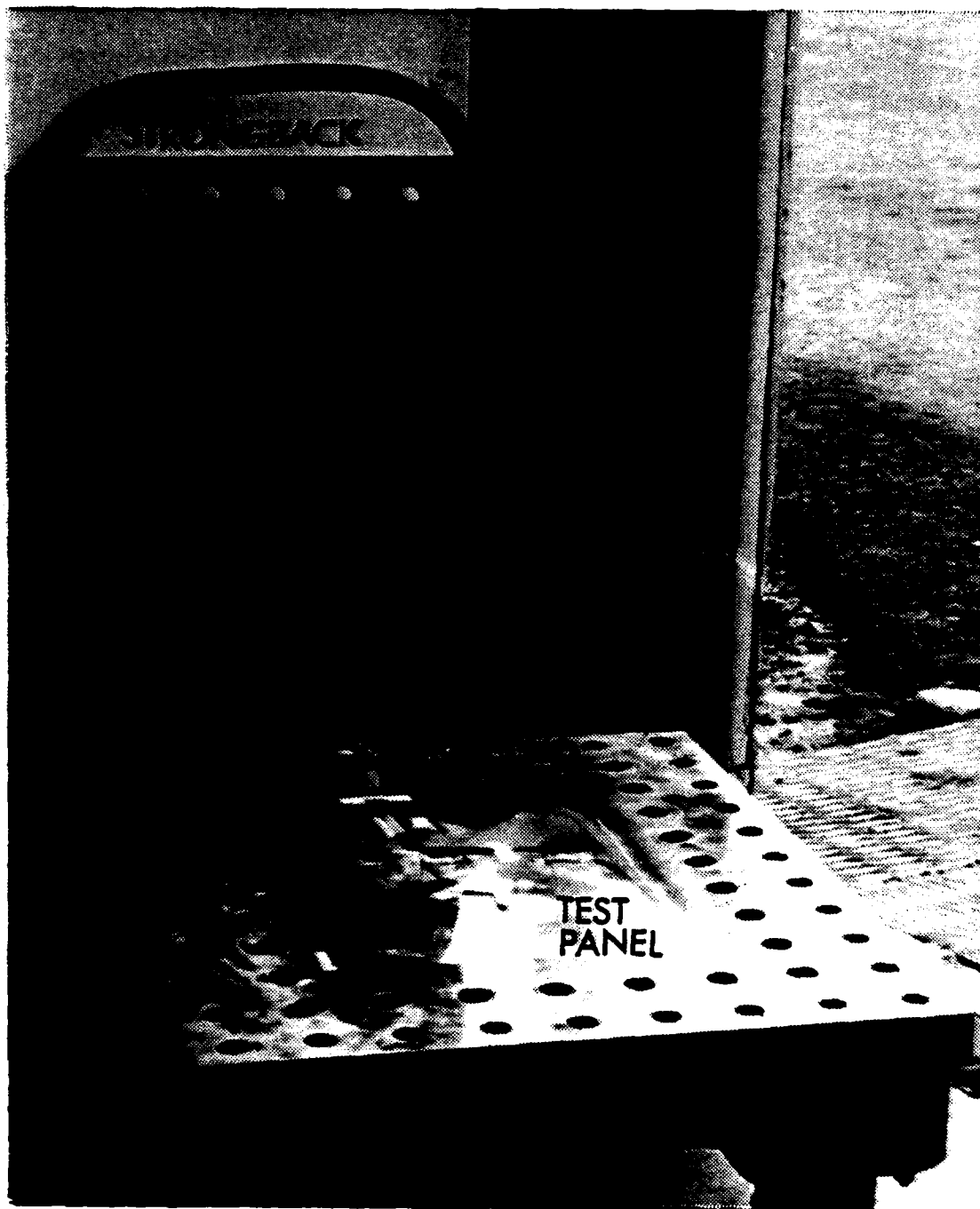
Figure 3.3   Static Test Strongback (Upper),
Test Panel (Lower).

22

reloading from the explosive gas bubble and bubble migration, surface cutoff, and bottom reflections can be avoided or ignored [Ref. 17].

The initial studies mentioned used eight pounds of TNT at a depth of four feet with a nine foot stand-off in an attempt to produce the necessary plate deflection to force stiffener tripping. Post-shot analysis of the four undex tests' pressure data [Refs. 14,15,16: p. 80,116,59] indicated that the TNT charges were not of a calibrated type and were reacting typically thirty percent greater in charge size (i.e., an 8 lb charge was exploding with the force of a 10.4 lb TNT charge). Under the assumption that all other eight pound TNT charges used would continue to react as larger sized charges, all test panel standoff and explosive charge depth calculations were made on the basis that the the explosive charge would react approximately as a 10 pound TNT charge. Accordingly, it was determined that the charge depth be 4.5 feet with a test panel standoff of 10 feet. Using this test configuration and a four millisecond sample window, the response expected would be that of a test panel experiencing an approximately plane shock wave.

2. Test Configuration

All undex testing was performed at the West Coast Shock Facility (WCSF), Hunter's Point Naval Shipyard, San Francisco, California.

In order to simulate a hull configuration and to ensure fully clamped boundary conditions, the test panel was securely bolted to the air-back chamber shown in Figure 3.4, designed by Rentz [Ref. 14: p. 105]. Note that the stiffener is exposed so that the loading conditions at the plate center will be compressive (i.e., enhancing the possibility of tripping).

For the actual testing the test panel and chamber combination was suspended as shown in Figure 3.6 by steel

23

cables attached to two pneumatic fenders. Figure 3.5 illustrates the critical dimensions of the test configuration, charge depth set at 4.5 feet with test panel/chamber standoff of 10 feet. The free-field pressure gages were set to measure incident pressure at a ten foot standoff radius. A pressure gage was also attached to the test panel exposed surface to measure fluid pressure at the plate, Figure 3.7 .

Strain measurements were taken on both the water exposed side and the air-backed side of the test panel as shown by Figures 3.7, 3.8 and 3.9 . The strain gage placement was determined on the basis of symmetry and the stiffener position. Consequently, the strains observed should be consistent with their position on the plate and would approximate the values and trends exhibited by symmetrically equal positions on other portions of the plate. Additionally, gages on the stiffener flange should be the first to show tripping effects, with the longitudinal array of three gages on the airside centerline soon mimicking the same trend.

3. Instrumentation

Twelve strain gages and three pressure transducers were placed as previously discussed and depicted. The strain gages were attached as described in [Ref. 14: p. 132] and coated with silicone sealant to ensure water tight integrity. The tourmaline pressure transducers were tied in their respective positions.

Two Honeywell MD-101 Wideband II (direct record) tape units were used to record all data channels at a tape speed of 120 inches-per-second, Figure 3.10 . Post-shot processing of the recorded strain and pressure data was through the NPS Vibrations Laboratory's HP-5451C Fourier Analyzer. Equipment specifications are listed in Table I .

24

TABLE I

SPECIFICATIONS OF EQUIPMENT

EQUIPMENT	TYPE	RANGE
strain gages	CEA-350 ohms	50k microstrain
pressure transducers	.25" Tourmaline	10 ksi, 97% response ratio
amplifiers	Ektron 563F J	-------------
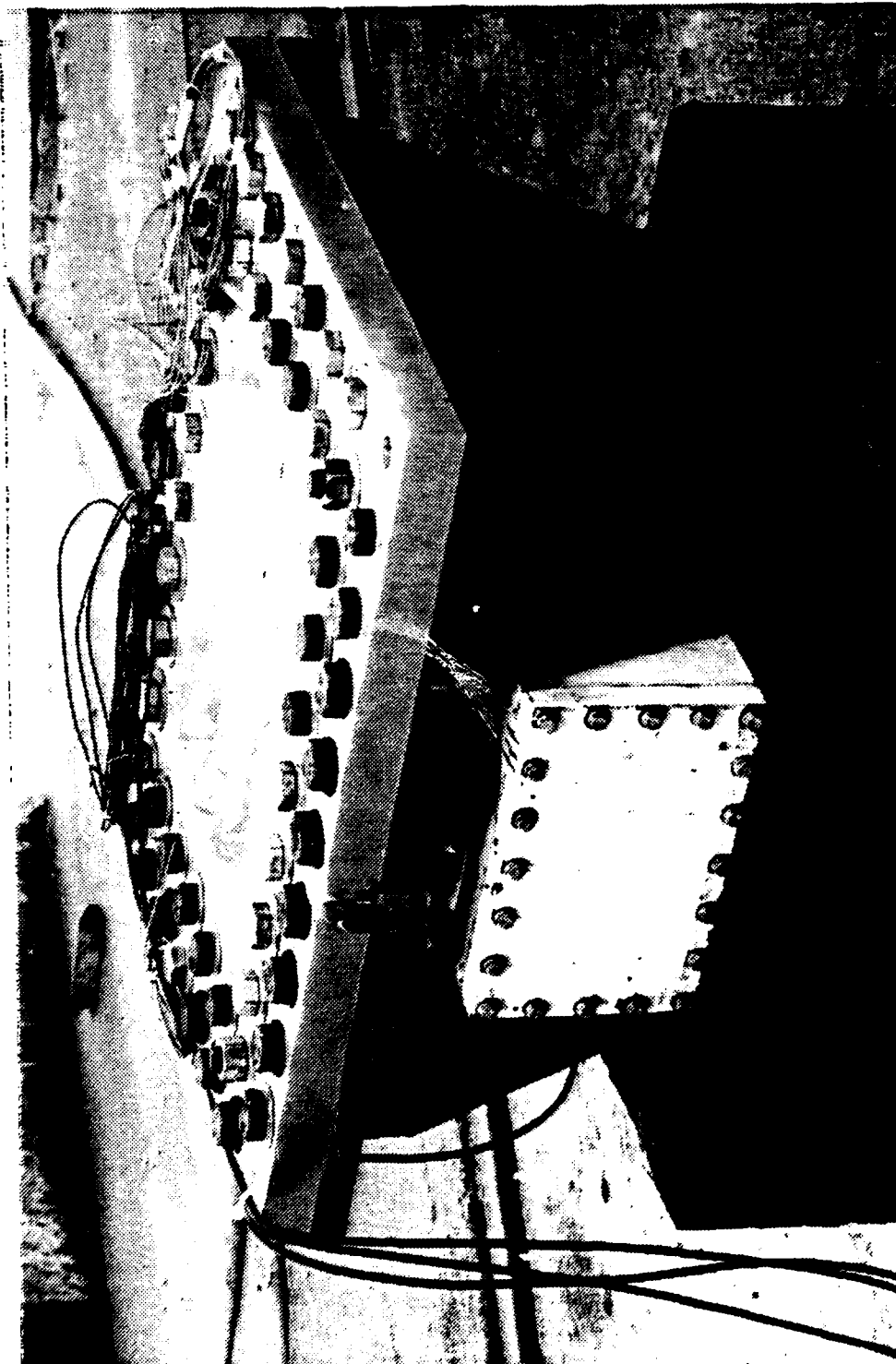
Figure 3.4   Test Panel Bolted to Air-back Chamber.

26

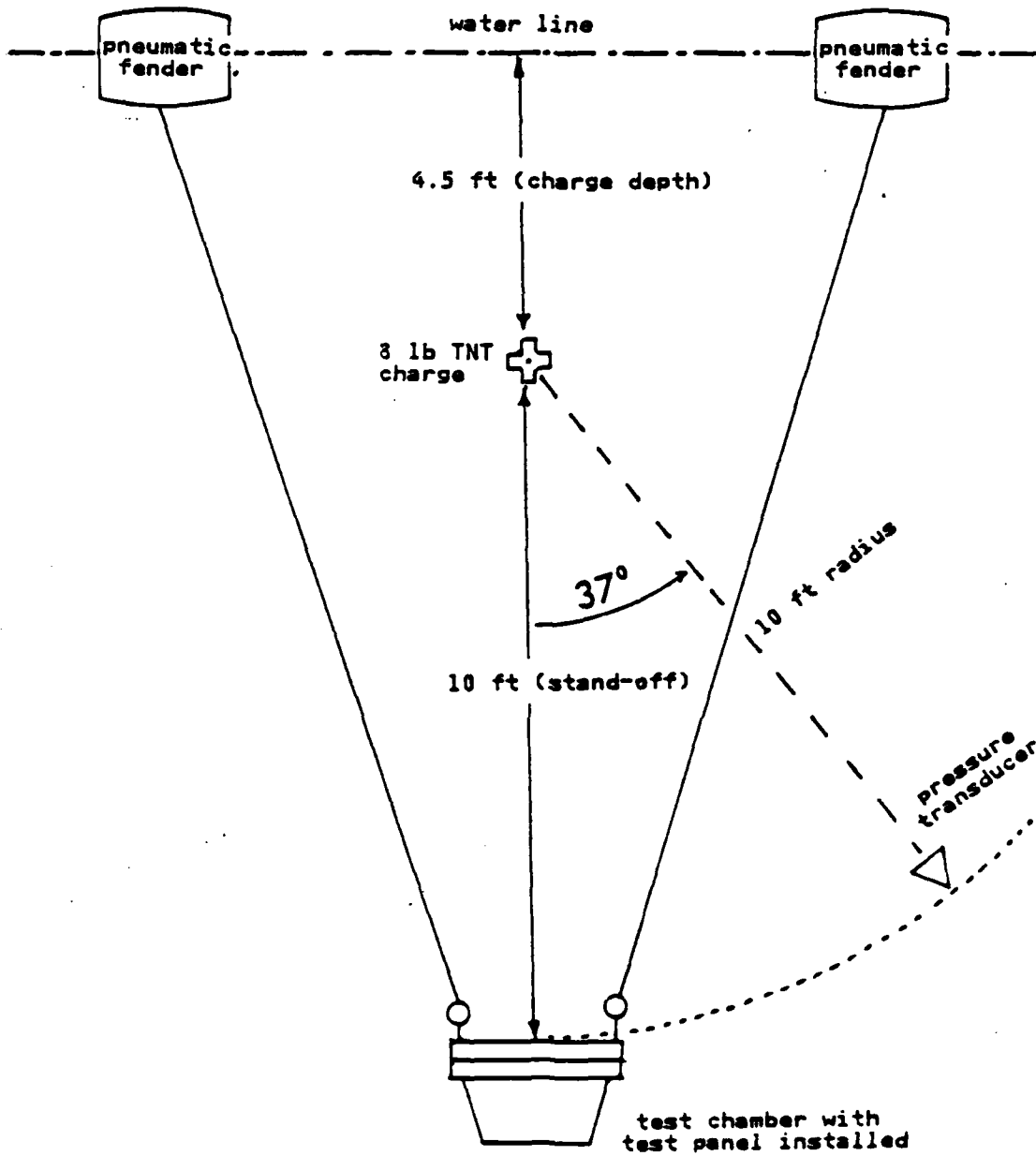Figure 3.5   Schematic of Undex Test Geometry.
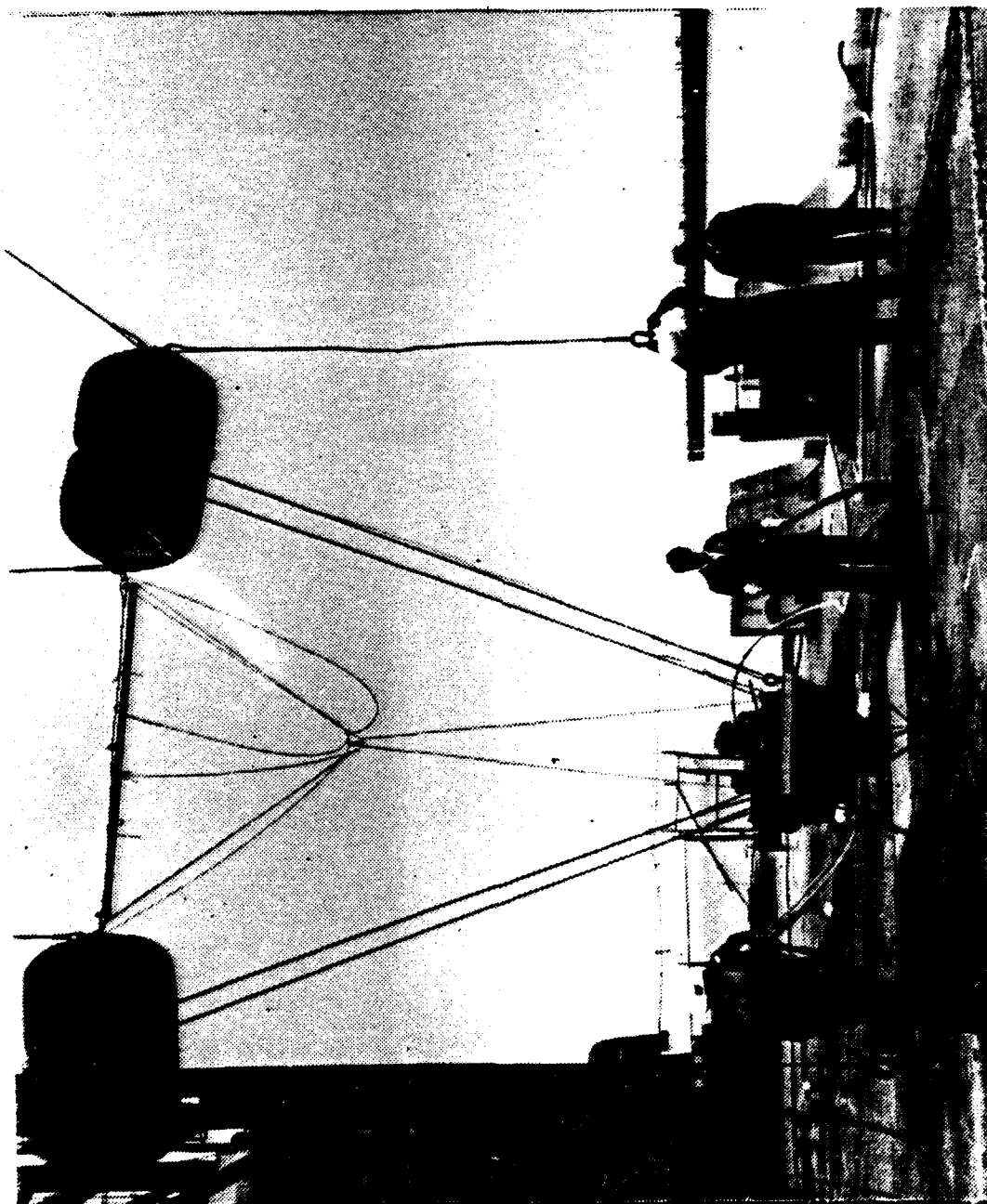
Figure 3.6   Test Panel and Chamber Slung from
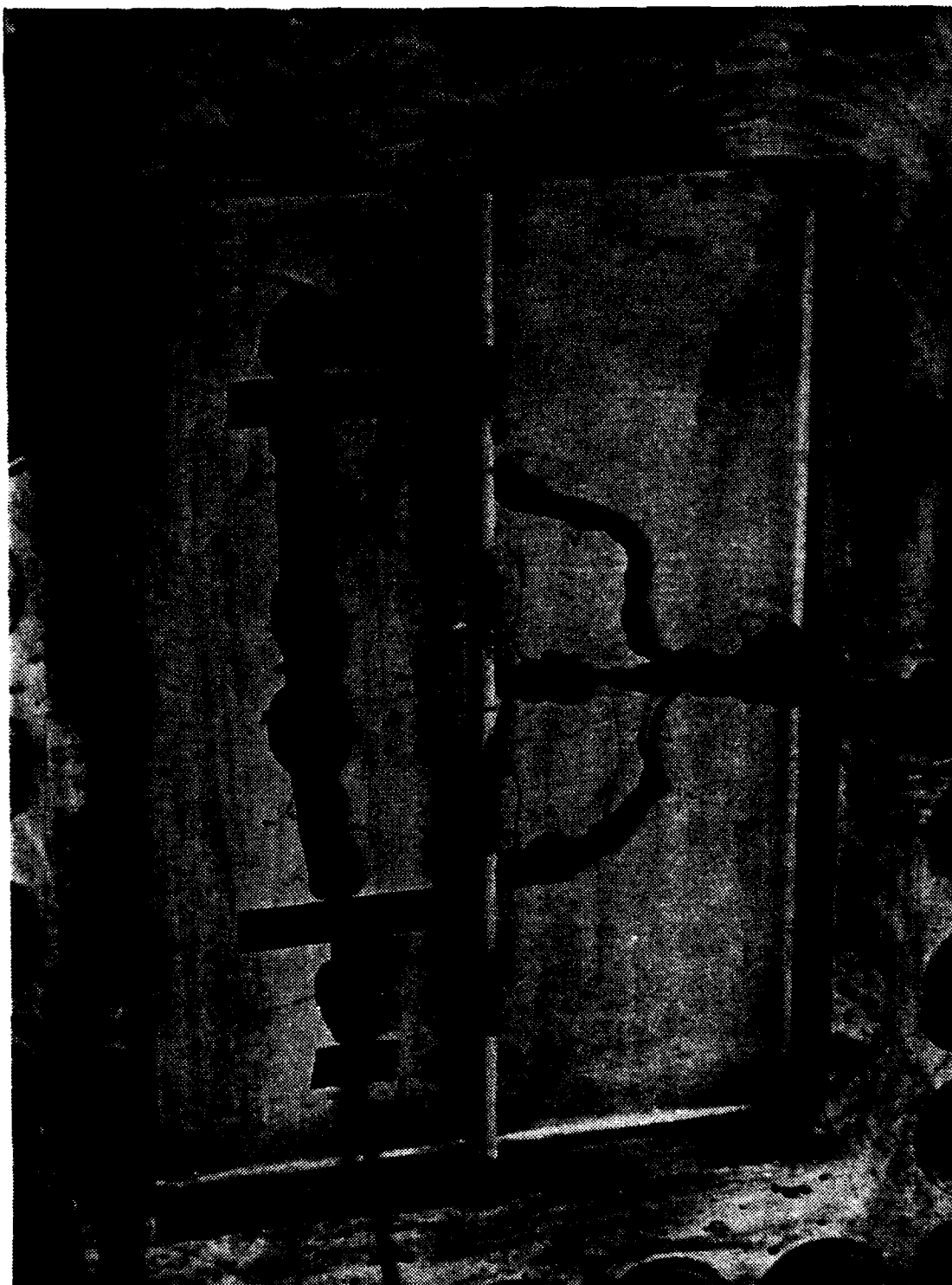Pneumatic Fenders.
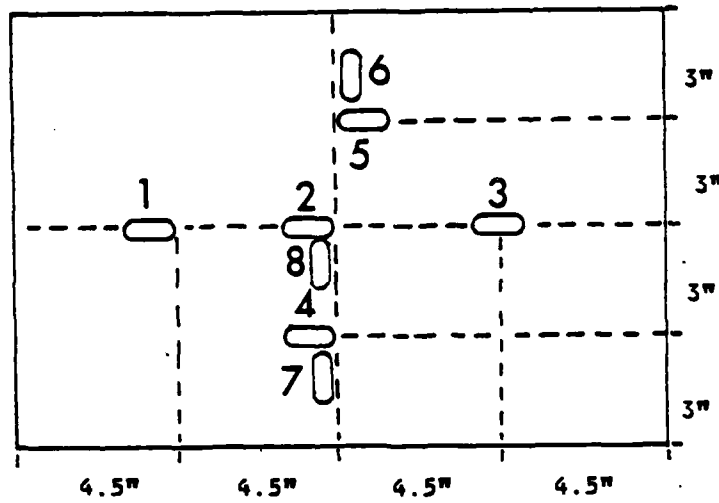
28

Figure 3.7   Strain Gage and Pressure Transducer
              Placement (waterside).

29

Figure 3.8   Strain Gages (Airside).

30

AIR SIDE

WATER SIDE
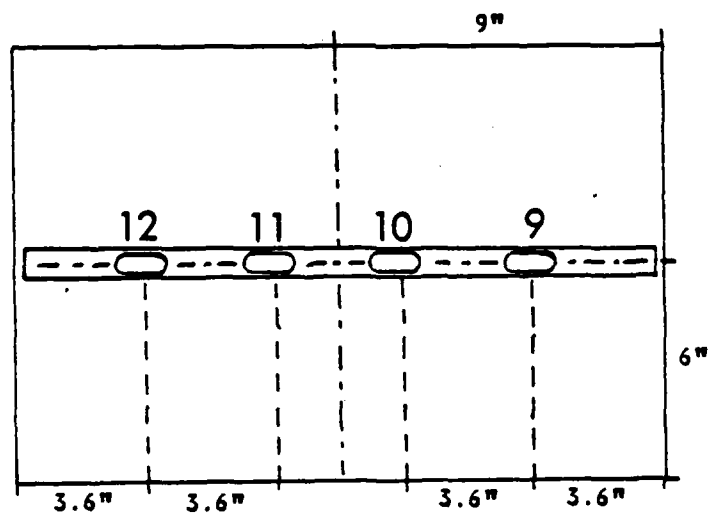
Figure 3.9   Diagram of Strain Gage Placement.

31
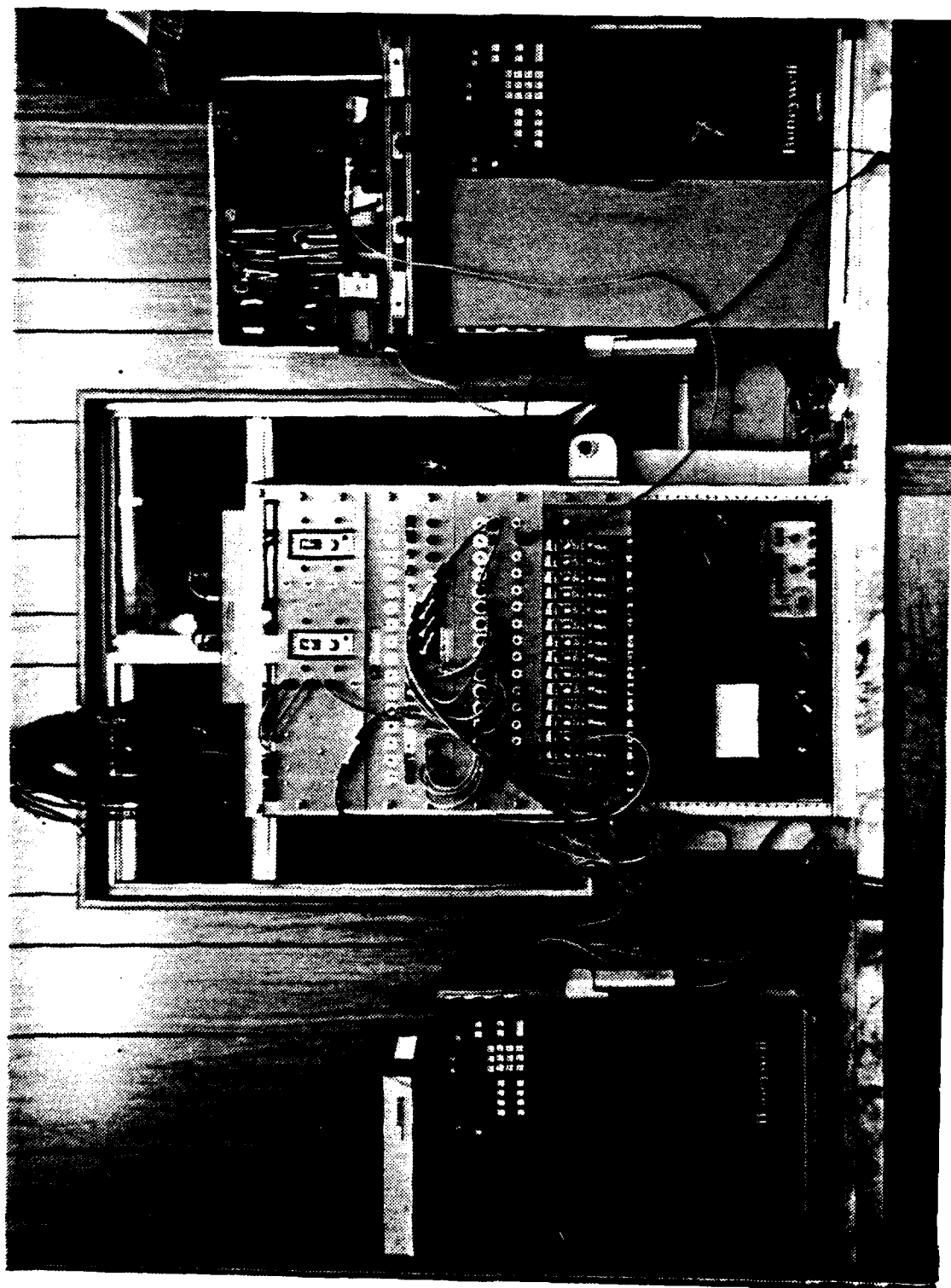
Figure 3.10   Undex Data Recording Instrumentation
Arrangement.

32

IV. RESULTS AND DISCUSSION OF DATA

A. STATIC TEST RESULTS

The static pressure deflection test of the panel machined for this purpose, proved to be a source of very good strain and deflection data showing the plate/stiffener behavior building up to elastic tripping as increasing water pressure deformed the plate. Figure 4.1 shows the plate segmented into 16 horizontal and 26 vertical elements for one "one-half symmetrical section" of the test panel. This was done to allow points on the plate to be denoted as nodes. Deflections were measured by dial indicators at positions 1 through 5 as shown in Figure 3.2, the results of which appear in Table II. Node (16,13) indicates the position at horizontal element 16 and vertical element 13. The nodal deflections across the horizontal element 16 (vertical element 1 through 26) are depicted in Figure 4.2 . Nodal deflection is again represented in Figure 4.3, but here deflection has been normalized to pressure at each 25 psi increment. Note the well defined regions for elastic, plastic, and elastic tripping behavior. These regions were approximately defined from the following information:

1. After completion of the test, pressure was released. The centerline node (16,13) retained a permanent set of 0.408 inches after a total deflection of 0.695 inches at 350 psi. This meant that approximately the first 0.287 inches of deflection were elastic (i.e., deflection corresponding to the initial one-hundred psi of pressure applied).

2. The elastic tripping behavior was noted initially on the strain histories for SG-2 and SG-4 at approximately 225 psi and continued through the end of the test.

3. Therefore, the region between elastic deflection and elastic tripping (i.e., 100 psi to 225 psi) can be considered plastic deformation of the plate and T-stiffener together. Again, referring to Figure 4.3, all five normalized deflection curves show the same trends and the same definite changes in slope at the regions indicated.

33

Strain data was continuously recorded on the Honeywell MD-II at a tape speed of 1.87 inches per second, over the entire forty minute period needed to perform the test. Ten strain gages performed very satisfactorily while two (SG-5 and SG-11) failed for unknown reasons. The recorded strain history for each surviving gage was then displayed by a strip-chart recorder, thus providing the traces seen in Figures 4.4 through 4.13 . Table III contains the strain values recorded at each pressure increment for each strain gage.

The effect of stiffener unloading and stress redistribution as the stiffener began to elastically trip can be clearly seen in Figures 4.14 and 4.15 . The region of the plate most sensitive to symmetrical stiffener tripping would be the area near the toe of the web, accordingly strain gage SG-2 would and did first sense the stiffener unloading. Additionally the center of the plate and the stiffener continued to be areas of largest strain (SG-2 and SG-10) until elastic tripping occurred at approximately 225 psi, at which point the stiffener web was elastically buckling and unloading as was demonstrated in all other regions of the plate (Figures 4.16 and 4.17). Also note that strains monitored at the far ends of the stiffener (SG-1, 3, 9, 10 and 12) continued to increase until elastic tripping occurred, at which point the rate of strain-increase became greater at these positions. This was not typical in the case of SG-10 (located 1.8 inches off the center of the point of maximum vertical deflection of the flange) where strain continued to increase but at a decreasing rate, demonstrating that the stiffener load was being redistributed to the regions of the stiffener where the web had not yet begun to rotate out of the vertical plane. The redistribution of the stresses throughout the stiffener is best illustrated in Figure 4.18 which is strain normalized at each 25 psi increment for

34

strain gages SG-1, 3, 9, 10 and 12. None of these plate and stiffener gage locations showed the same elastic tripping "unloading" as did SG-2, 4, 5, 7, and 8. Accordingly SG-1, 3, 9, 10, and 12 best represented the response of the stiffener flange (SG-9, 10, and 12) and web toe (SG-1 and 3) to elastic tripping. In Figure 4.18 it again can be seen how the center of the stiffener flange (SG-10) begins to unload as the web rotates elastically out of the vertical plane (symmetrical tripping) and the remaining portion of the stiffener assumes the load. The strain histories also indicate that the stiffener was rotating out of the vertical plane towards strain gage SG-6, which is why SG-7 and SG-8 values were not sensitive to the initial tripping action until 275 psi, versus 250 psi for SG-6 (Figure 4.16).

As a consequence of this test it was determined that more than four plate thicknesses deflection would be required to initiate inelastic tripping. Lateral measurements of the stiffener (after the 0.695 inch centerline vertical deflection of the test panel, i.e., approximately four plate thicknesses) indicated no permanent deformation of the flange or web out of the vertical plane. Additionally, the progressive behavior of this specific plate-stiffener combination when loaded was found to be well defined, qualitatively predictable, and sensitive to tripping. The static field test had shown also that the equipment to be used in the underwater explosion data collection was reliable and performed well.

B. UNDERWATER SHOCK TEST RESULTS

The shot went off as planned and, as predicted, the 8 lb charge reacted as a 10 lb charge (determined by post-shot calculations). The dome and plume from the explosion were symmetrical, as was expected for the cylindrical charge used, see Figures 4.19 and 4.20 . Also, as had happened during the Langan test [Ref. 16: p. 46], the pneumatic fenders were ruptured from the force of the explosion.

35

TABLE II
STATIC TEST DEFLECTION AND PRESSURE DATA

| | PLATE DEFLECTION (inches) | | | | |
| | - NODES - | | | | |
PRESSURE (psi)	(5,13)	(10,13)	(16,13)	(16,8)	(16,4)
25	.043	.079	.095	.080	.040
50	.080	.148	.180	.154	.075
75	.110	.204	.247	.211	.103
100	.139	.255	.304	.260	.131
125	.180	.308	.361	.311	.165
150	.197	.352	.407	.352	.190
175	.223	.394	.451	.392	.217
200	.248	.434	.492	.430	.242
225	.275	.473	.532	.466	.267
250	.297	.506	.566	.497	.288
275	.321	.540	.601	.529	.311
300	.342	.570	.632	.557	.333
325	.364	.601	.664	.586	.354
350	.387	.632	.695	.615	.376

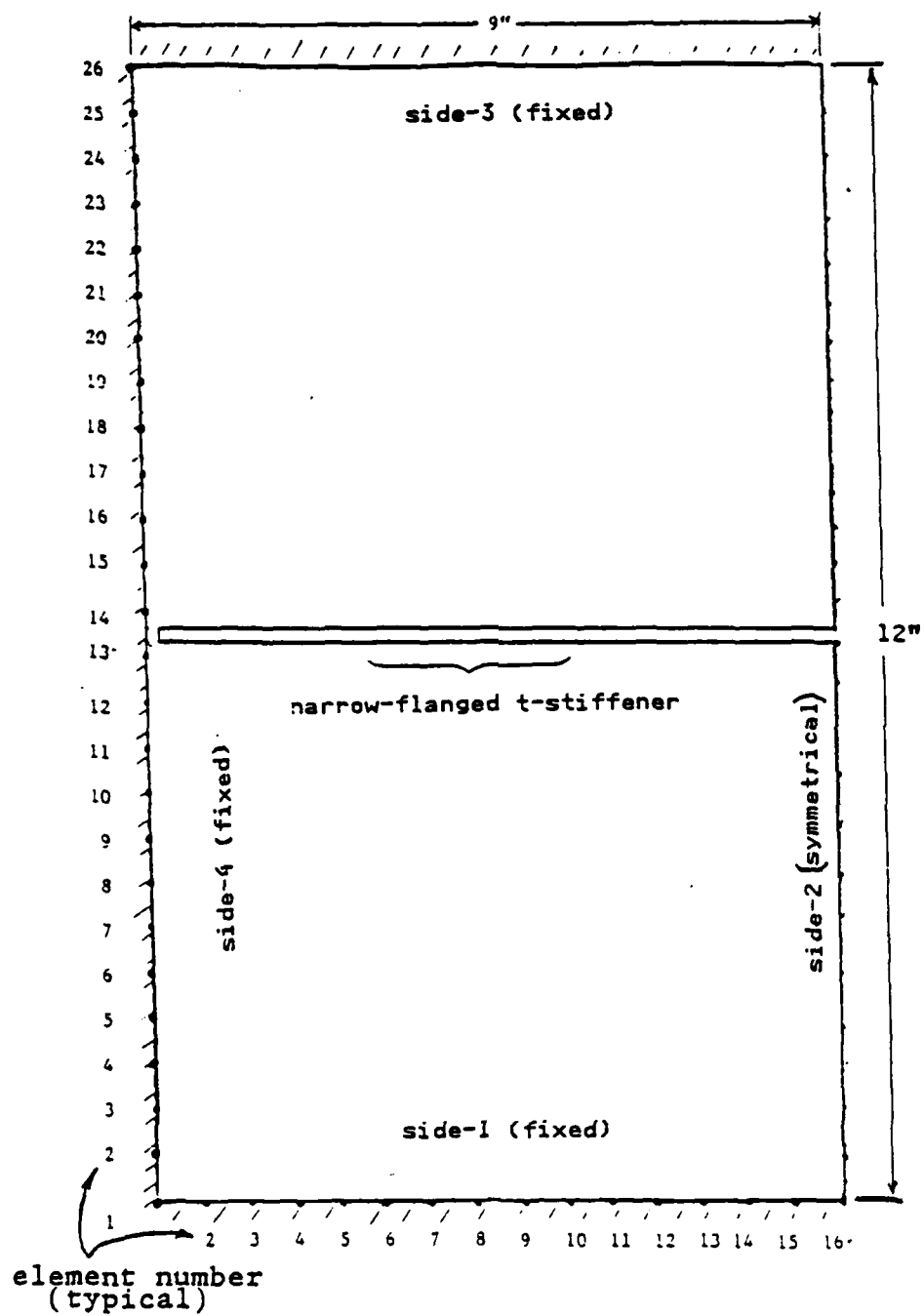NOTE: AFTER PRESSURE WAS VENTED OFF, A PERMANENT SET OF 0.408 INCHES REMAINED AT NODE (16,13).
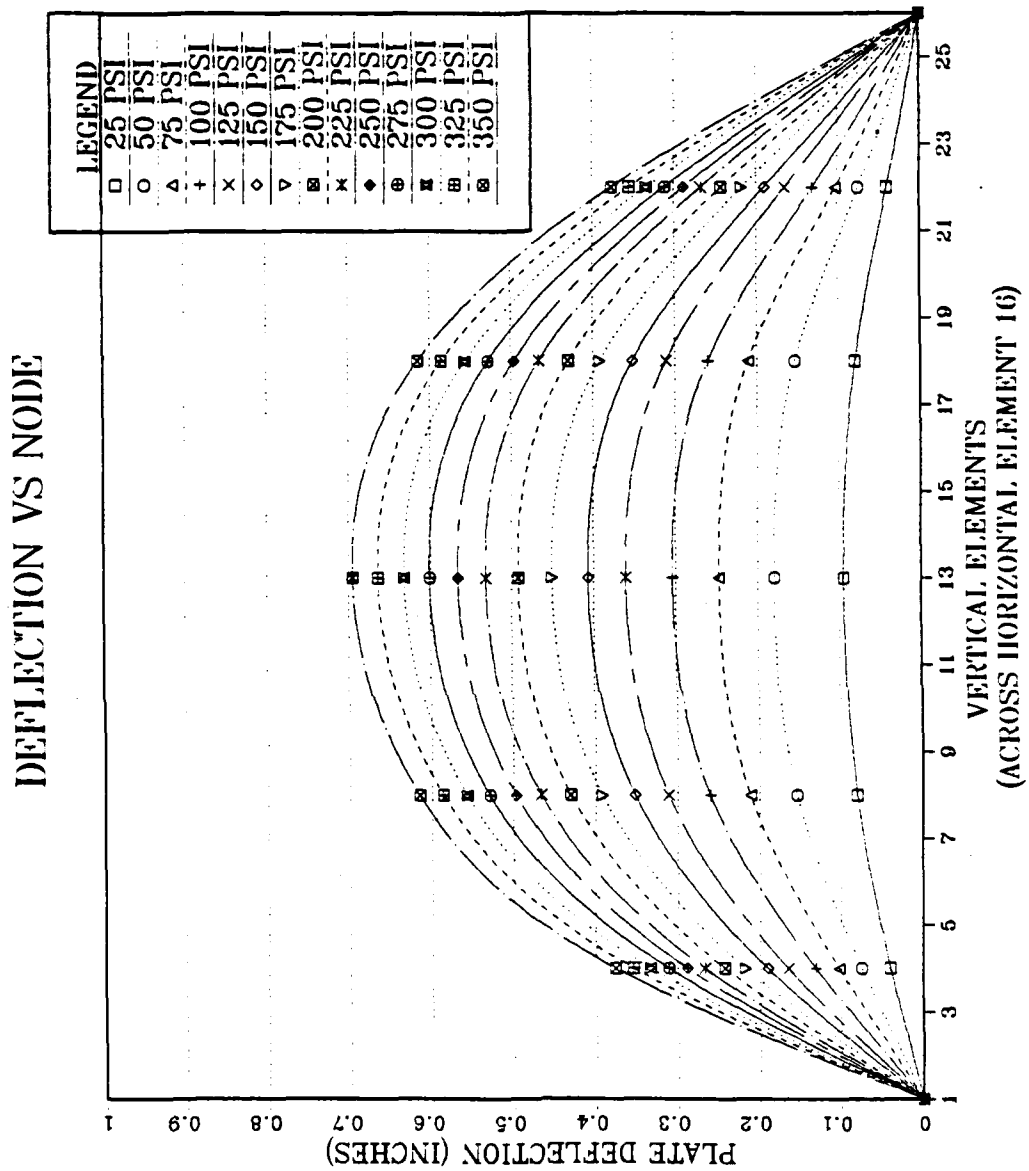
Figure 4.1   Segmentation of Half-plate.

37

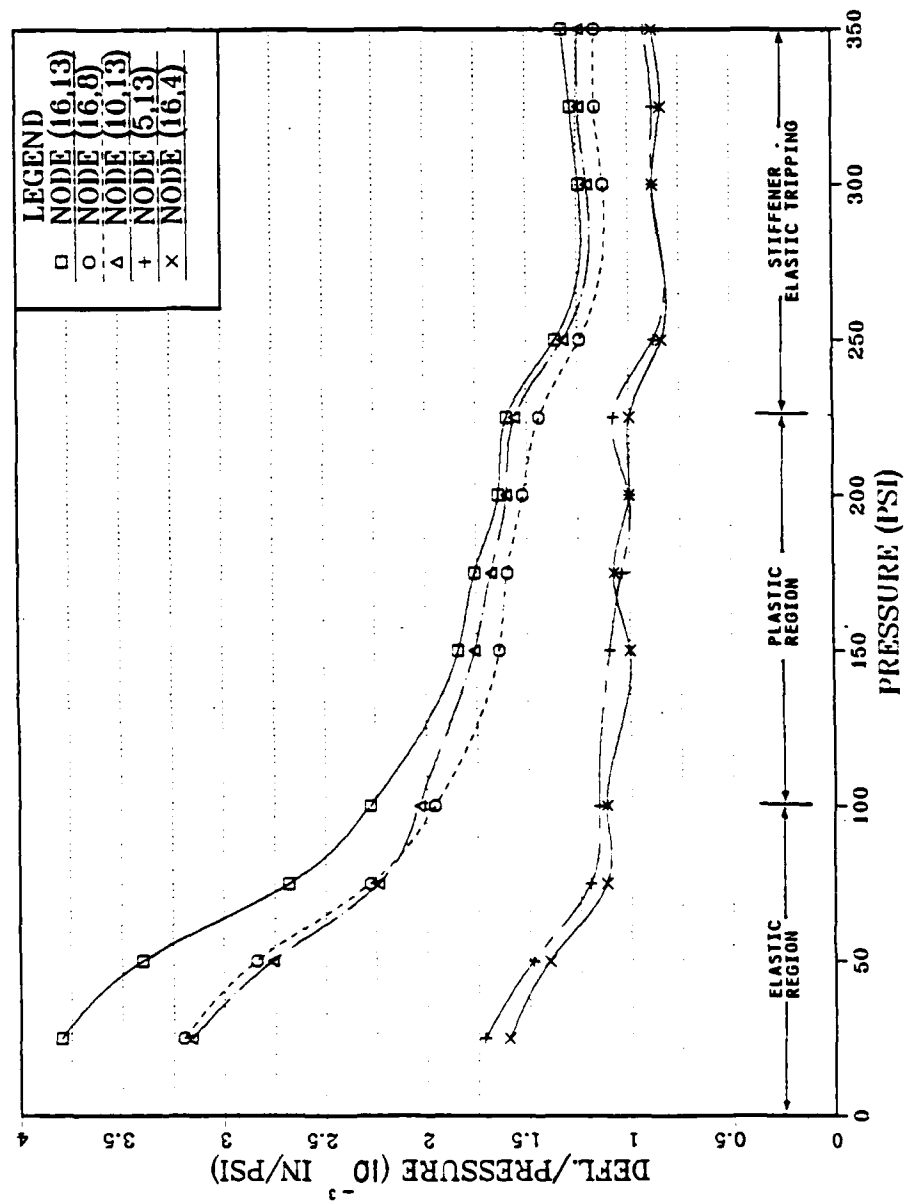Figure 4.2   Plot of Static Deflection Test Results.

38

Figure 4.3   Plot of Static Deflection Normalized to Pressure.

TABLE III
STATIC TEST STRAIN AND PRESSURE DATA

STRAIN GAGE DATA (microstrain)

-STRAIN GAGE POSITIONS-

PRESSURE (psi)	1	2	3	4	6	7	8	9	10	12
25	403	616	373	242	622	579	745	1156	2655	1236
50	781	1243	741	509	1271	1186	1697	2015	4348	1988
75	1140	1716	1083	694	1846	1763	2595	2681	5132	2608
100	1522	2026	1451	841	2448	2340	3314	3253	7644	3155
125	1995	2297	1882	977	3098	3030	4025	4018	9720	3907
150	2440	2537	2342	1100	3654	3572	4769	4781	11122	4789
175	2922	2802	2802	1231	4334	4274	5550	5669	12074	5992
200	3408	3053	3281	1359	5014	5031	6183	7081	12948	7323
225	3975	3330	3833	1515	5830	5942	6778	8613	13458	9014
250	4456	2633	4340	1542	6548	6708	7351	9911	13877	10574
275	5070	1261	4938	1258	6288	7512	7901	11552	14132	12359
300	5637	871	5490	1073	2754	2686	5401	13078	14314	14181
325	6223	760	6089	1030	1873	2462	3091	14910	14496	15985
350	6913	734	6779	996	1743	2377	2964	16742	14678	17770
VENT	3266	284	3189	485	1048	691	1236	10102	8190	11137

NOTE: STRAIN GAGES SG-5 AND SG-11 FAILED PRIOR TO TEST. ALSO STRAIN VALUES IN THE VENT ROW INDICATE STRAIN REMAINING AFTER PRESSURE WAS VENTED OFF (I.E. AT ATMOSPHERIC PRESSURE).

40
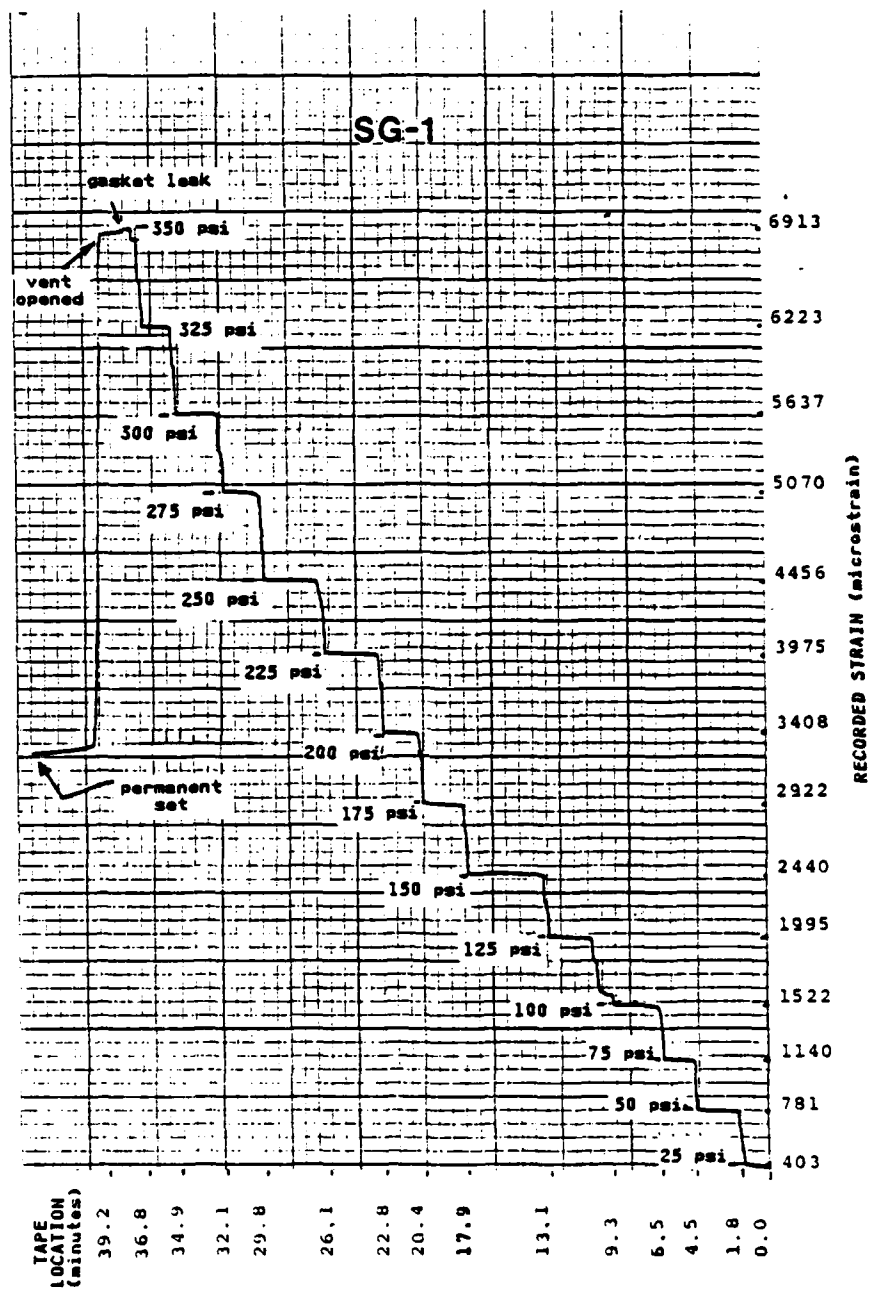
Figure 4.4   Strain Gage NO. 1 Strain History.
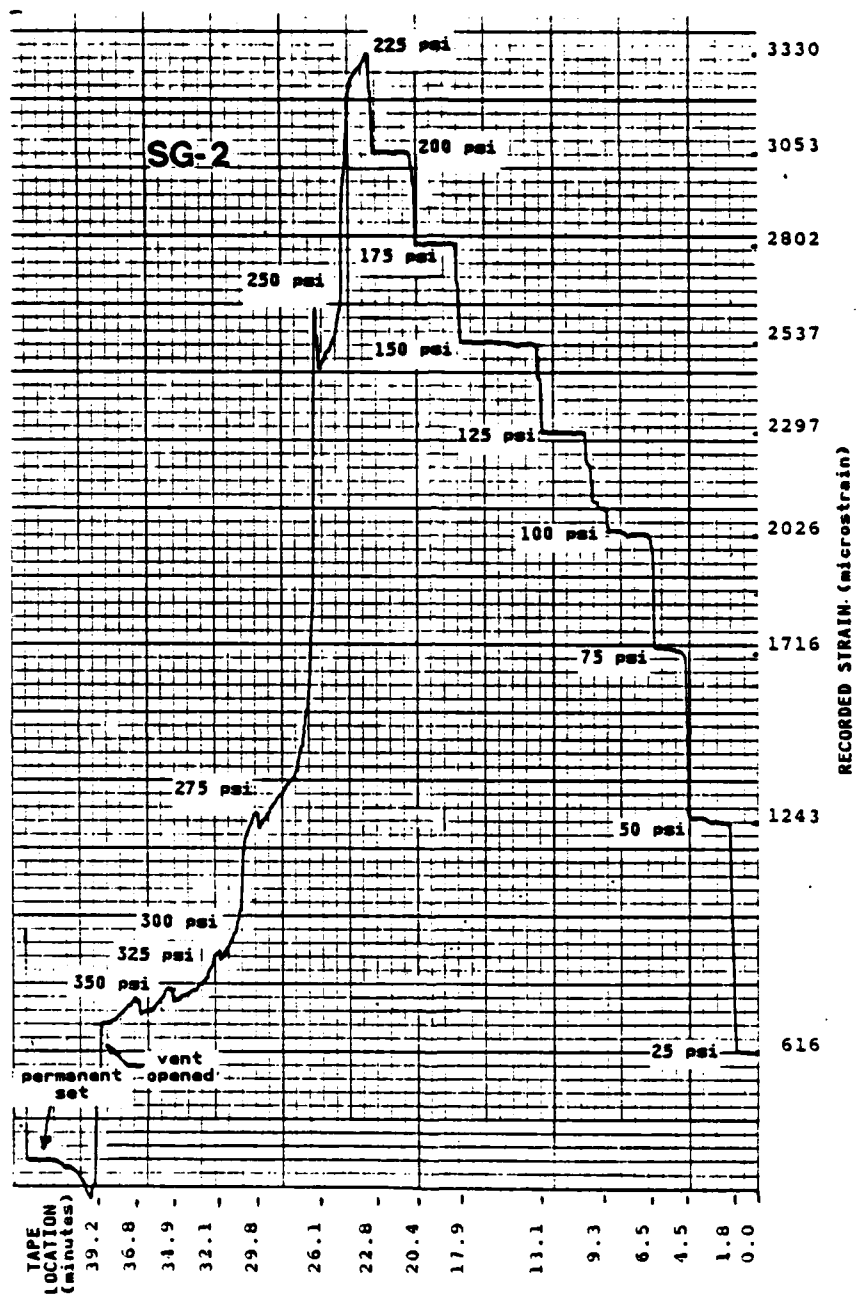
Figure 4.5   Strain Gage NO. 2 Strain History.

42
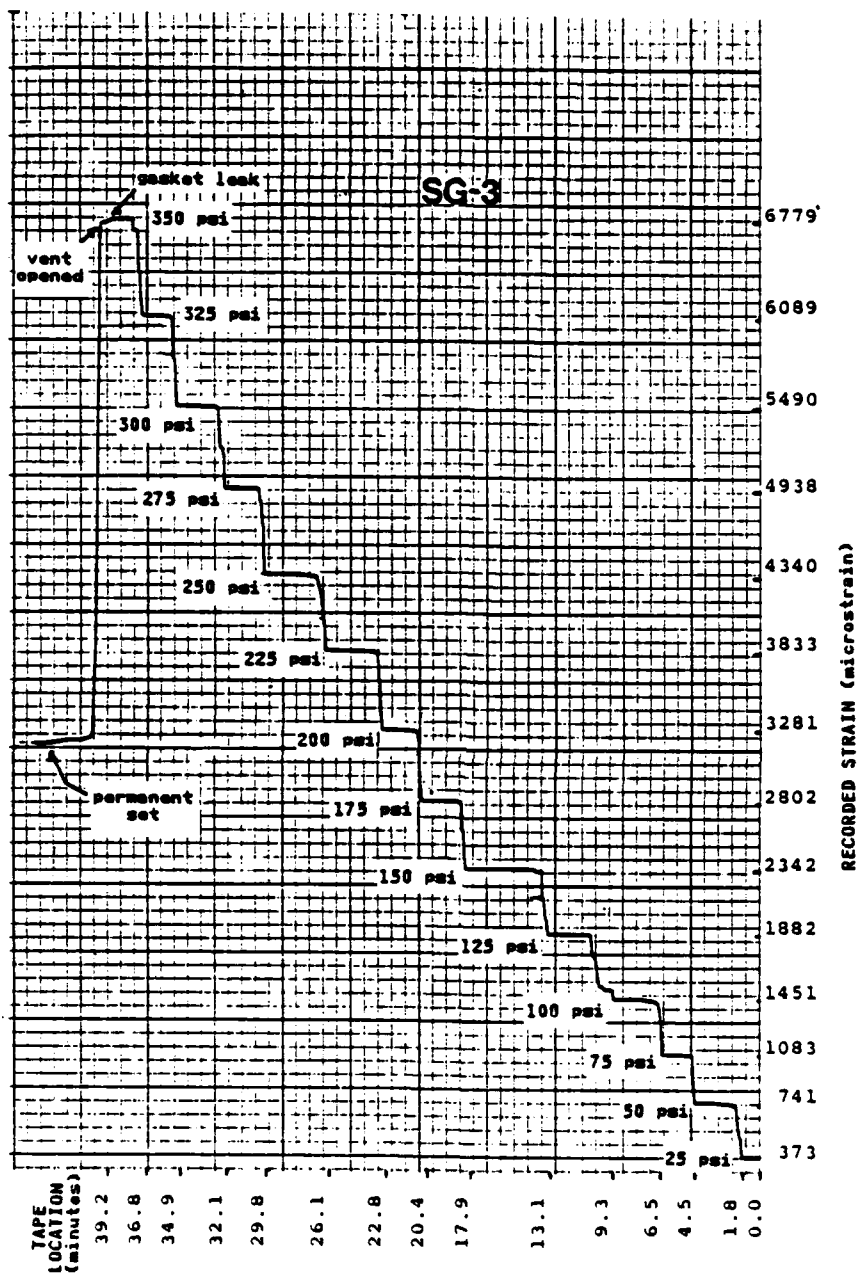
Figure 4.6   Strain Gage NO. 3 Strain History.
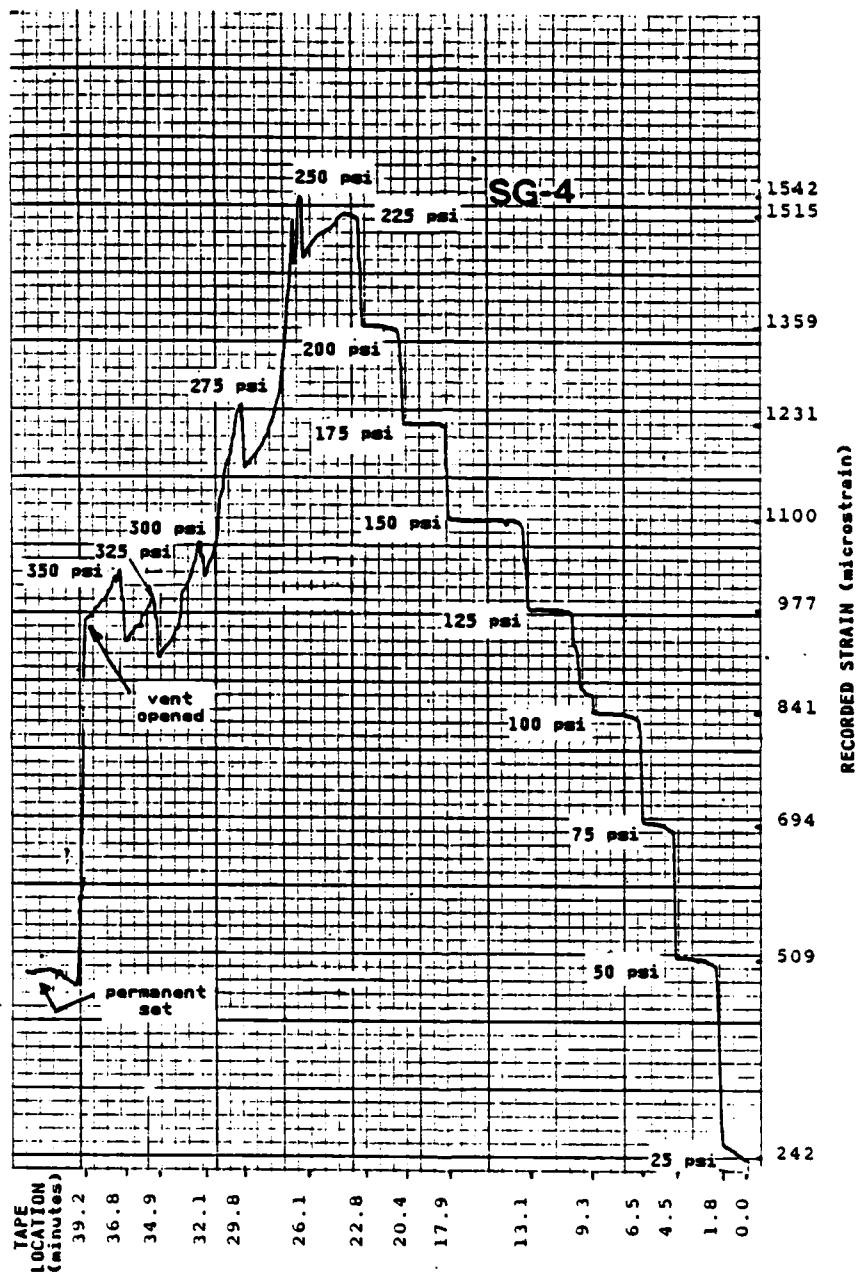
Figure 4.7   Strain Gage NO. 4 Strain History.

44
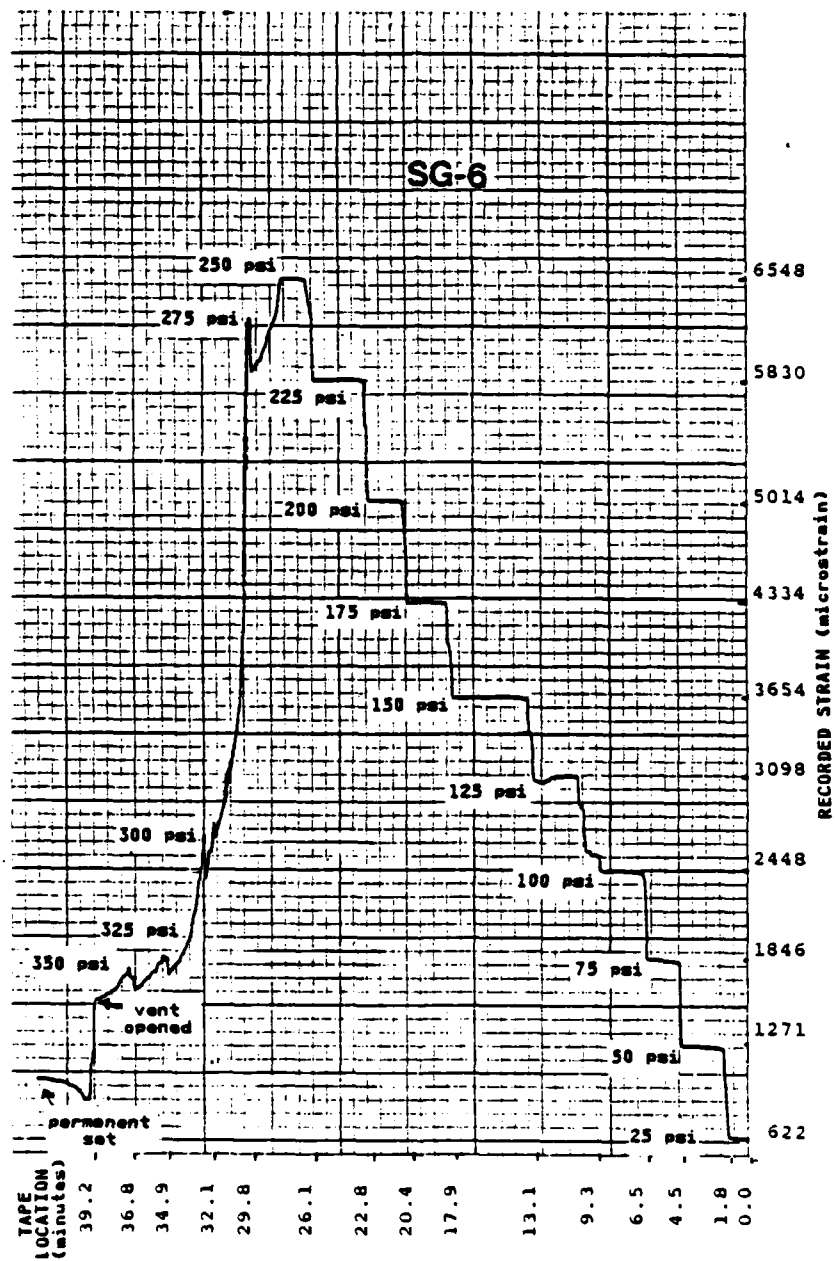
Figure 4.8   Strain Gage NO. 6 Strain History.

45
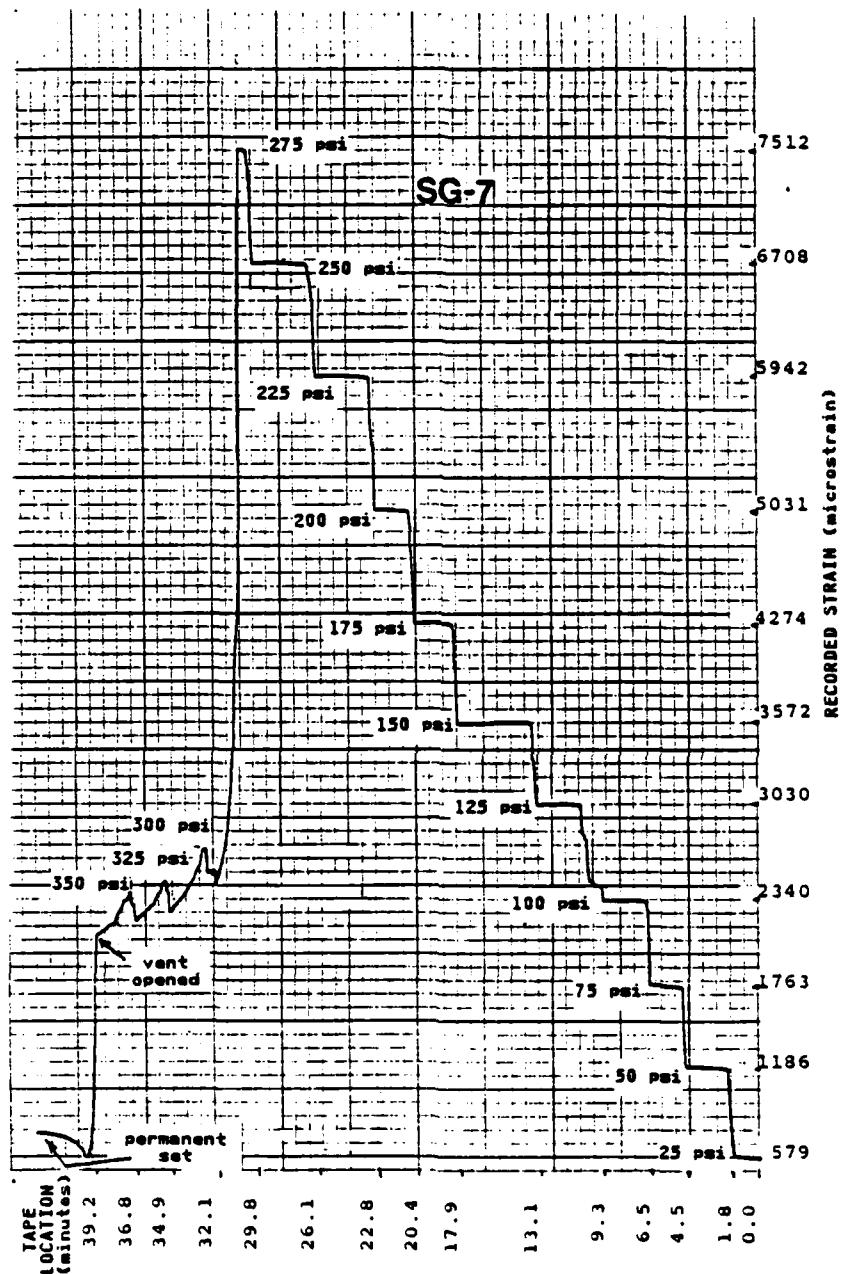
Figure 4.9   Strain Gage NO. 7 Strain History.
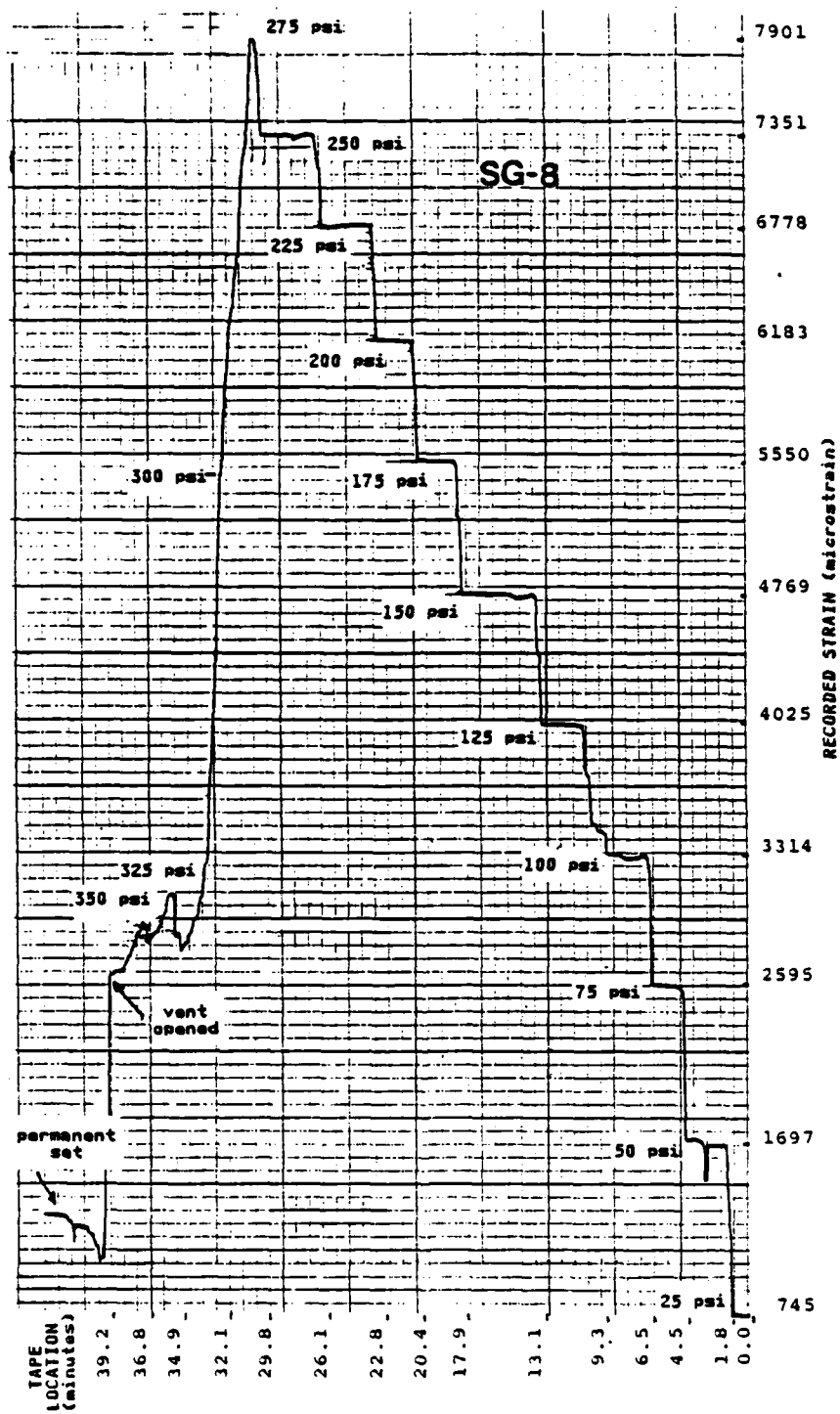
Figure 4.10   Strain Gage NO. 8 Strain History.

47
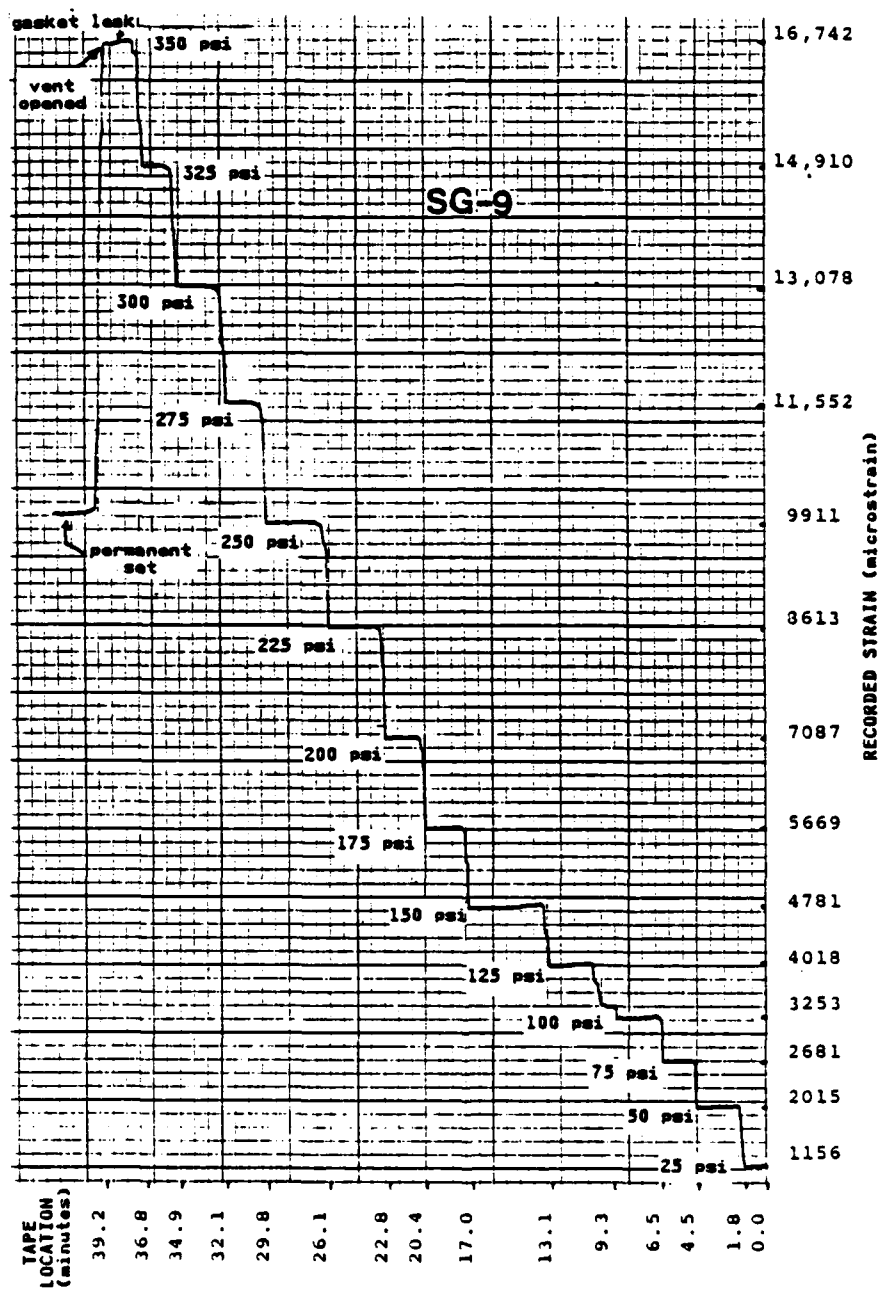
Figure 4.11   Strain Gage NO. 9 Strain History.

48
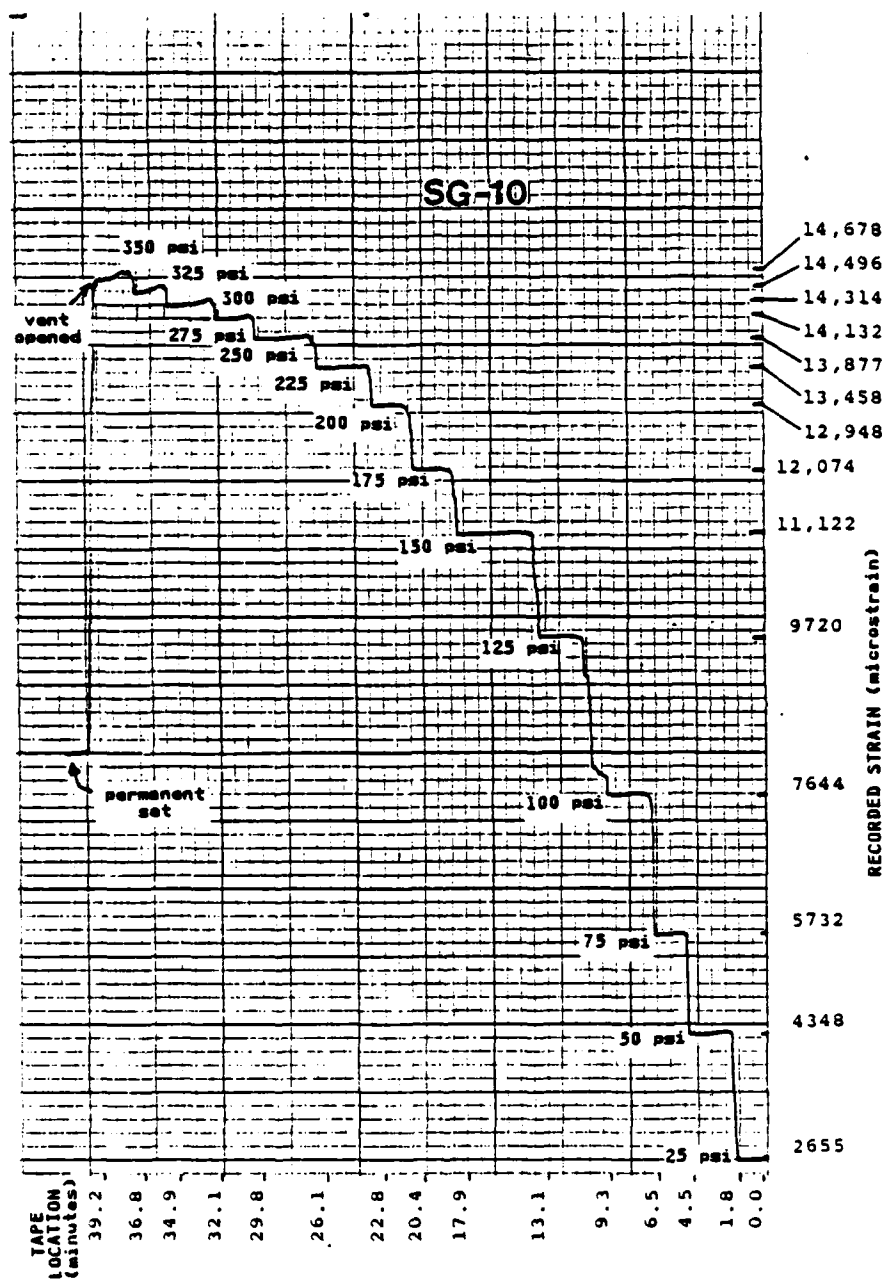
Figure 4.12   Strain Gage NO. 10 Strain History.
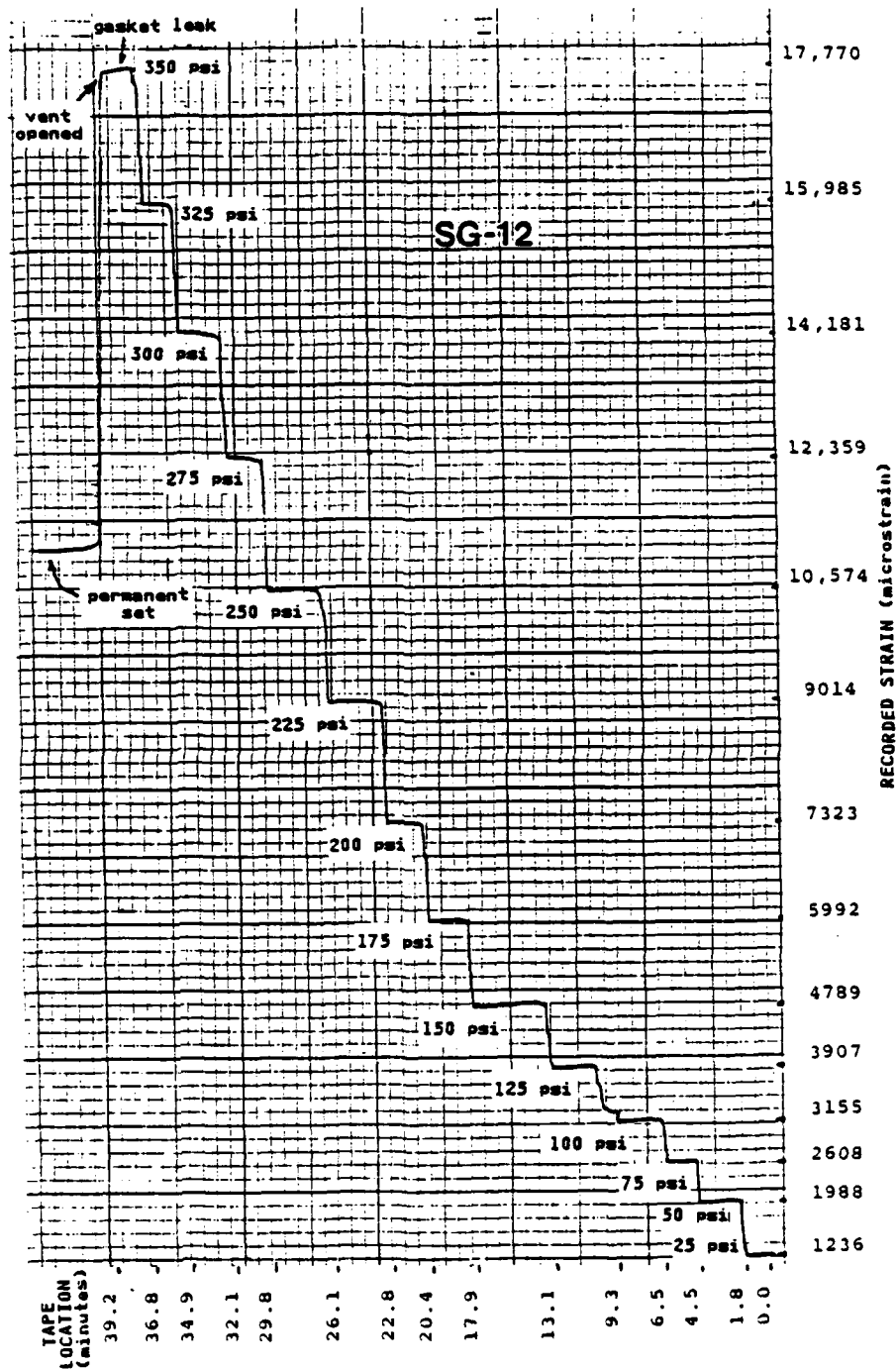
Figure 4.13   Strain Gage NO. 12 Strain History.
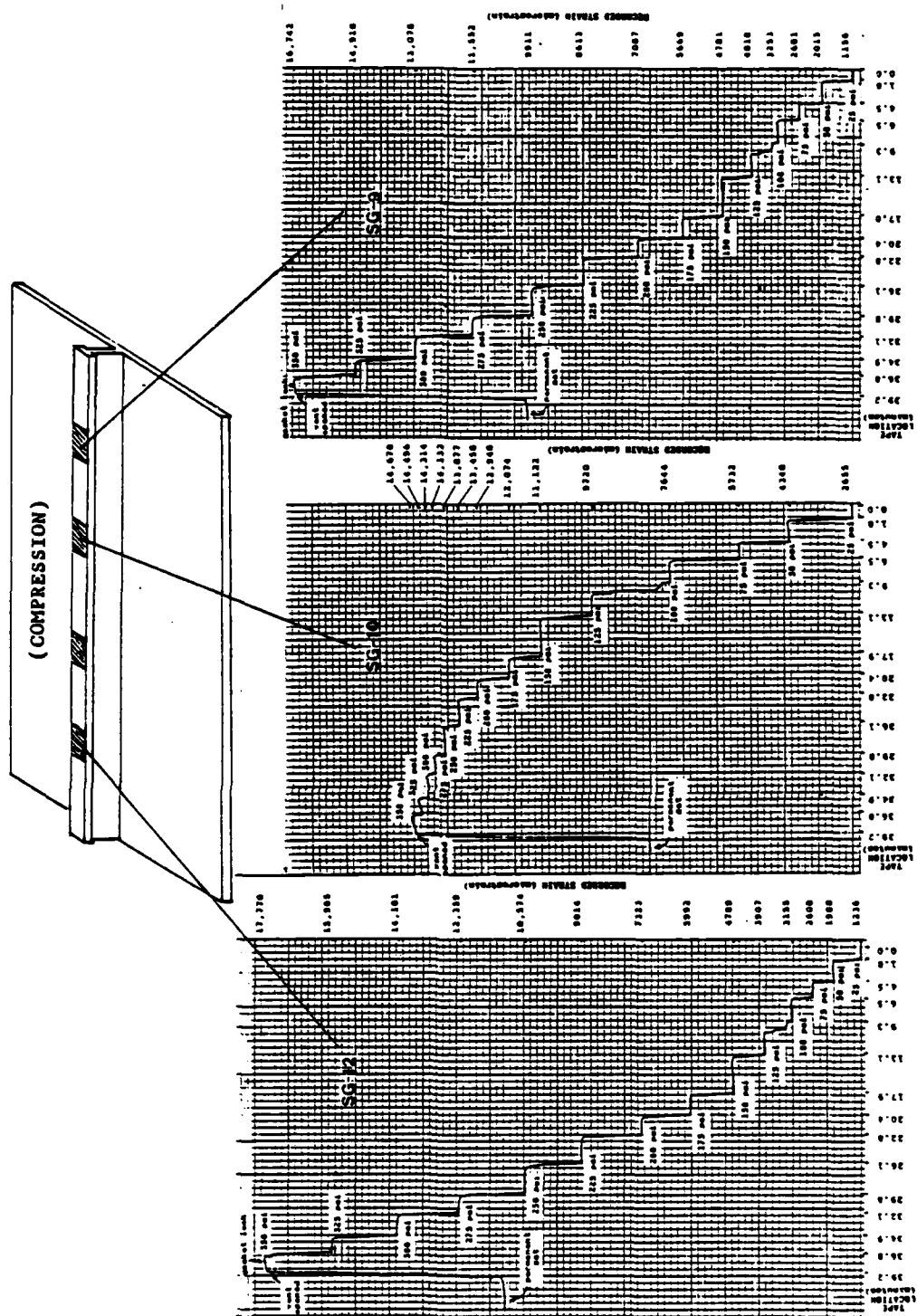
Figure 4.14   Strain History Recorded Longitudinally
Across Flange of T-stiffener.

51
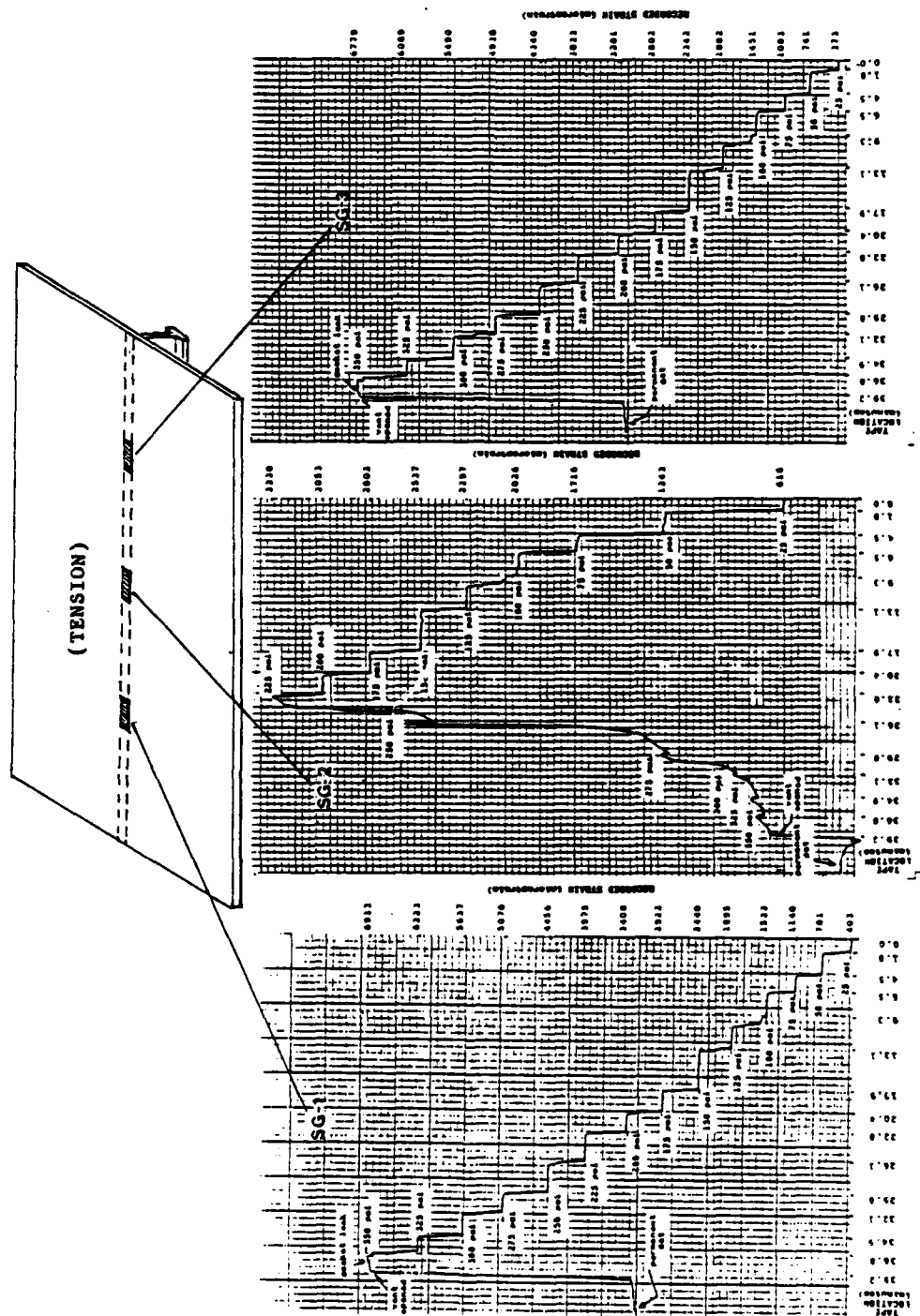
Figure 4.15   Strain History Recorded Longitudinally
Across Centerline of Plate Back.

52
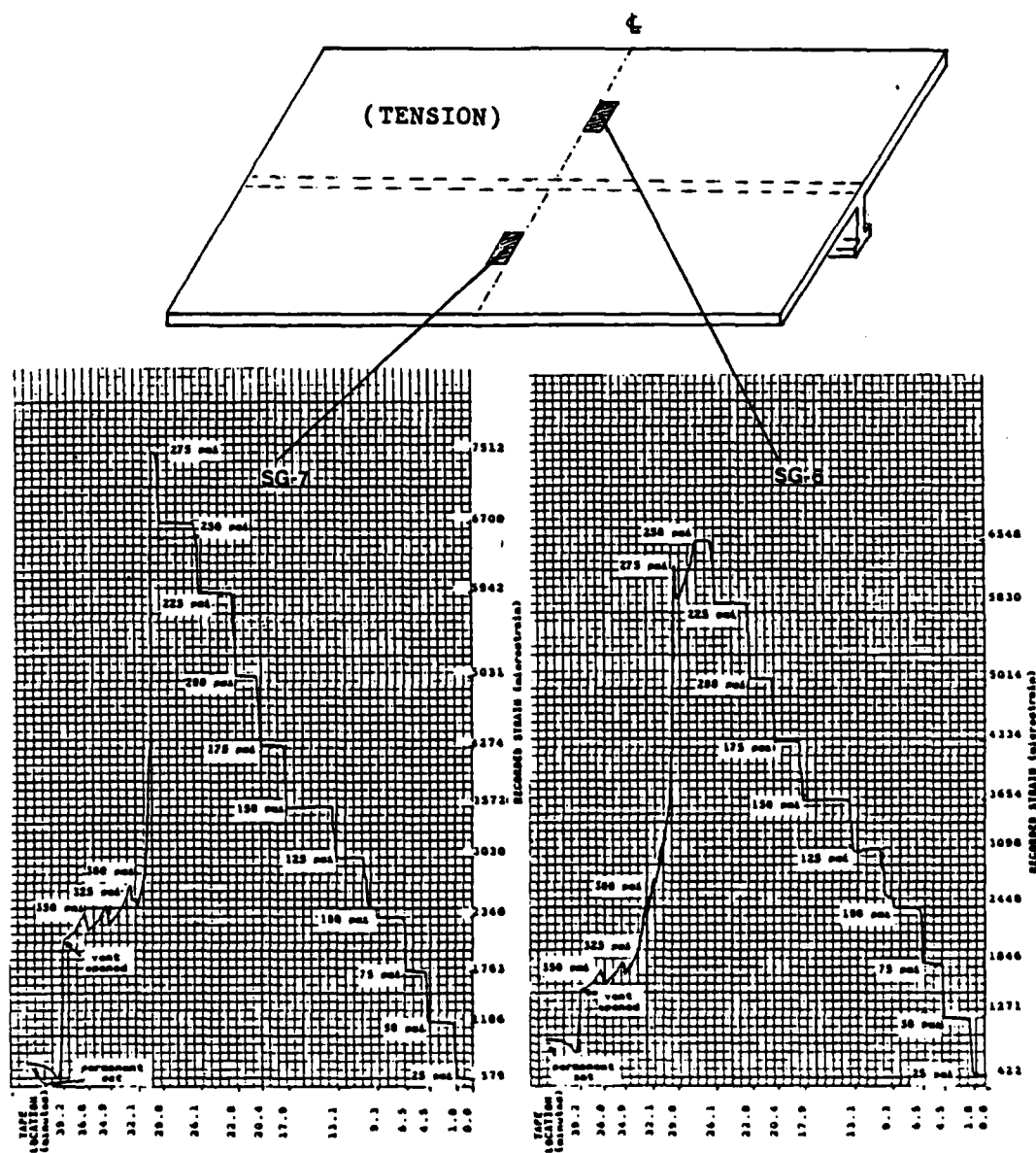
Figure 4.16   Strain History Recorded Across
Transverse Centerline of Plate Back.

53
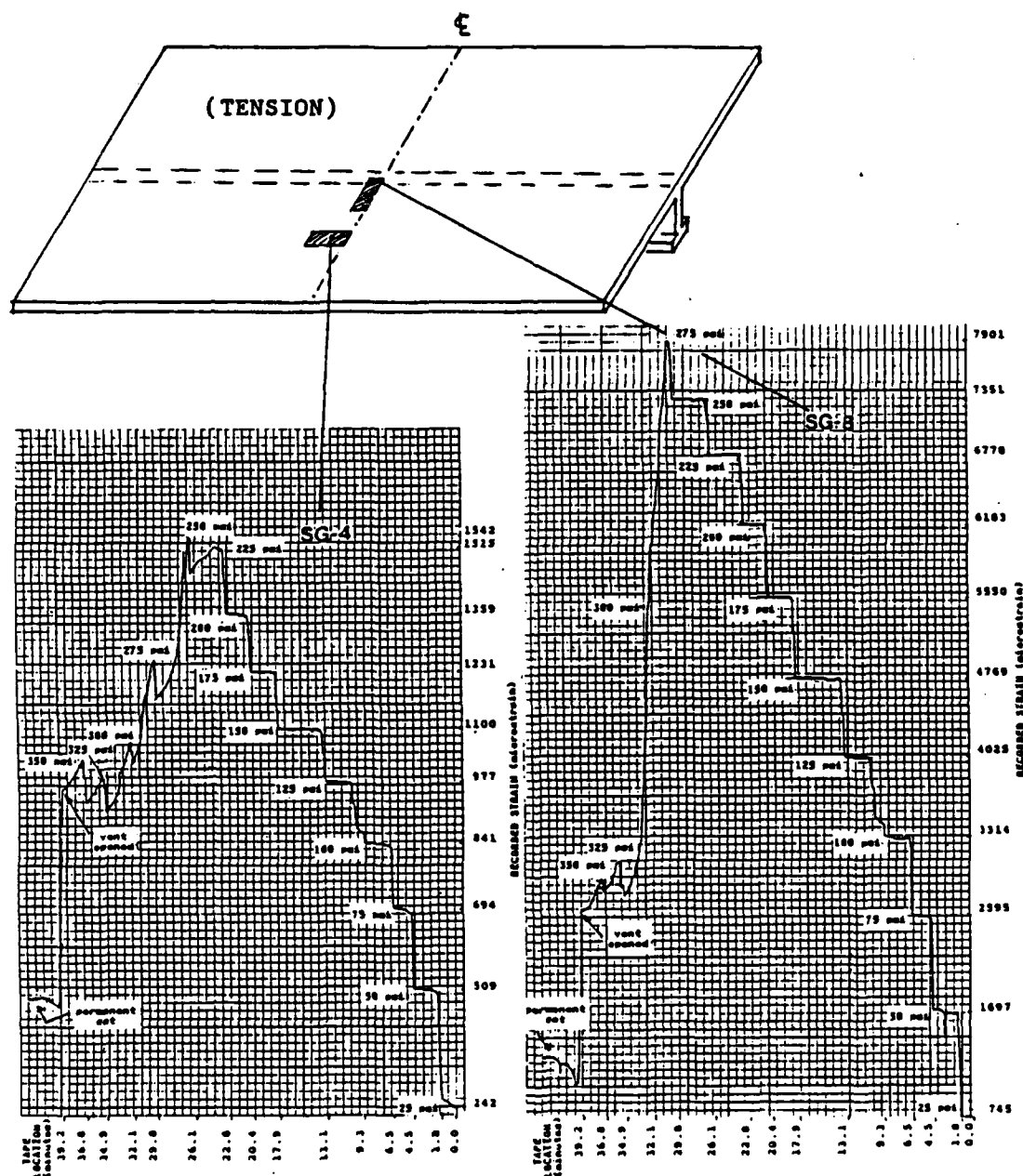
Figure 4.17   Strain History Recorded on Lower Half of
Transverse Centerline of Plate Back.

54
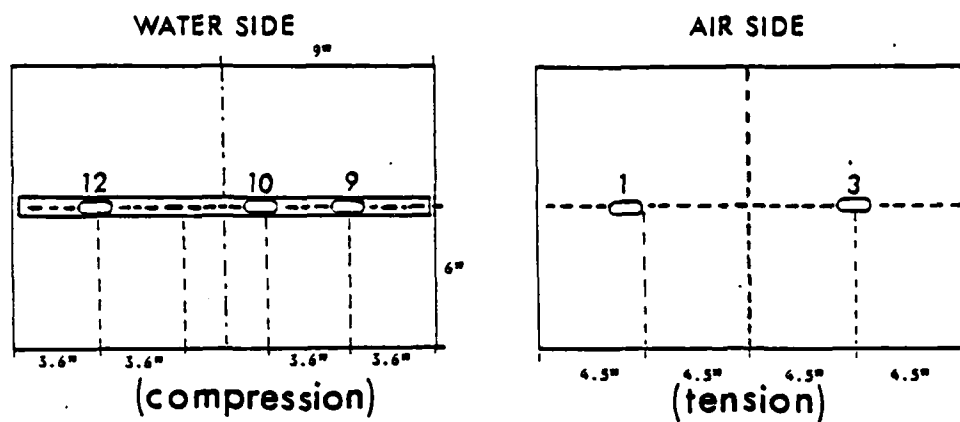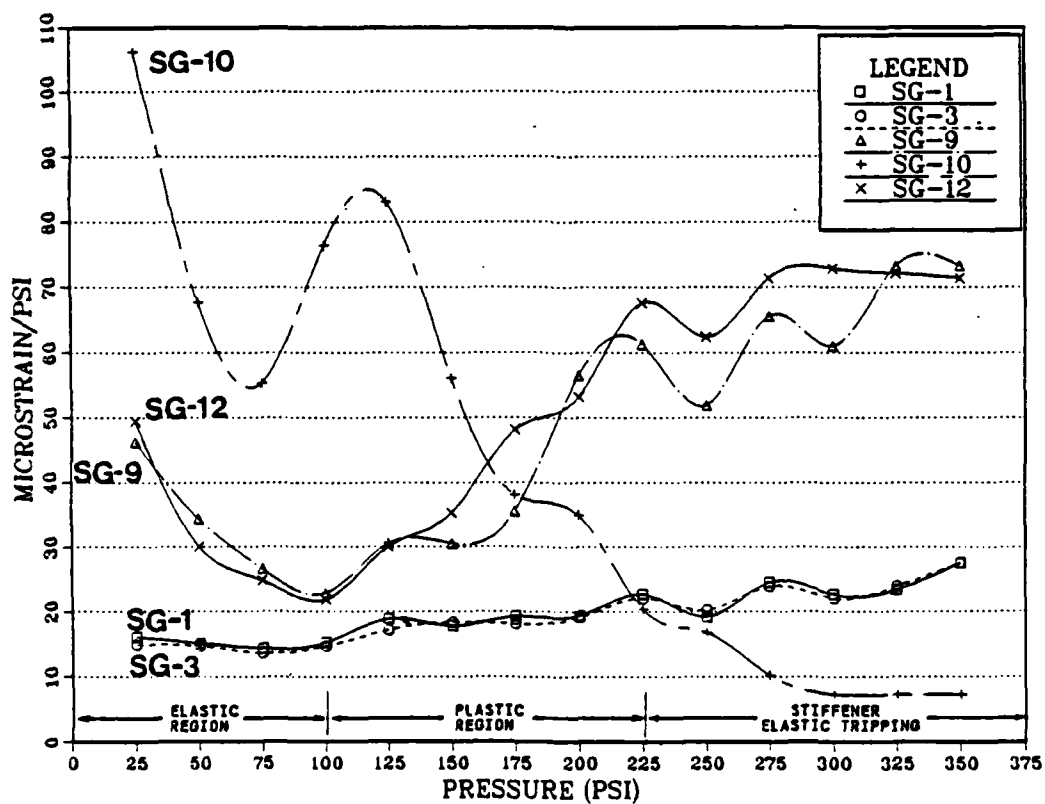
Figure 4.18   Plot of Static Strain Normalized to Pressure.

As the chamber was pulled from the water immediately
after the shot (Figures 4.21 and 4.22) it was readily
obvious that over three-quarters of the test plate surface
area was blown free from the rest of the test panel. Upon
closer inspection (Figure 4.23) it was discovered that the
missing section had been cleanly torn along the boundaries
of the test panel and was lying in the bottom of the air-
back chamber (Figure 4.24). As can be seen in Figure 4.25,
the stiffener exhibited an anti-symmetric displacement
configuration (i.e., the stiffener remains vertical) as
described in [Ref. 8: p.361]. This type of deformation is
the initial stage of inelastic tripping before collapse of
the stiffener. The web had begun to buckle at the point of
attachment to the flange in three separate areas spaced
symmetrically along the length of the stiffener: the center
and four inches on either side as shown in Figure 4.25 .
The stiffener, though it had not rotated out of the vertical
plane, was showing indications of doing so and collapsing to
the left side of the plate. The center-most position of the
plate (node 16,13) retained a permanent vertical deflection
of approximately 1.30 inches, a deflection of seven plate
thicknesses. Even at this extreme amount of deformation
there was not a total collapse of the stiffener.

The strain histories were expected to follow the same
symmetry and trends experienced in the static test, even
though now the applied pressure was 3780 psi (Figure 4.26)
and was generated by a shock wave which peaked 17.3 microse-
conds after arrival at the ten foot standoff radius.

The recorded peak strain values and arrival times are
listed in Table IV and associated strain histories are shown
in Figures 4.27 through 4.38 . Each strain gage history had
been transferred from the high speed tape to disk storage on
the HP-5451C Fourier Analyzer, where individual records were
reviewed and out-putted graphically. Typically, one gage
strain history would cover fourteen records (approximately

56

4.48 milliseconds). Note that the voltage values on the vertical axis were multiplied by each strain gage's calibration factor to obtain the peak strain values which are annotated on each strain gage history. The strain gage histories are also marked at the time of arrival of the wave front and the "individual record" containing the peak value (top plot) was annotated on the extended strain histories of each strain gage (bottom plot). Each "individual record" is 320 microseconds in length.

A characteristic of every strain history was an eventual peak strain drop-off to a negative value. This represented the plate detaching from the water (due to cavitation at the plate surface) allowing the plate to come to rest until it was reloaded microseconds later by an on rush of water from the explosion [Ref. 13: p. 84-91]. A summary of strain gage shockwave arrival times, peak times before reloading (multiple peaks in many cases), times to cavitation (i.e., last peak time less the arrival time), and reload times is provided in Table V . Note that reload times for all strain histories in the center of the plate and across the stiffener (SG-1, 2, 3, 8, 9, and 12) were consistent at approximately 3.44 to 3.49 microseconds. Additionally, the time period prior to the onset of surface cavitation was also uniform in the plate center (SG-1, 2, 3, and 8) at 540 to 590 microseconds.

A comparison of observed symmetry and trends was made in Figures 4.39, 4.40, 4.41, and 4.42 . Initially after making a general overview of all the strain histories, it became evident that the upper left end of the plate (Figure 4.25) was exposed to the shock wave earliest and experienced the highest strain values. The shock wave arrival time for the left side gages SG-4 and SG-7 was 2.5 msec., while the arrival time for the stiffener gages SG-9, 10, and 12 was 2.56 msec and for the gages on the opposite side of the plate it was even later. This information suggests that the

57

test panel and air-back chamber were not parallel relative to the shock front but slightly canted to oneside. The angle of incline to one side was approximated by assuming that the shock wave was planar and, from the data, the wave front reached the stiffener gage SG-10 and the plate gages SG-4 and SG-7 at about the same time (i.e., 2.5 msec). Then, using the geometry of Figure 4.43, the angle of inclination was calculated as 22 degrees. This indicates that the left side of the plate was about 4.5 inches higher than the right, which is why all other plate strain gage arrival times were approximately 2.8 msec. (i.e., 0.3 milliseconds later). This confirmed the belief that the cabling and junction box mounted to the side of the air-back chamber could possibly tilt the chamber once it was lowered into the water and only supported by the pneumatic fenders. For later undex tests, this situation can be avoided by mounting the junction box directly beneath the test chamber.

The plate rectangular geometry additionally dictated that all longitudinally measured strains would be less than those measured transversely across the width of the plate in the same positions. This proved to be the case in the undex test (as well as the static test) where the peak values of strains for SG-6, 7, and 8 (measured 90 degrees from the longitudinal gages SG-2, 4, and 5) were higher. As expected, except for the region of the plate affected by the chamber tilt, all arrival times measured on the plate were later than those for the stiffener. Additionally, it can be seen that the general shapes of the recorded strain histories in regions which are symmetrically equal are very similar (specifically Figure 4.40 (SG-1 and SG-3), Figure 4.41 (SG-6 and SG-8), and Figure 4.42 (SG-9 and SG-12)). As far as determining the correlation between strain histories and the physical deformation of the stiffener, it can only be speculative. For illustrative purposes Figure 4.42 containing SG-9, SG-10, and SG-12 strain histories will be

58

used. Again in comparison to static test trends, it would be expected that the strain values experienced at SG-10 would never get quite as large as elsewhere on the stiffener, but build up, unload, and build up again as the stiffener experiences its progressive deformations. Undoubtedly, the three areas of stiffener deformation shown in Figure 4.25 occurred progressively starting with the region initially of highest compressive stress (the center of the plate) and then progressed to the next highest, probably the SG-9 portion of the stiffener, and lastly SG-12. This sequence seems to follow especially well the strain history undulations depicted in the curves for SG-9 and SG-12, and somewhat for all the other strain histories.

As can be seen, the underwater explosion shock test strain histories clearly depict the interaction between the shockwave front and the test panel in arrival times, reload times, and peak strain values.

C. GEOMETRY AND MATERIAL CONSIDERATIONS

The results of the underwater shock test are unique for the specific test panel geometry and material used. To put this "uniqueness" in the correct perspective, a discussion of the impulsive load effects on geometry and materials follows.

The deformation of the test panel is more than just a property of the material, it also depends on the geometry of the test panel and the process used to deform it. It has been found [Ref. 13: p. 91] that dynamic yielding occurs only at pressures 3 to 10 times the static yield value. This is due to the fact that materials which undergo a transition from ductile to brittle behavior at lowered temperatures will generally undergo a similar transition when the loading has changed from static to dynamic.

59
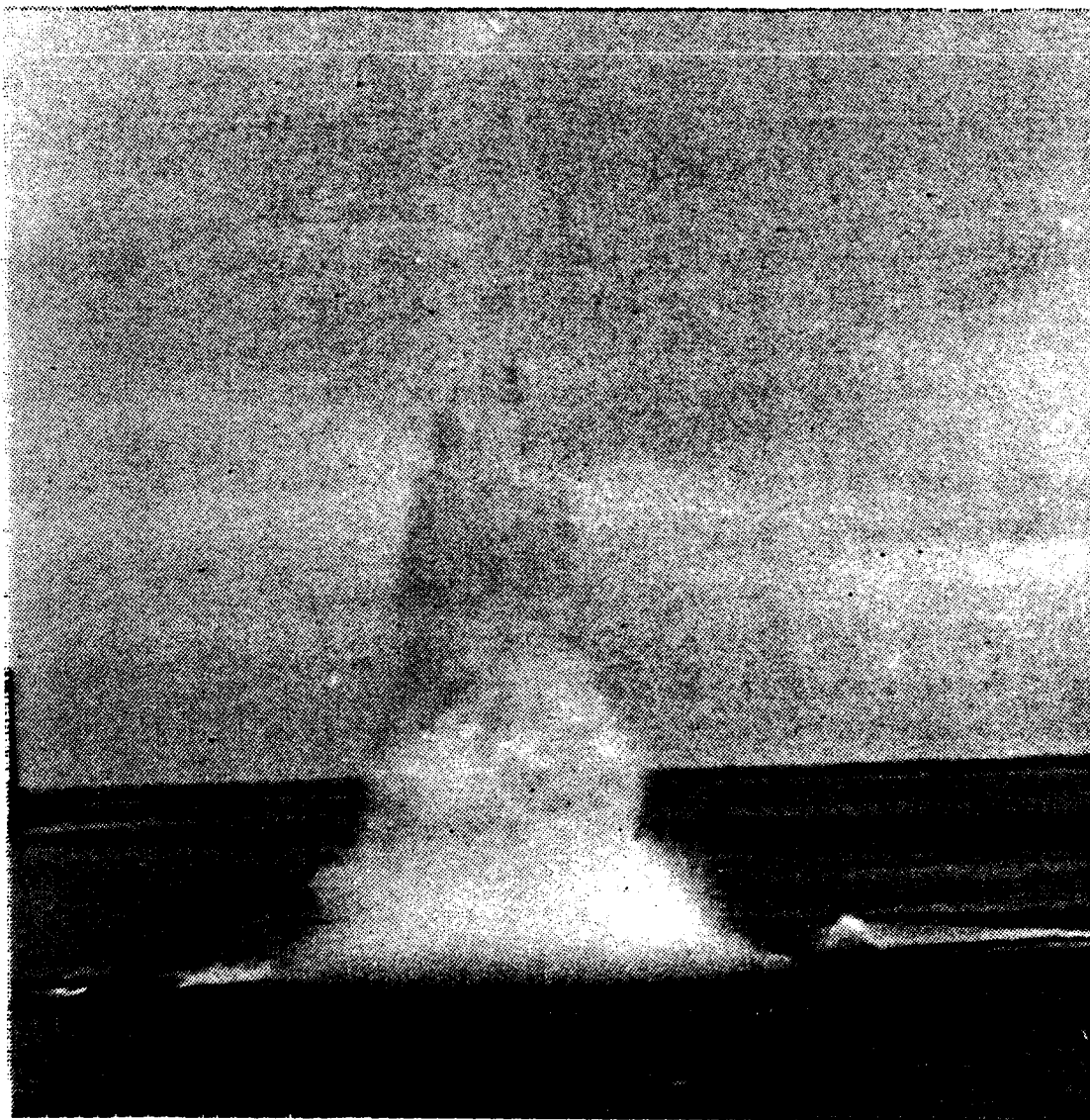
Figure 4.19   Eight-pound Charge Explosion Dome and
Initial Venting.
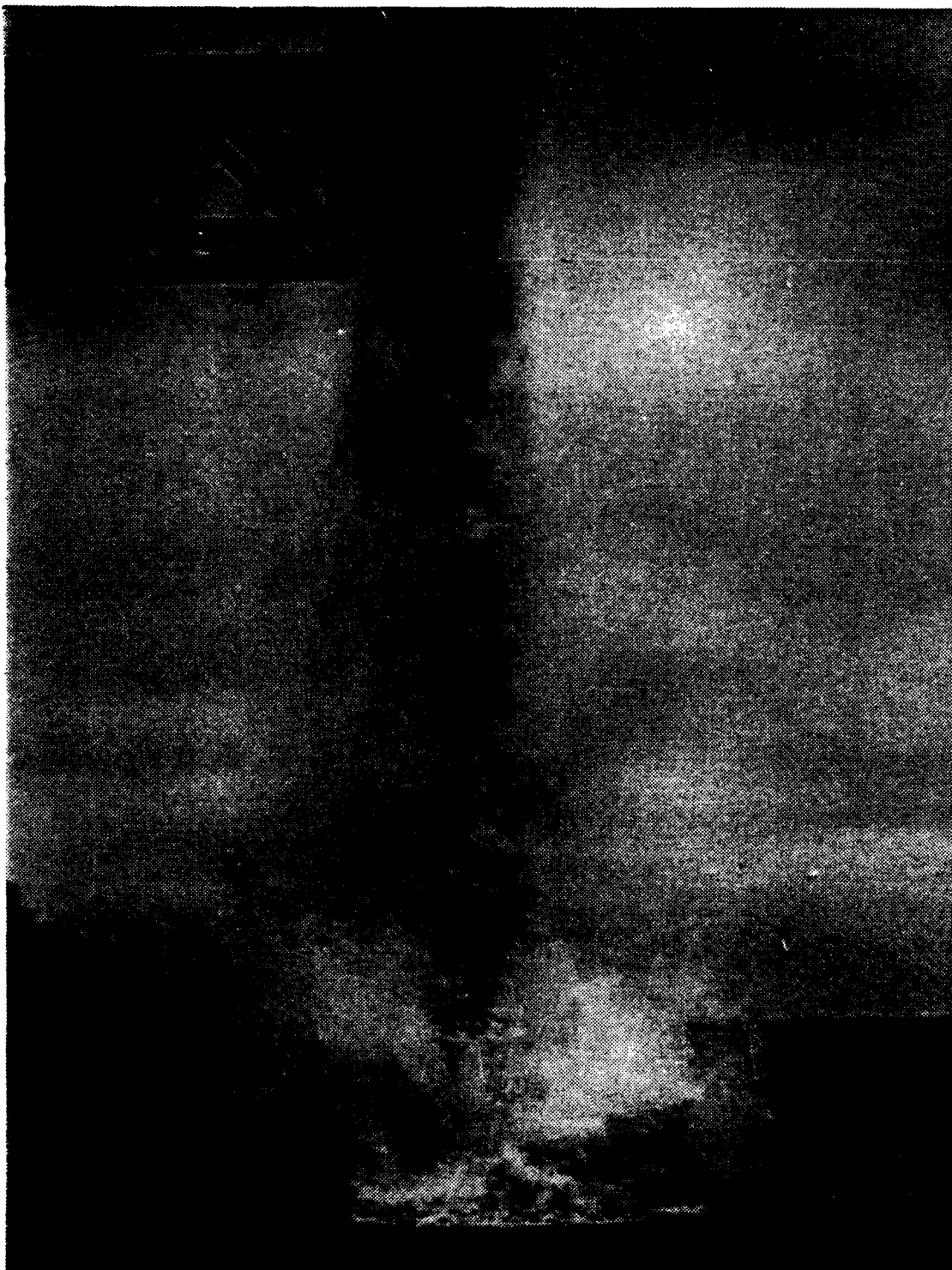
Figure 4.20   Eight-pound Charge Explosion Plume.

TABLE IV

SUMMARY OF PEAK STRAIN VALUES AND SHOCK
WAVE ARRIVAL TIME DATA

SENSOR	ARRIVAL TIME (milliseconds)	RECORDED PEAK (microstrain)
SG-1	2.85	20.2 k
SG-2	2.82	30.0 k
SG-3	2.88	44.0 k
SG-4	2.50	17.0 k
SG-5	2.76	23.0 k
SG-6	2.82	25.2 k
SG-7	2.50	40.0 k
SG-8	2.88	35.0 k
SG-9	2.56	36.0 k
SG-10	2.56	16.0 k
SG-11	----------FAILED-------------	
SG-12	2.56	36.0 k
P-XDCR-1	2.42	3780 psi
P-XDCR-2	2.40	3500 psi

TABLE V

SUMMARY OF SHOCK WAVE ARRIVAL TIMES, PEAK TIMES, TIME TO CAVITATION, AND RELOAD TIMES

SENSOR	ARRIVAL TIME (milliseconds)	*PEAK TIMES (milliseconds)	ELAPSED TIME PRIOR TO CAVITATION (microseconds)	RELOAD TIME (milliseconds)
SG-1	2.85	<u>3.35</u>/3.39/3.41	560	3.45
SG-2	2.82	3.30/3.31/3.39/<u>3.41</u>	590	3.44
SG-3	2.88	<u>3.39</u>/3.42	540	3.44
SG-4	2.50	2.64/<u>2.74</u>	240	2.75
SG-5	2.76	<u>3.08</u>	320	3.09
SG-6	2.82	<u>3.09</u>/3.13	310	3.16
SG-7	2.55	<u>2.67</u>	120	>2.70
SG-8	2.88	3.32/3.40/<u>3.44</u>/3.46	580	3.49
SG-9	2.56	2.65/<u>2.85</u>/2.97/3.05/<u>3.27</u>	710	3.49
SG-10	2.56	2.77/<u>2.92</u>/3.11	550	>3.18
SG-11	---------------FAILED---------------			
SG-12	2.56	2.68/<u>2.75</u>/2.91/3.07/<u>3.39</u>	830	3.49

*UNDERLINED PEAK TIME INDICATES TIME OF MAXIMUM STRAIN VALUE.

63
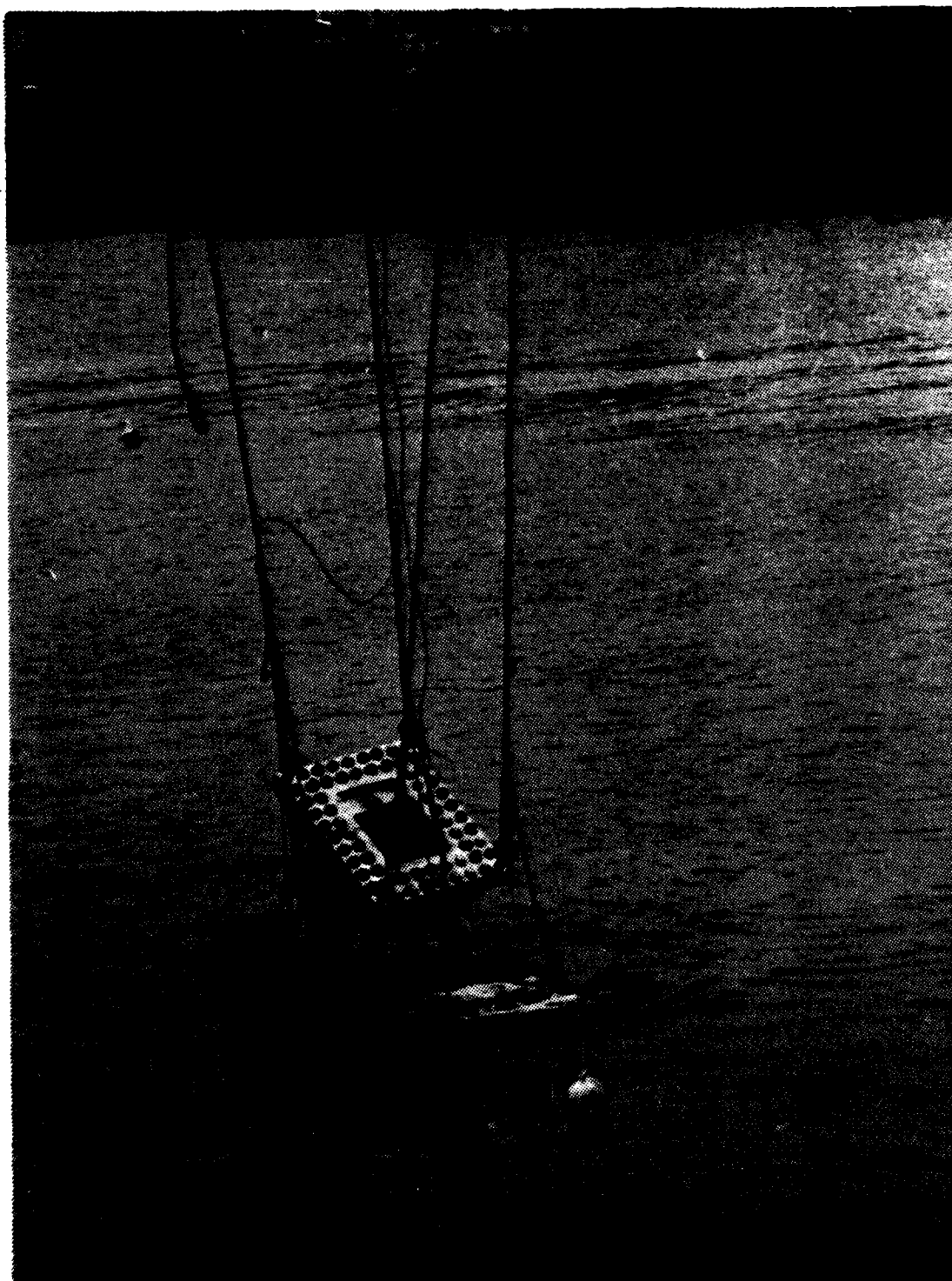
Figure 4.21   Raising Test Chamber Immediately After
Eight-pound Charge Detonation.
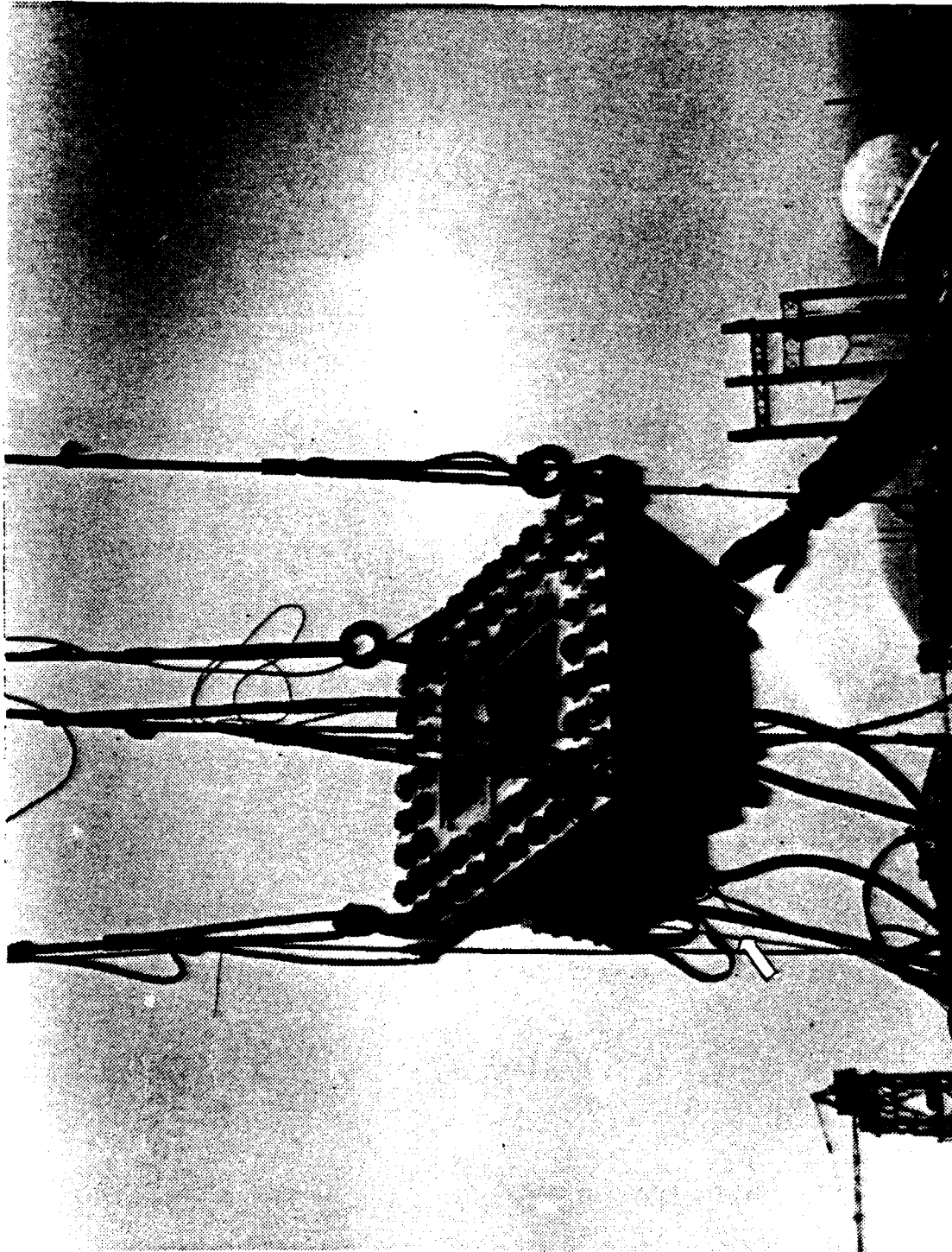
Figure 4.22   View Showing Test Chamber Cabling
Still Attached After Undex.

Figure 4.23   Top View of Test Panel After Undex.

66

Figure 4.24   Blown-out Plate Section Found Inside
of Test Chamber.
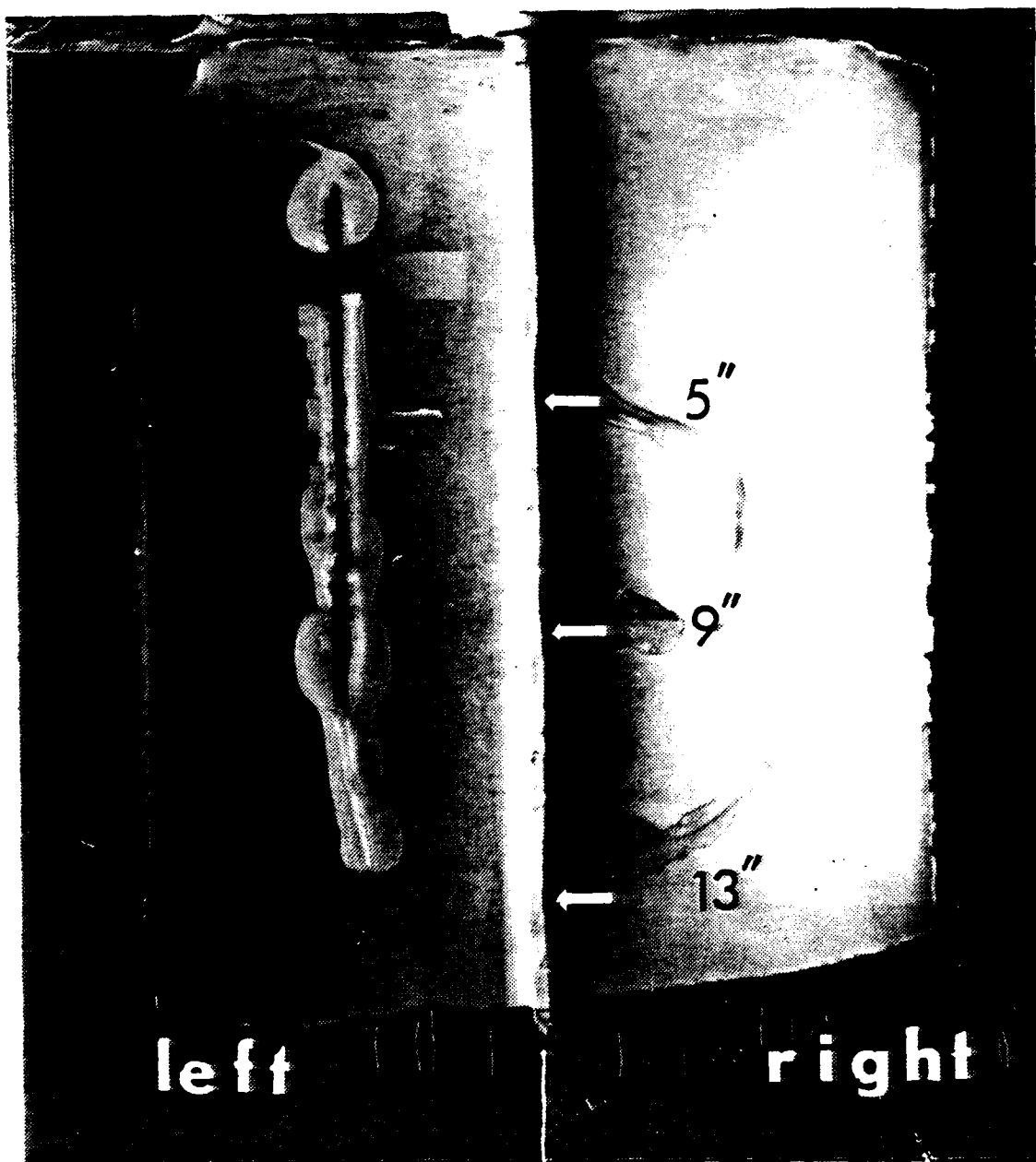
Figure 4.25   View of Plate Section Showing
Anti-symetrical Tripping.

68

this shock pressure history at a 10 foot standoff represents 640 microseconds and contains the pressure transducer peak pressure value and arrival time of the shock front

arrival time: 2.42 milliseconds

peak pressure: 3780 psi

this is the extended shock pressure history at a 10 foot standoff

arrival time: 2.42 milliseconds

peak pressure: 3780 psi

640 microseconds
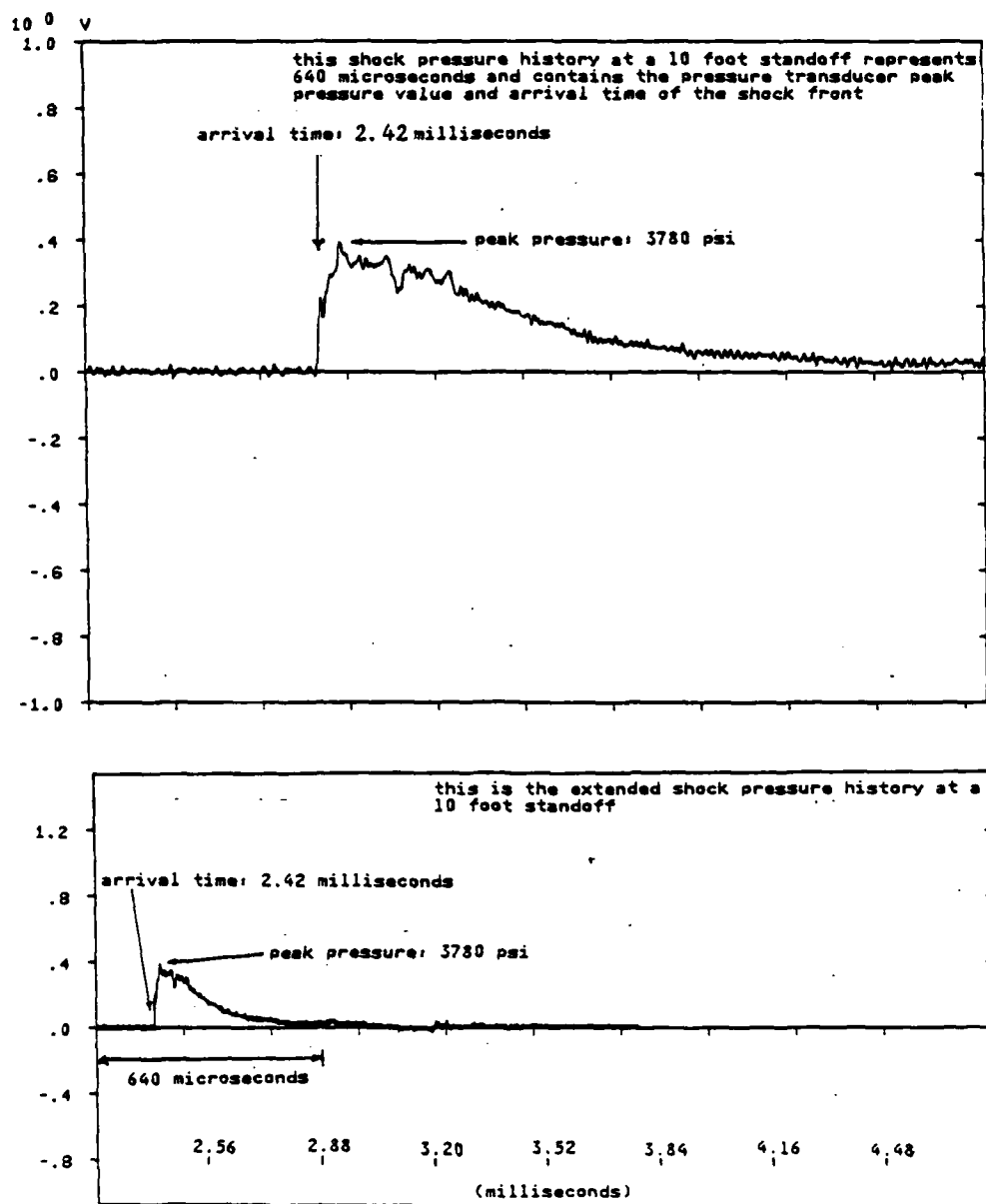
Figure 4.26   Free-Field Pressure and Arrival Time.

69

Figure 4.27   Strain Gage NO.1 Strain History.

70

Figure 4.28   Strain Gage NO. 2 Strain History.
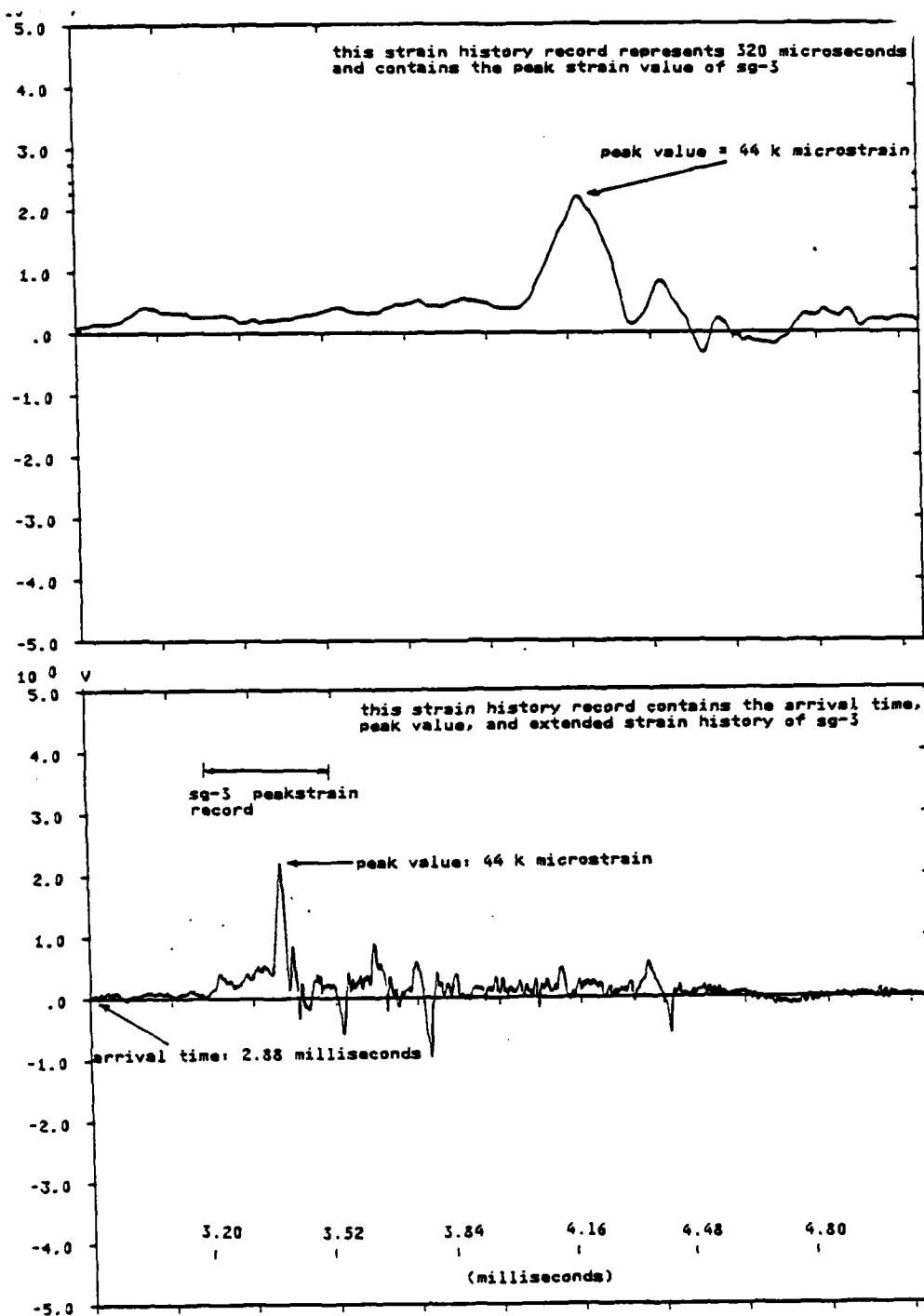
Figure 4.29   Strain Gage NO. 3 Strain History.
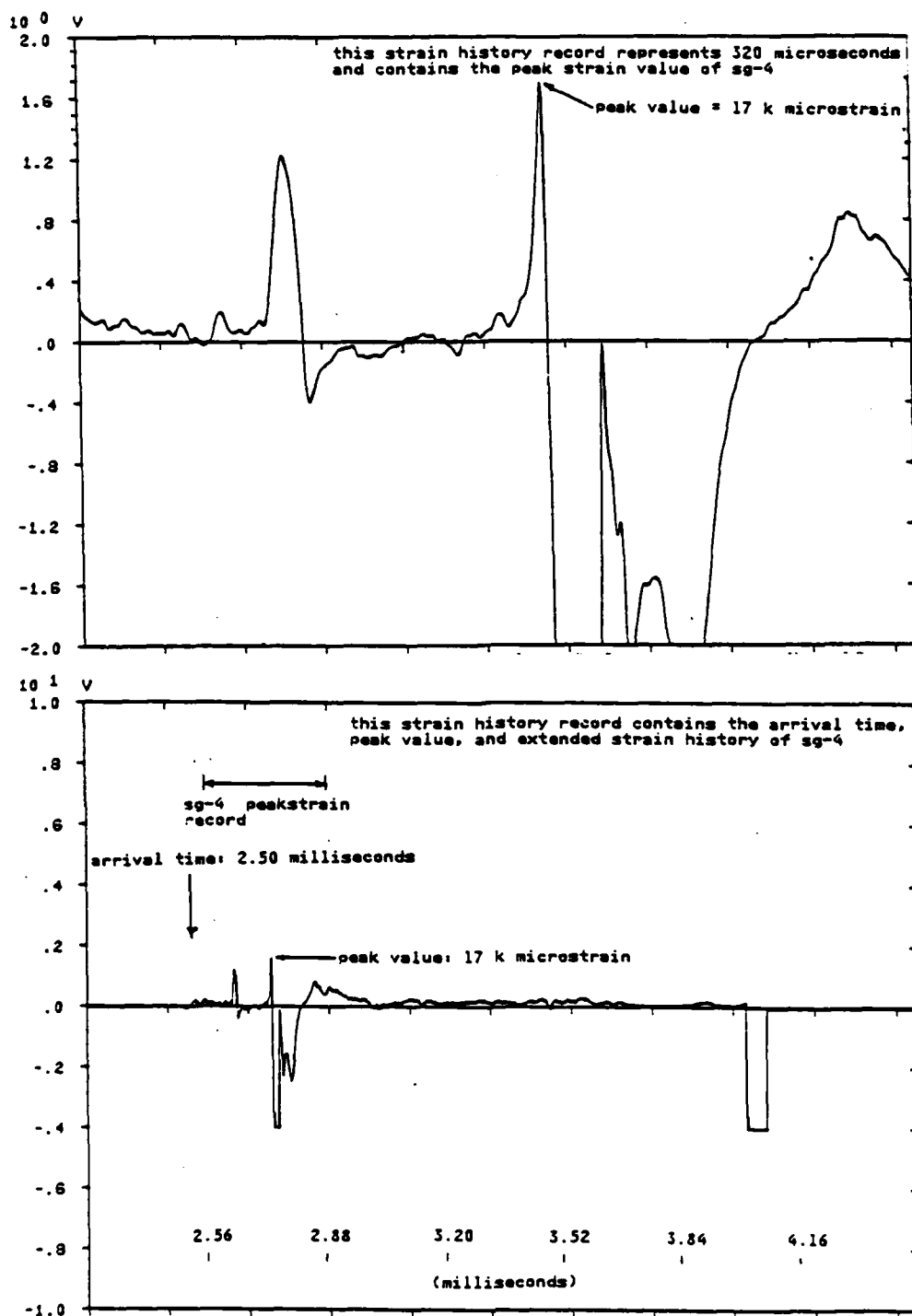
Figure 4.30   Strain Gage NO. 4 Strain History.

73
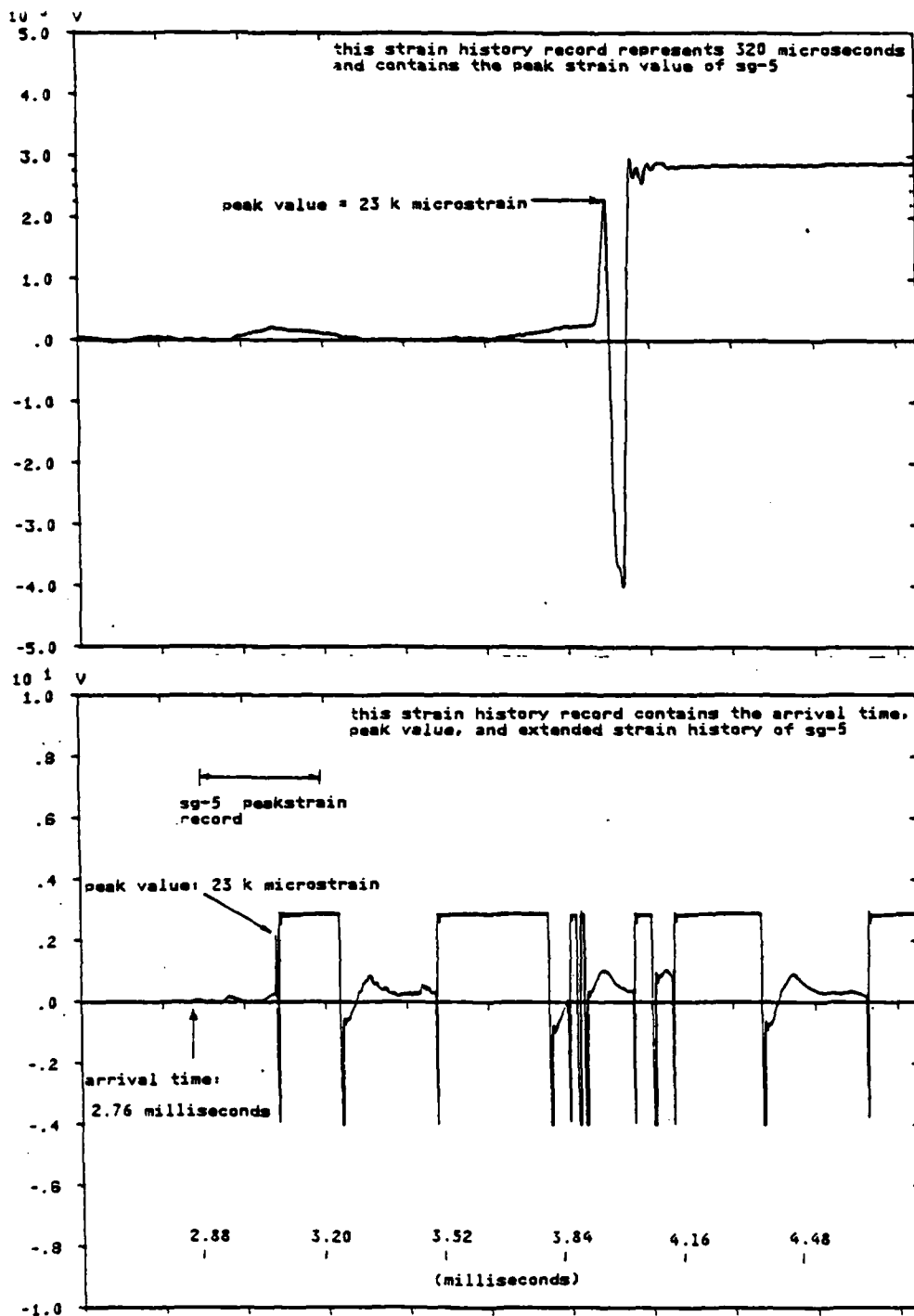
Figure 4.31   Strain Gage NO. 5 Strain History.

this strain history record represents 320 microseconds and contains the peak strain value of sg-6

peak value = 25.2 k microstrain

this strain history record contains the arrival time, peak value, and extended strain history of sg-6

peak value: 25.2 k microstrain

arrival time:
2.82 milliseconds

sg-6 peakstrain
record

2.88   3.20   3.52   3.84   4.16   4.48

(milliseconds)
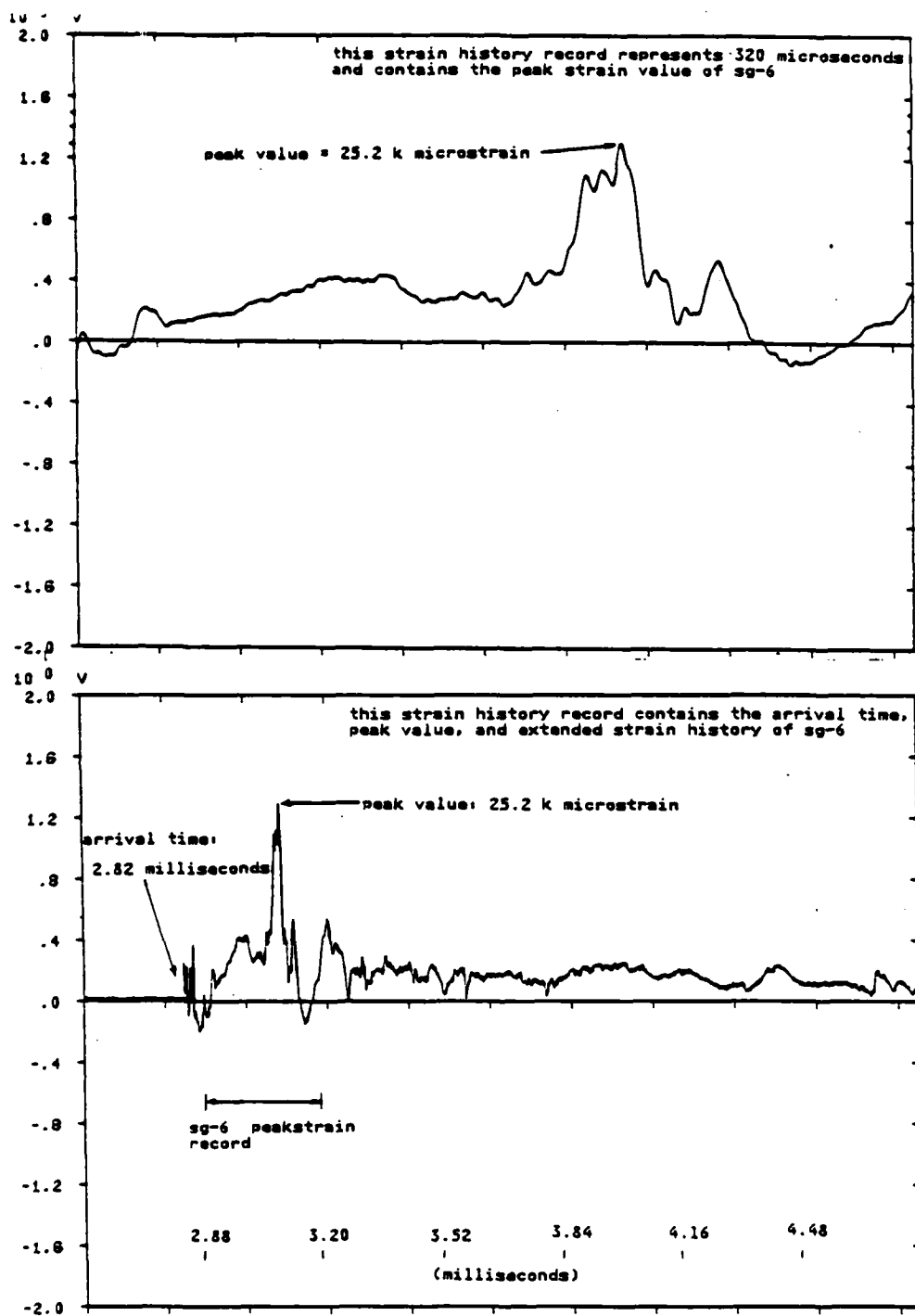
Figure 4.32   Strain Gage NO. 6 Strain History.
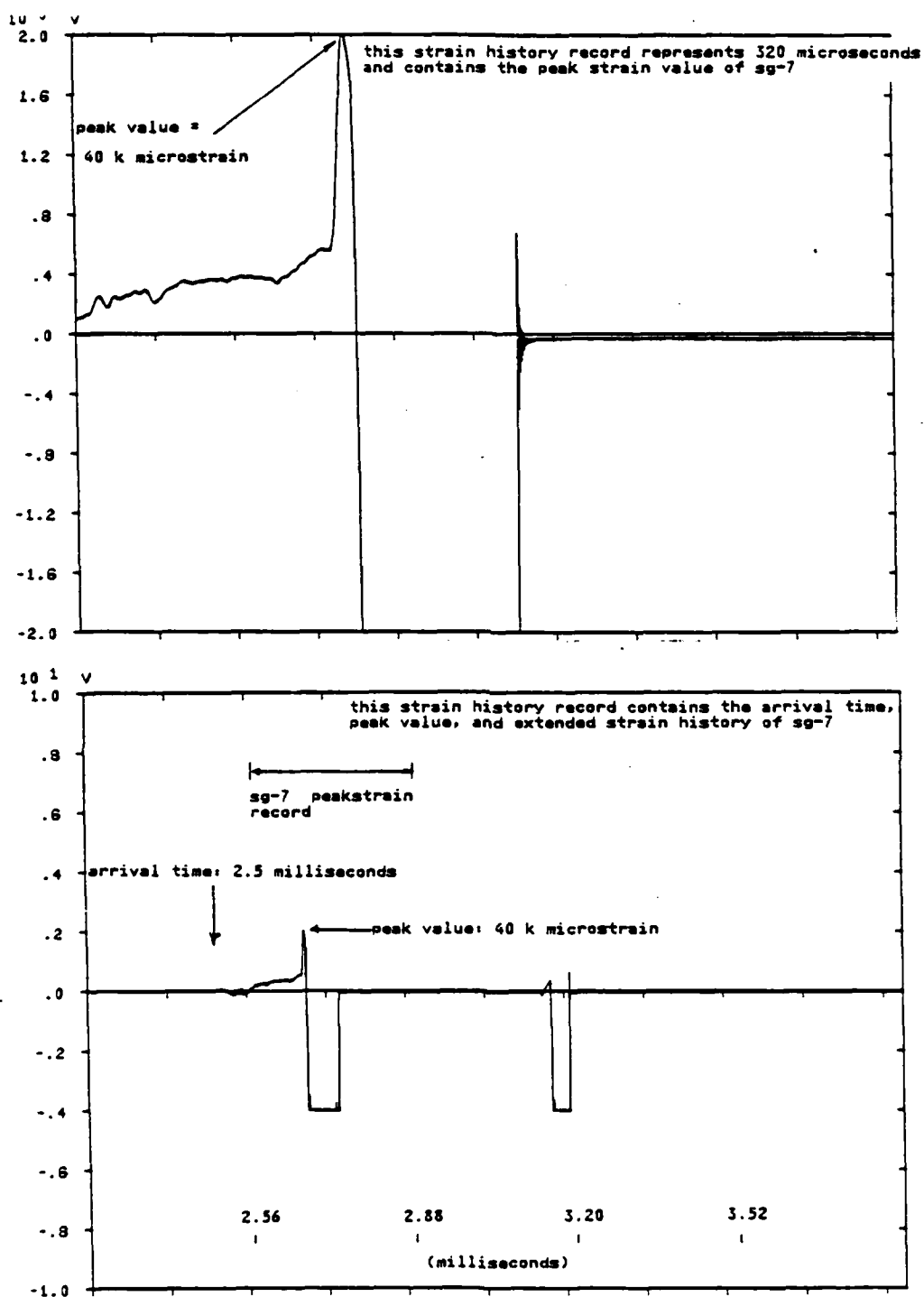
Figure 4.33   Strain Gage NO. 7 Strain History.
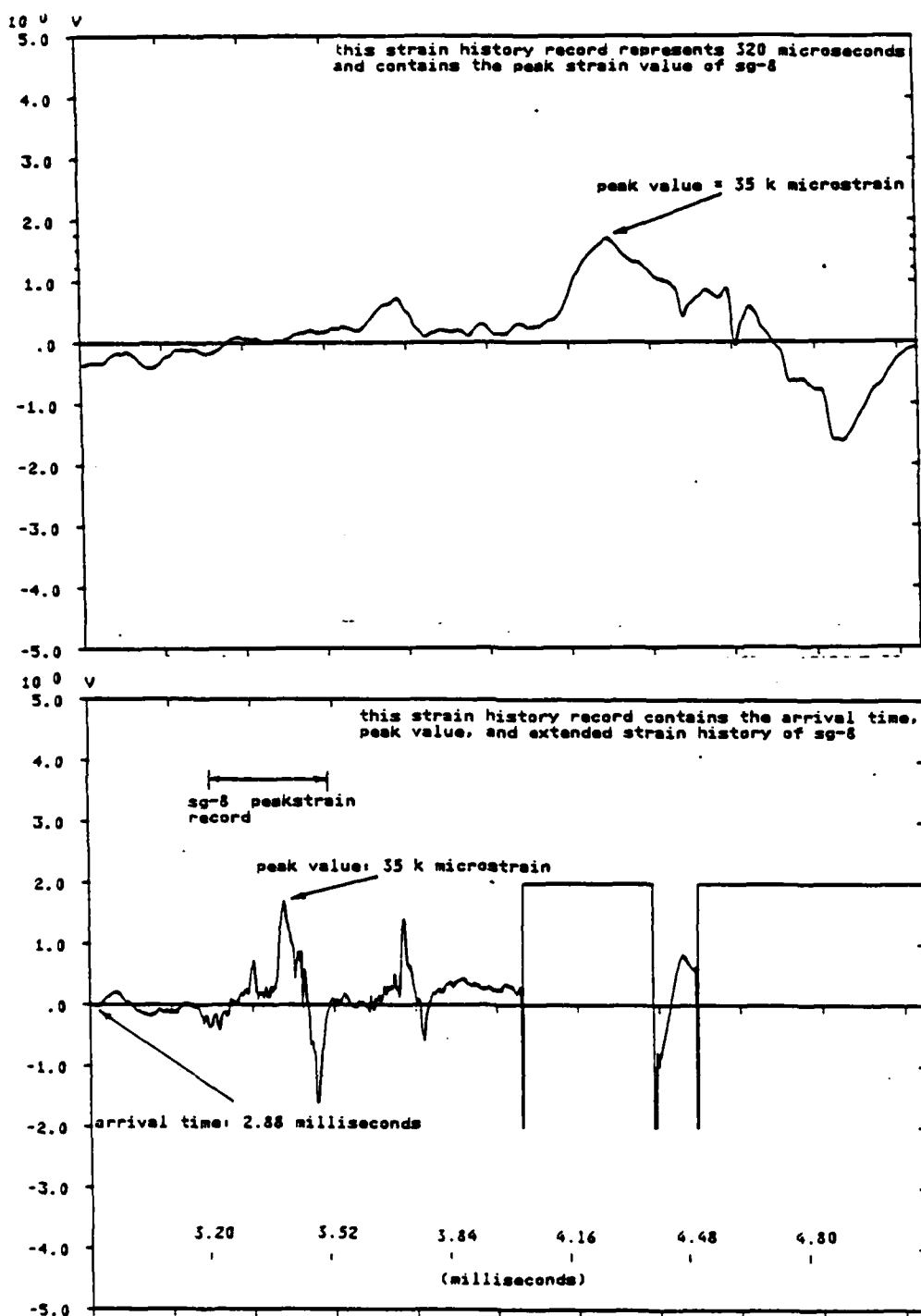
Figure 4.34   Strain Gage NO. 8 Strain History.

77

this strain history record represents 320 microseconds
and contains the peak strain value of sg-9

peak value = 36 k microstrain

this strain history record contains the arrival time,
peak value, and extended strain history of sg-9

sg-9 peakstrain
record

arrival time: 2.56 milliseconds

peak value: 36 k microstrain

2.56   2.88   3.20   3.52   3.84   4.16
(milliseconds)
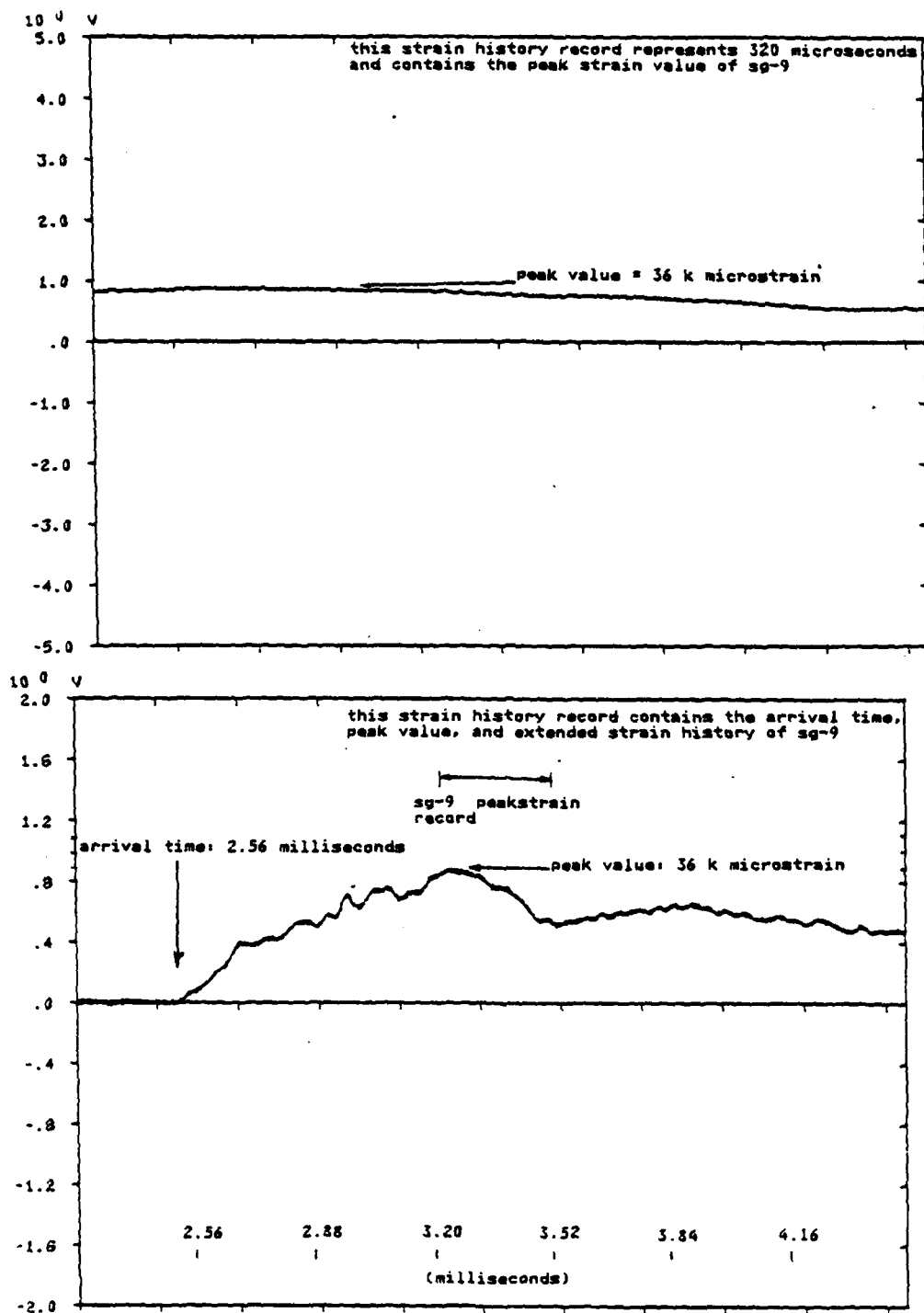
Figure 4.35   Strain Gage NO. 9 Strain History.

78
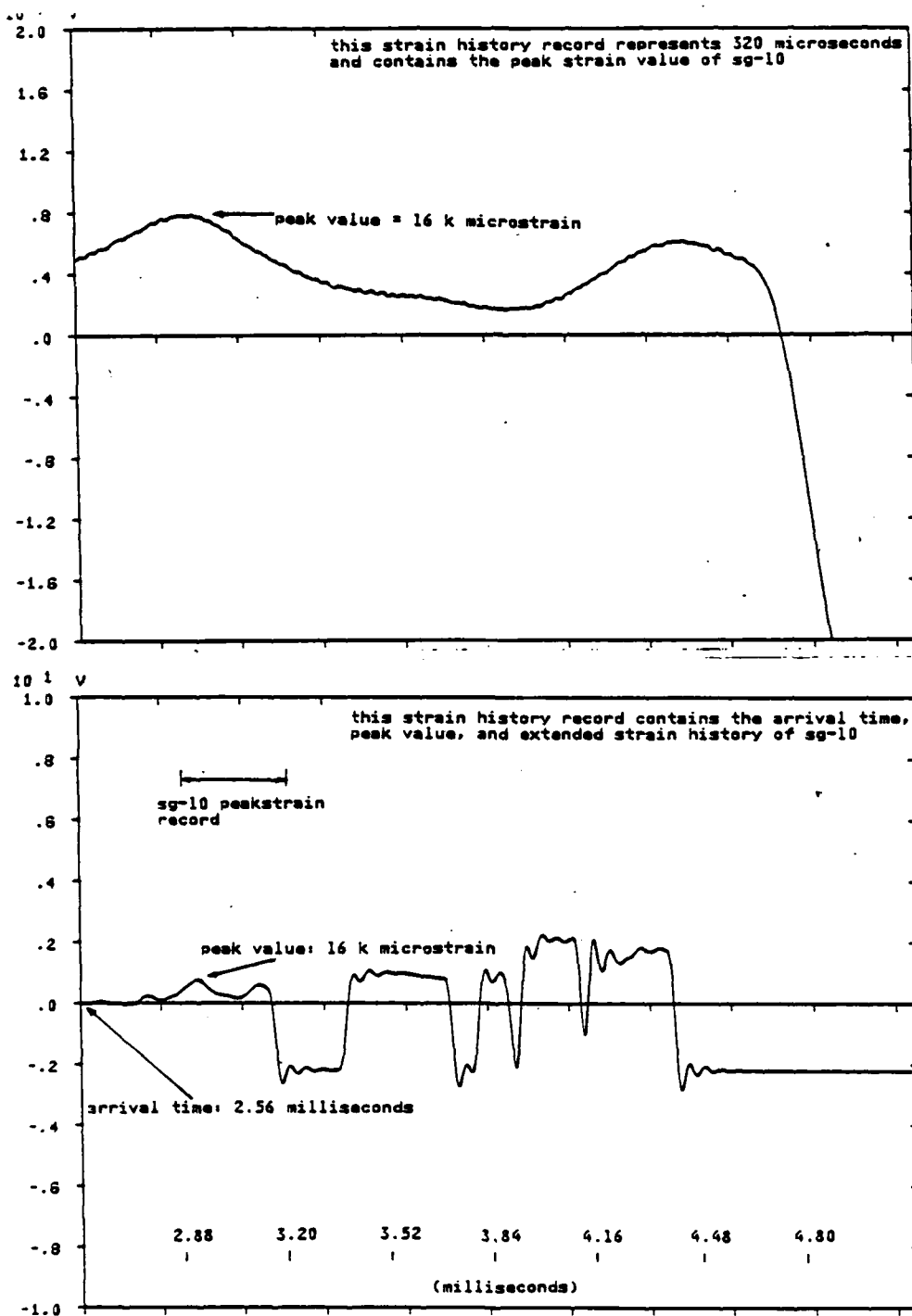
Figure 4.36   Strain Gage NO. 10 Strain History.

79

this strain history record represents 320 microseconds and contains the peak strain value of sg-11

peak value: (failed)

this strain history record contains the arrival time, peak value, and extended strain history of sg-11

sg-11 failed at 1.13 milliseconds

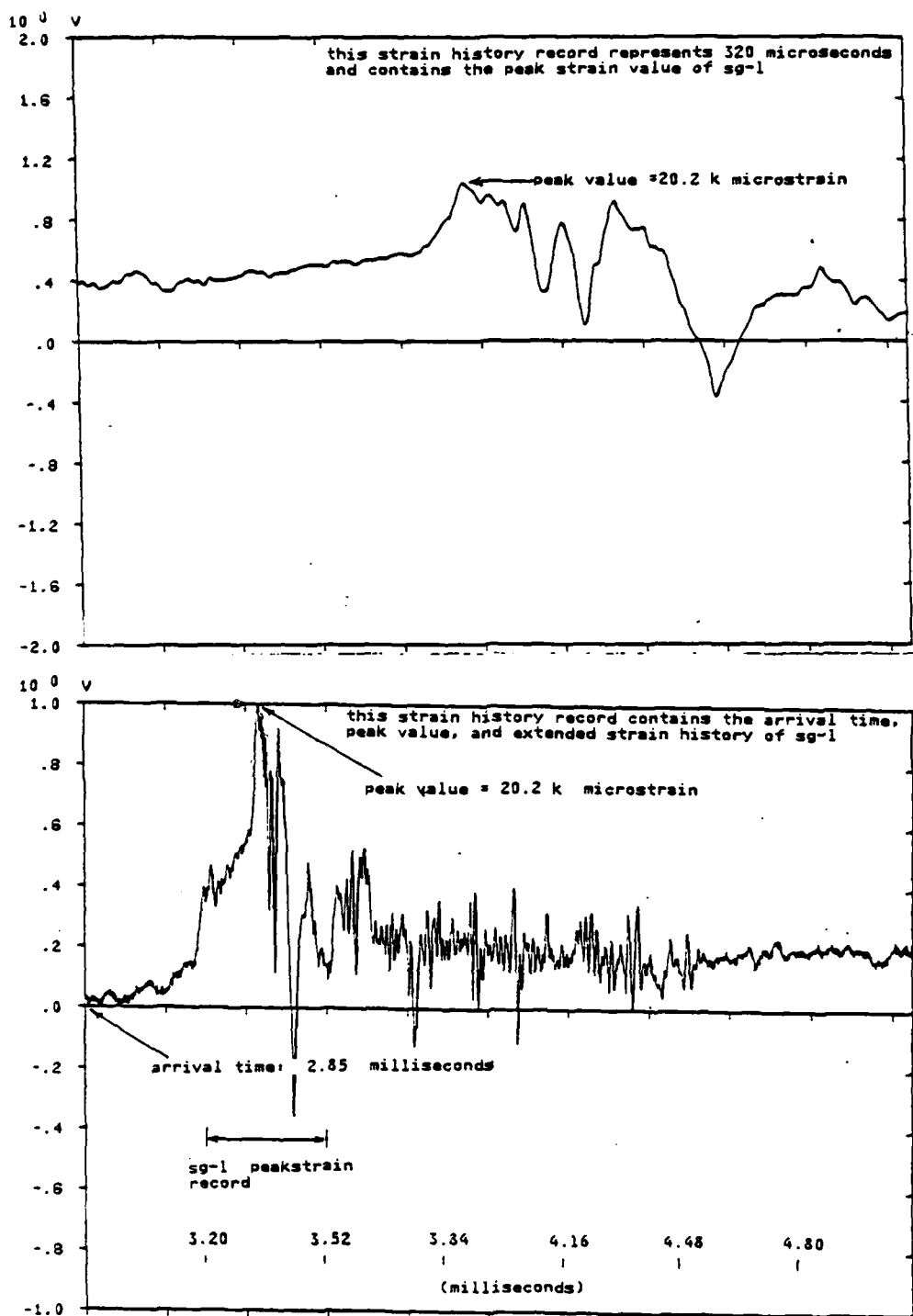sg-11 (failed)
record

0.64   0.96   1.28

(milliseconds)
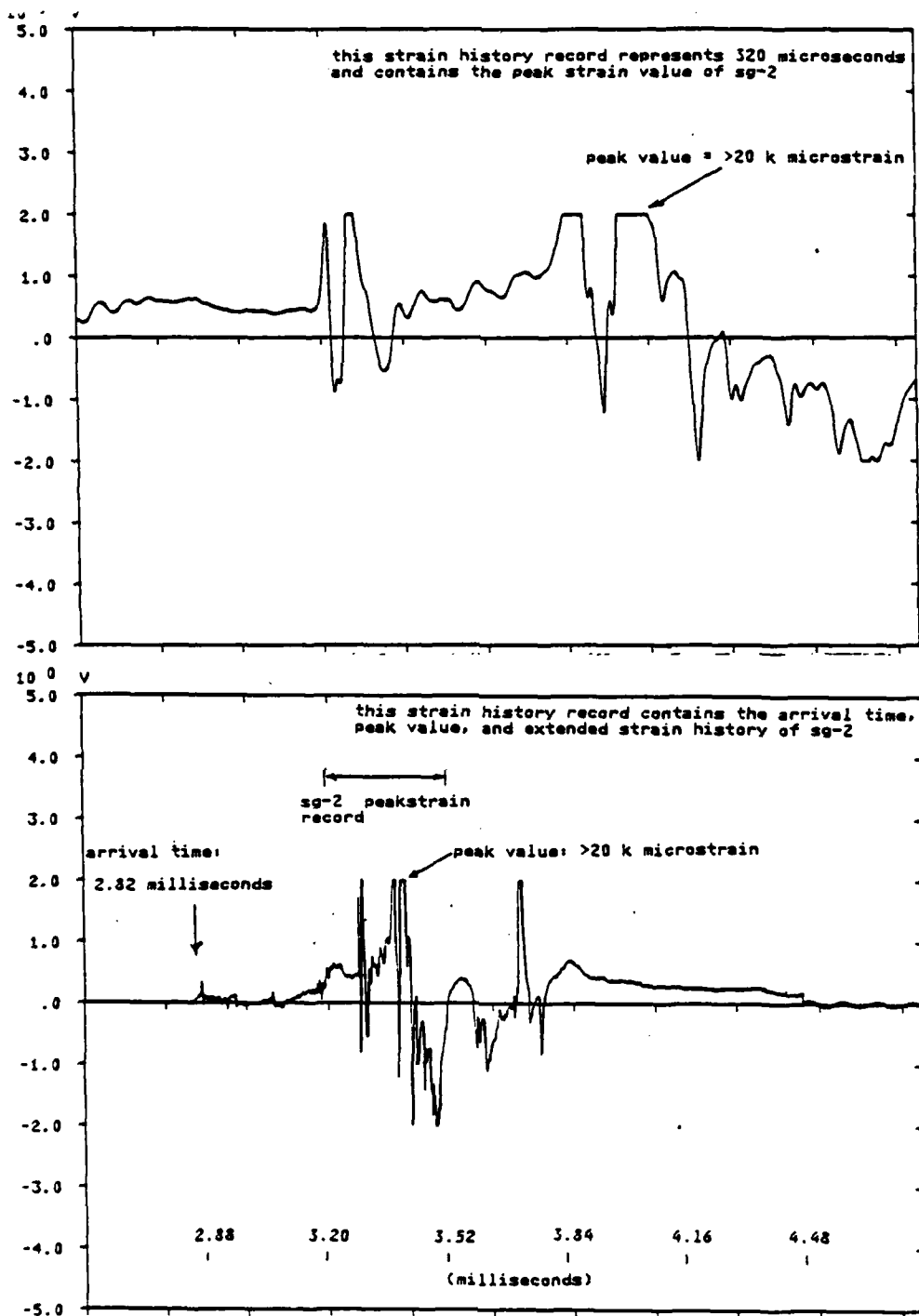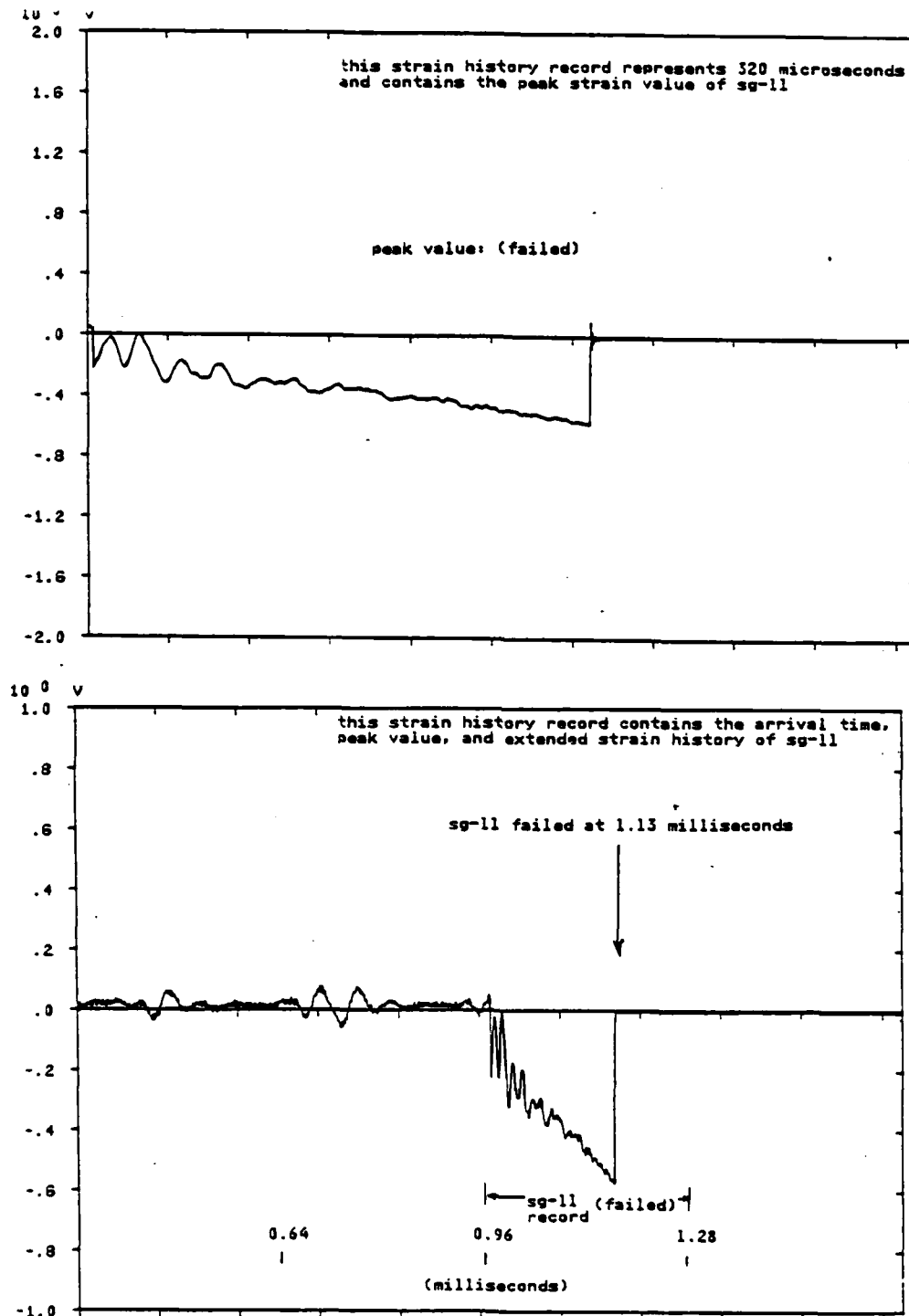
Figure 4.37   Strain Gage NO. 11 Strain History.

80
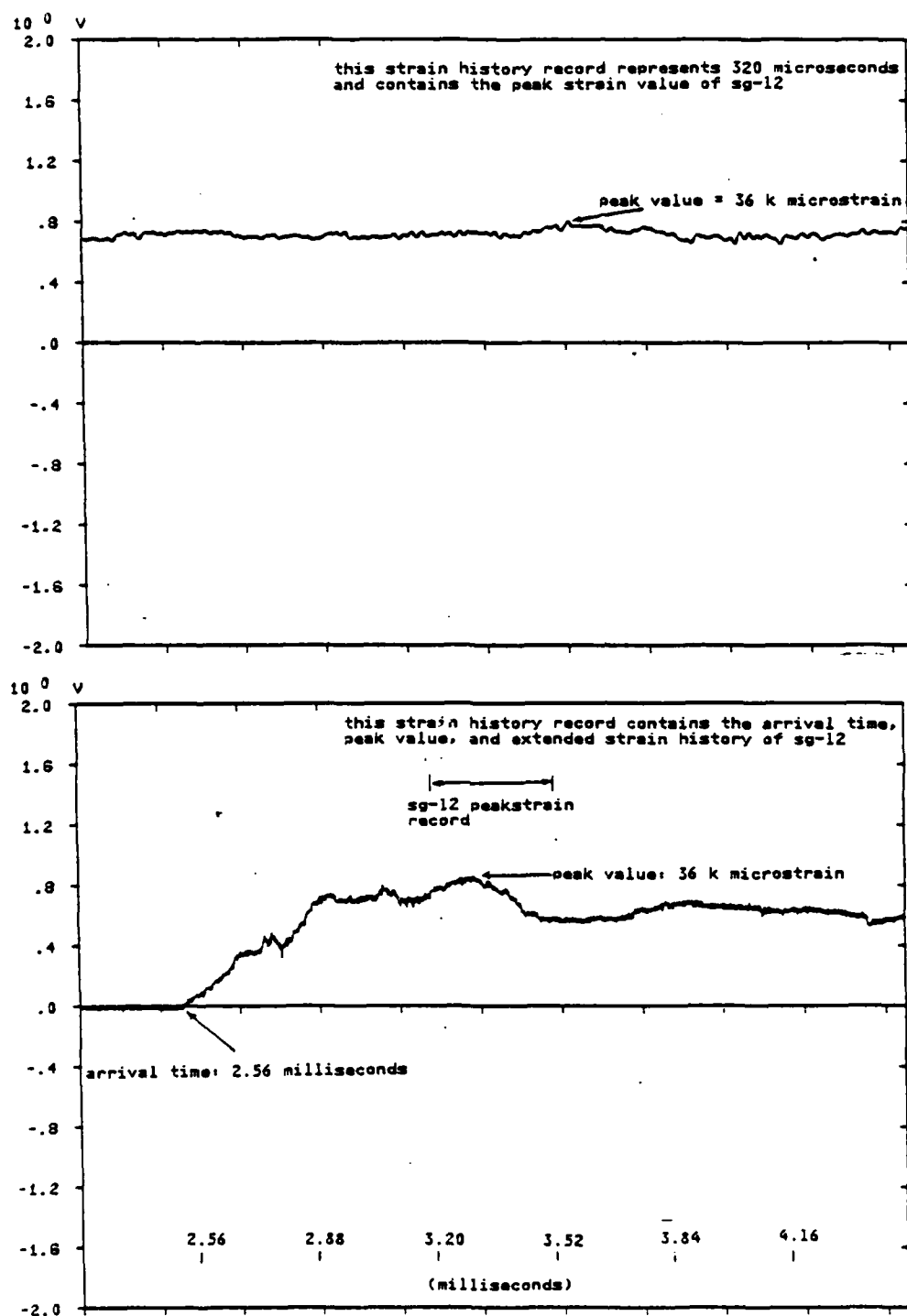
Figure 4.38   Strain Gage NO. 12 Strain History.

Figure 4.39   Strain History Recorded Longitudinally
Across Centerline of Plate Back.
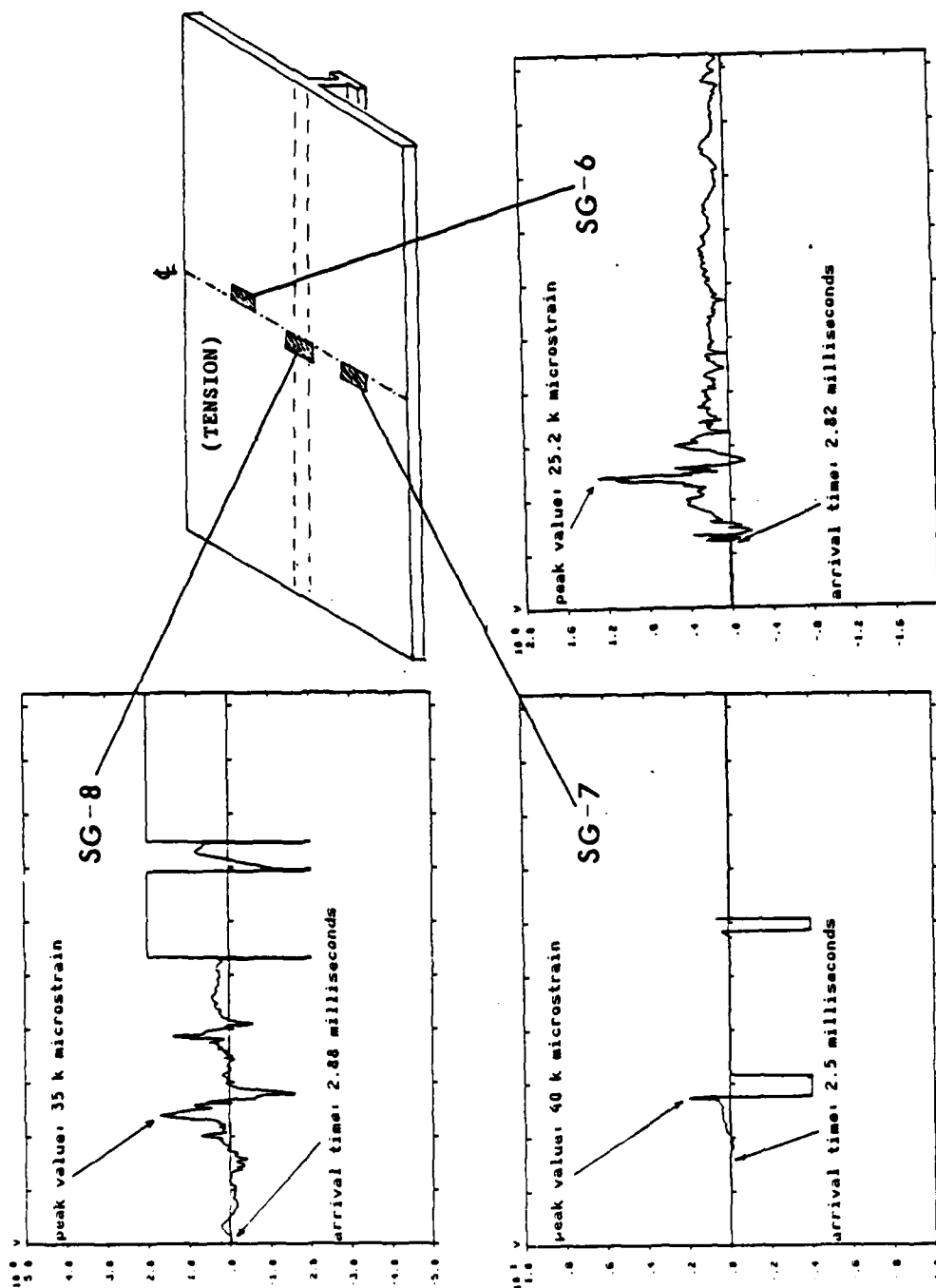
Figure 4.40   Strain History Recorded Across
Transverse Centerline of Plate Back.

83
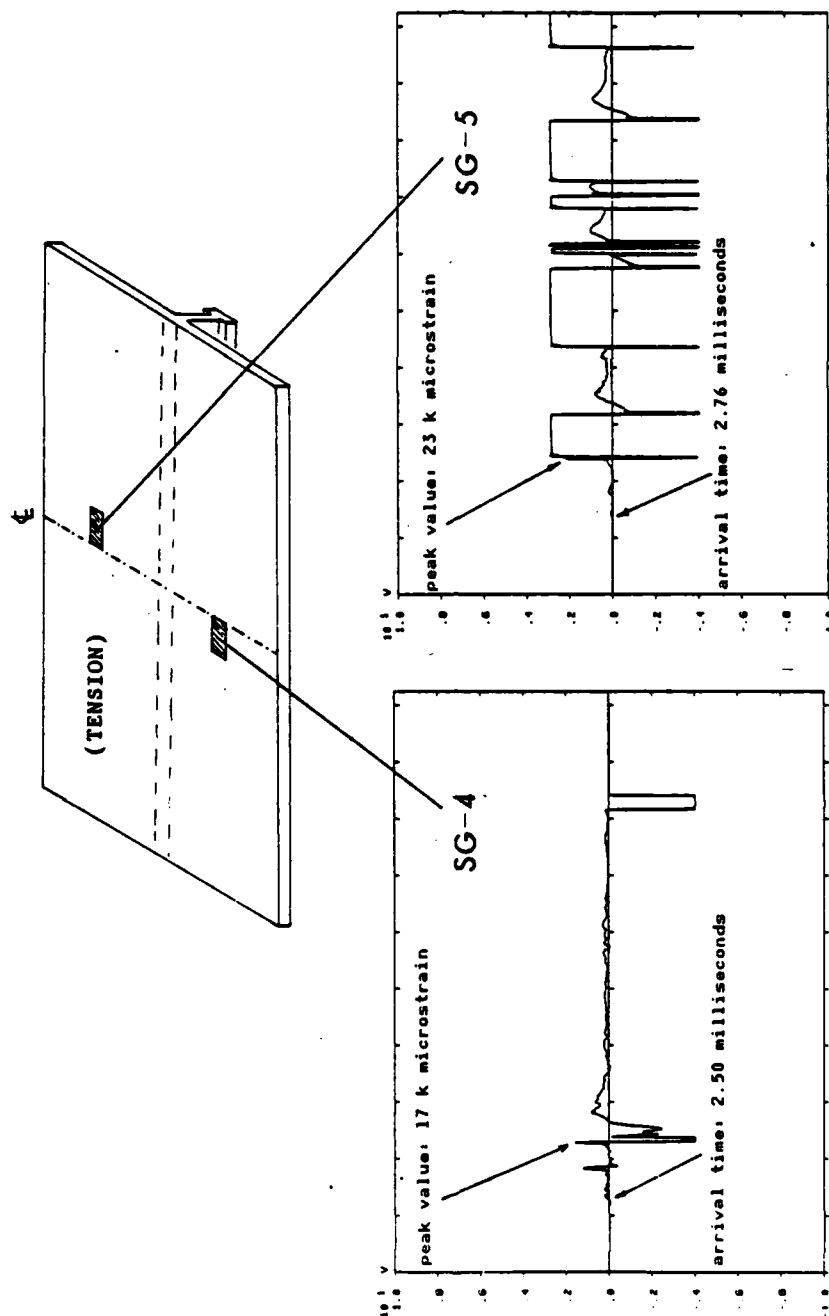
Figure 4.41   Strain History Recorded Across
Transverse Centerline of Plate Back.

84
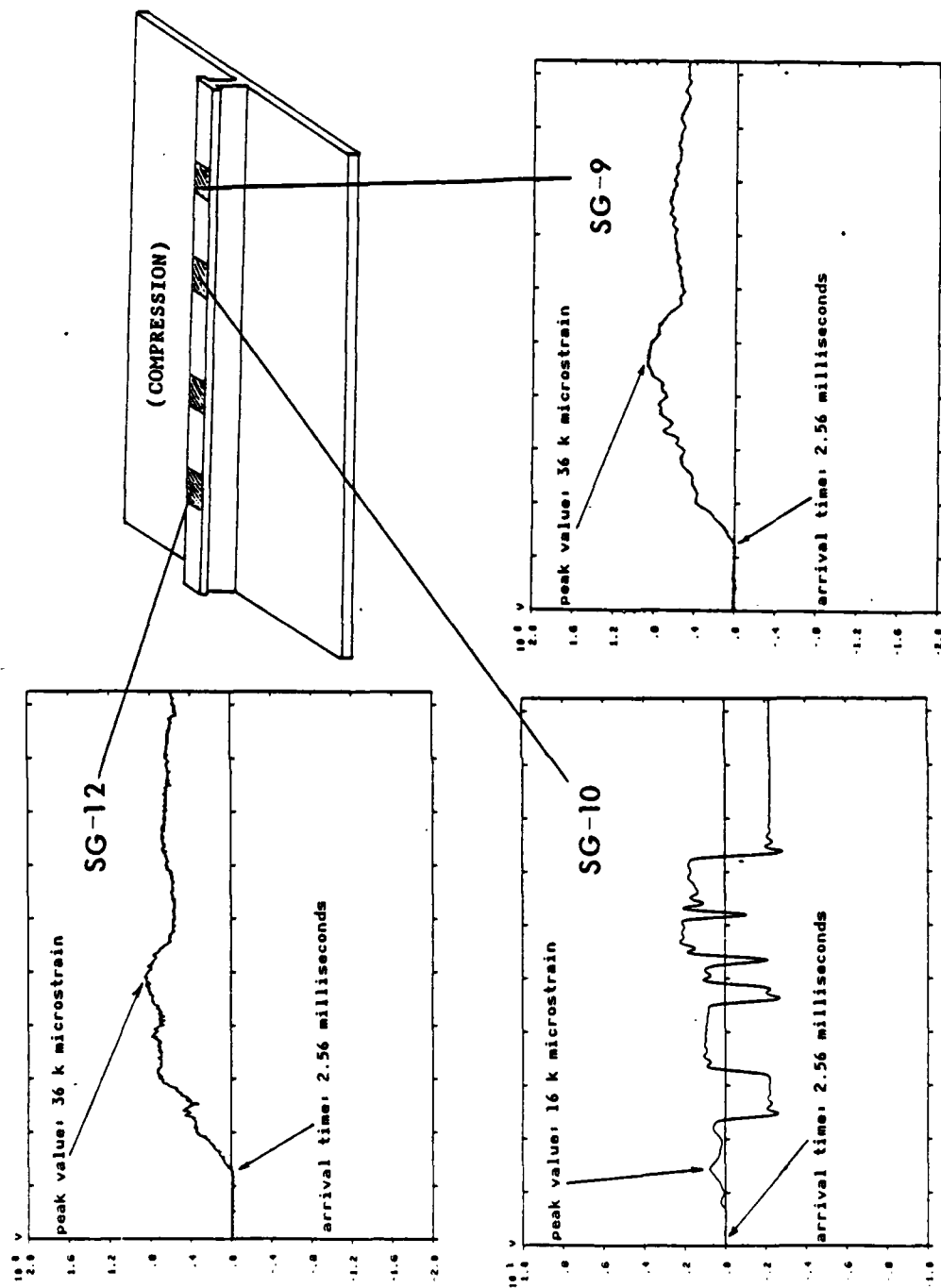
Figure 4.42   Strain History Recorded Longitudinally
Across Flange of T-stiffener.
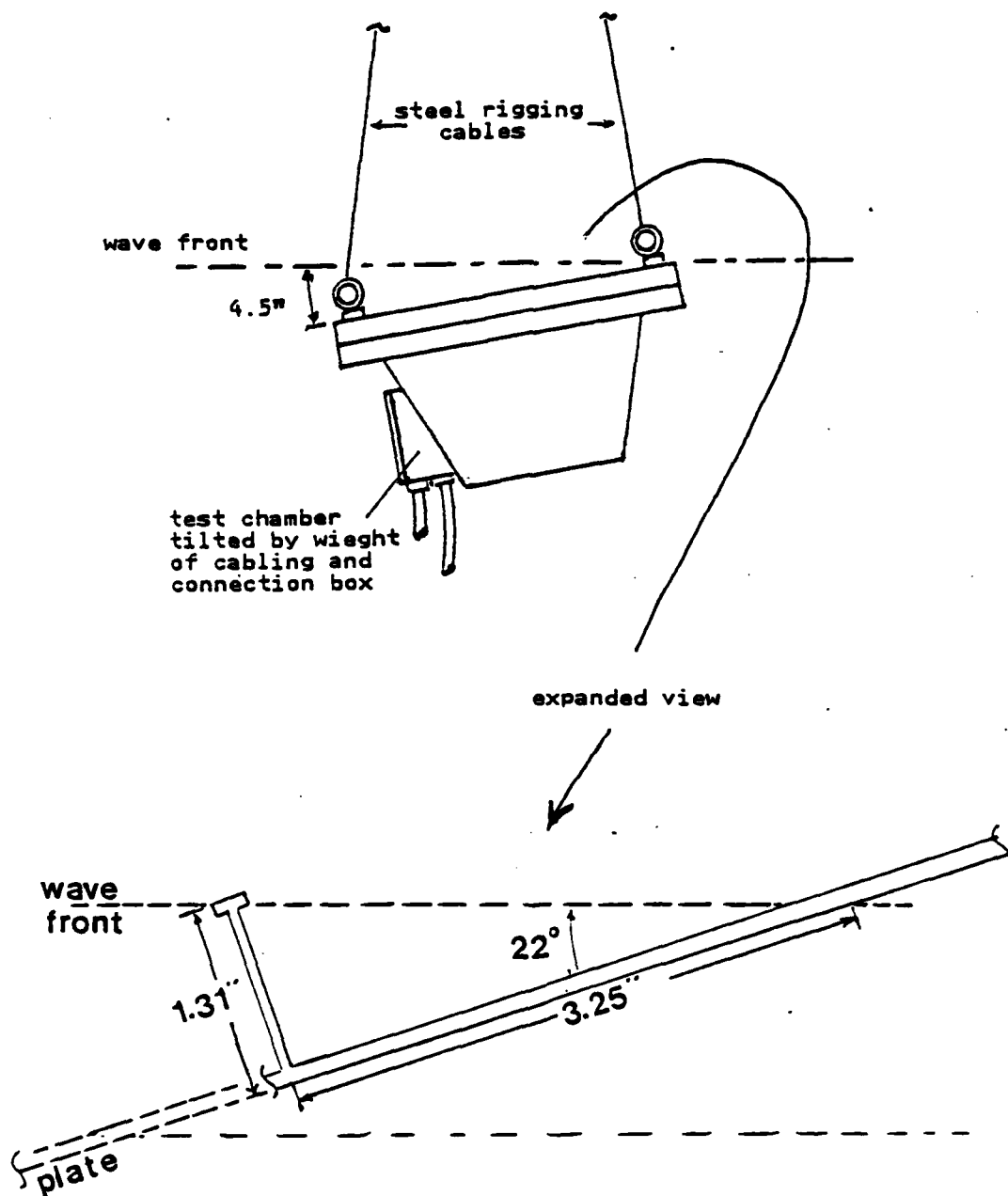
Figure 4.43   Geometry of Inclined Test Panel.

Additionally, materials which are ductile at low temper-
atures tend to remain ductile under dynamic loading
[Ref. 12: p. 153]. The flow charateristics of most metals
will be influenced by the high strain-rates involved, espe-
cially in iron which has a very noticeable loss of ductility
at high strain-rates. This strain-rate sensitivity deter-
mines the magnitude of the permanent deflections. It was
because of materials' typical strain-rate sensitivity that a
relatively strain rate independent metal was selected for
the test panel material, since the less strain-rate sensi-
tive a material is, the less explosive charge required to
cause the necessary deformations. Aluminum 6061-T6 was
believed to be almost strain-rate insensitive compared to
steel plate at the same strain-rates, yet it is known that
the flow stress required for plastic straining of 6061-T6
aluminum increases significantly with increasing strain-rate
at strain rates above 10,000 1/s [Refs. 18,19,20].
Nonetheless, 6061-T6 aluminum was still the best readily
available material.

The anatomy of a shock front interaction with a plate is
shown in Figure 4.44 . The reflected incident wave is
compressive and is the reactive force which causes the plate
to deform. Additionally, the amplitude and shape of the
incident wave changes rapidly as it passes through the
plate. The steady decrease in the amount of permanent
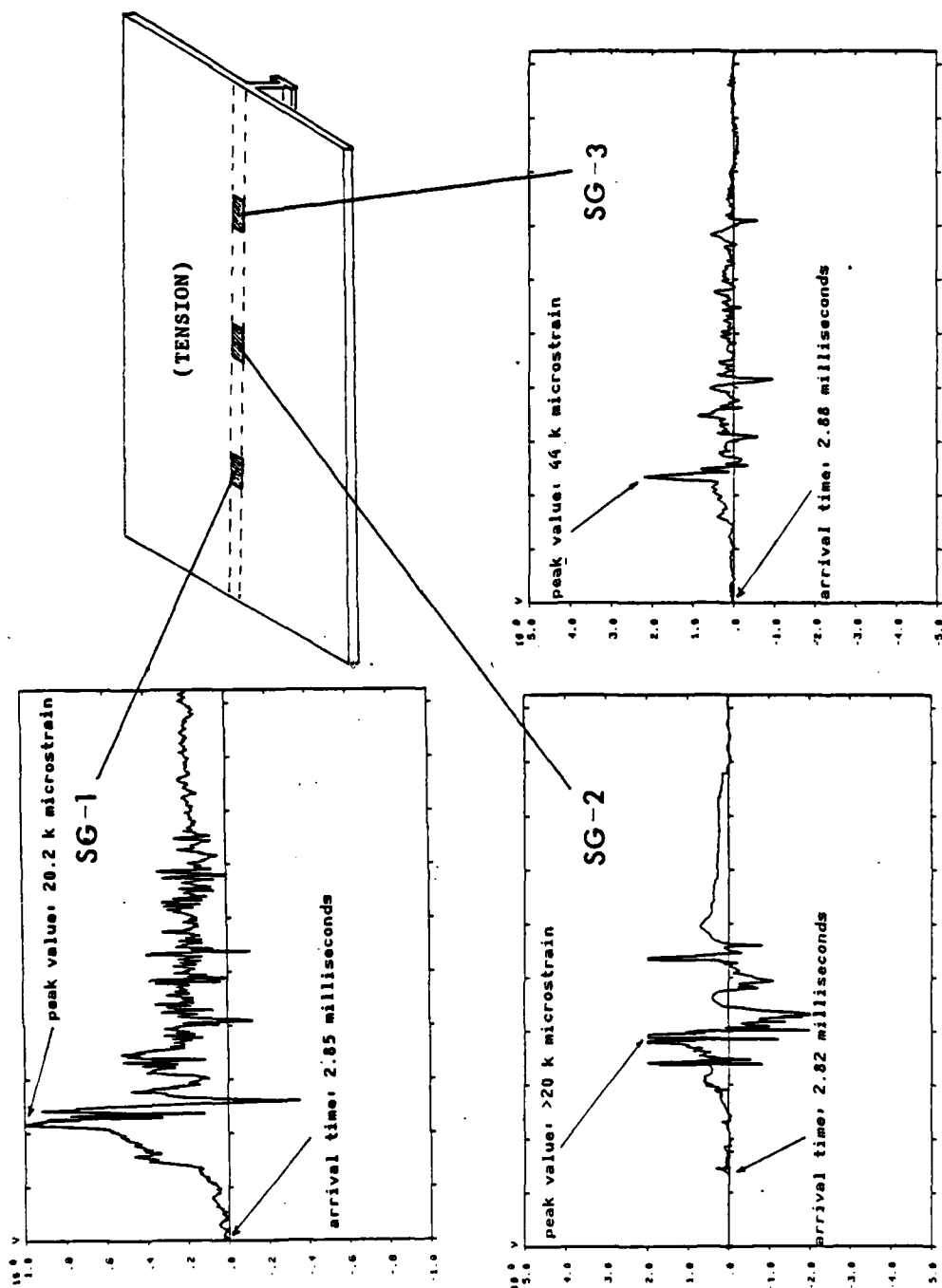deformation is due primarily to the decay of the wave. The
transmitted incident wave, which is microseconds later,
reaches the backside free surface of the plate and is
reflected as a tensile rarefaction wave. This free surface
reflected wave in many cases can lead to the development of
tension fractures. Finally, the reflected tension wave is
partly transmitted back into the water. [Refs. 13,21: p.
101,18]

87

The shock front interaction with the plate can be complicated extensively by the shape of the test panel since the geometry of a body and its constraints determine both the location and the amount of plastic flow that will take place. In most cases, interpreting the deformation and fractures that occur can be facilitated by considering the effects that the geometrical shape has on the stress waves. Behavior of Metals Under Impulsive Loads [Ref. 12: p. 147] best describes the three ways plastic deformation is influenced by geometry:

1. Stress inhomogeneities which result from reflection and interaction of stress waves can influence the deformation. Very highly localized regions of plastic deformation may be observed at the place where fracturing might have been expected.

2. Plastic flow usually involves no appreciable volume changes and hence changes in configuration must usually start at a free surface.

3. Fracturing under impulsive loading often leads to plastic deformations which result from the relative motions that are imparted to the different parts of the body as a result of the fracturing.

For example, fracturing may occur at a corner due to the reinforcement between two (or more) tension waves that eat in simultaneously from the edge of the corner. Additionally, entrapment of the incident shock wave by the corner causes multiple reflections from the walls of the corner (pressure increasing stepwise with each further reflection), leading to a significant increase in the pressure at the corner. This combination of reinforced tension waves and pressure amplification is undoubtedly the source of the initiation of the fracturing observed in the test panel and eventual 360 degree tearing of the plate from the test panel, Figures 4.23 and 4.24 .

As a closing remark to this section, it should be mentioned that the test panel incurred two surface gouges (less than three-thirtyseconds of an inch deep) near the plate edge while being machined. One was weld repaired and one was left as is, and after exposure to the underwater
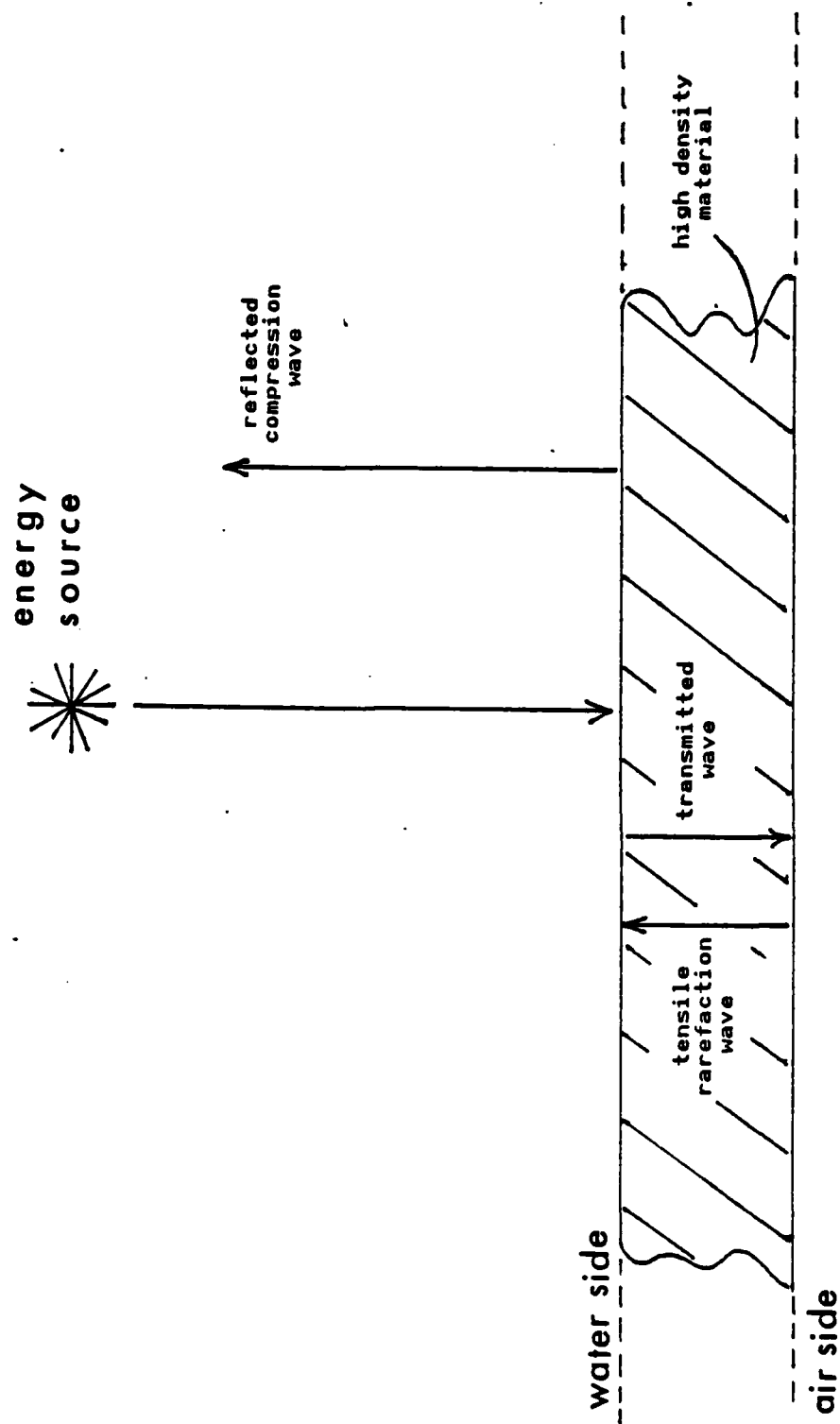
Figure 4.44   Shock Front Interaction With a Plate.

89

explosion neither defect showed any involvement in the plate fracturing or deformation and apparently were not stress concentrators in this situation. This was also observed in Ref. 12, page 147, ". . . the presence of notches may have little effect in impulsive load situations." However, spalling (or scabbing) was observed in the weld repaired defect. Spalling (Figure 4.45), an unsusual type of fracturing, occurs near a free-surface relatively far removed from the area of application of a pressure impulse [Ref. 12: p. 124]. The spalling observed was a consequence of the applied load generating both longitudinal and transverse waves which progressively struck the weld fusion boundary creating additional waves (Figure 4.45) giving rise to highly localized stresses which were sufficient to cause localized fracturing in the center of the weld repair.

LOAD

water side

reflected wave
produced from
incident transverse
wave

weld fusion boundary

weld fusion boundary

incident
transverse wave

reflected waves
produced from
incident longitudinal
wave

incident
longitudinal wave

internal cracking

air side

surface separation (spalling)
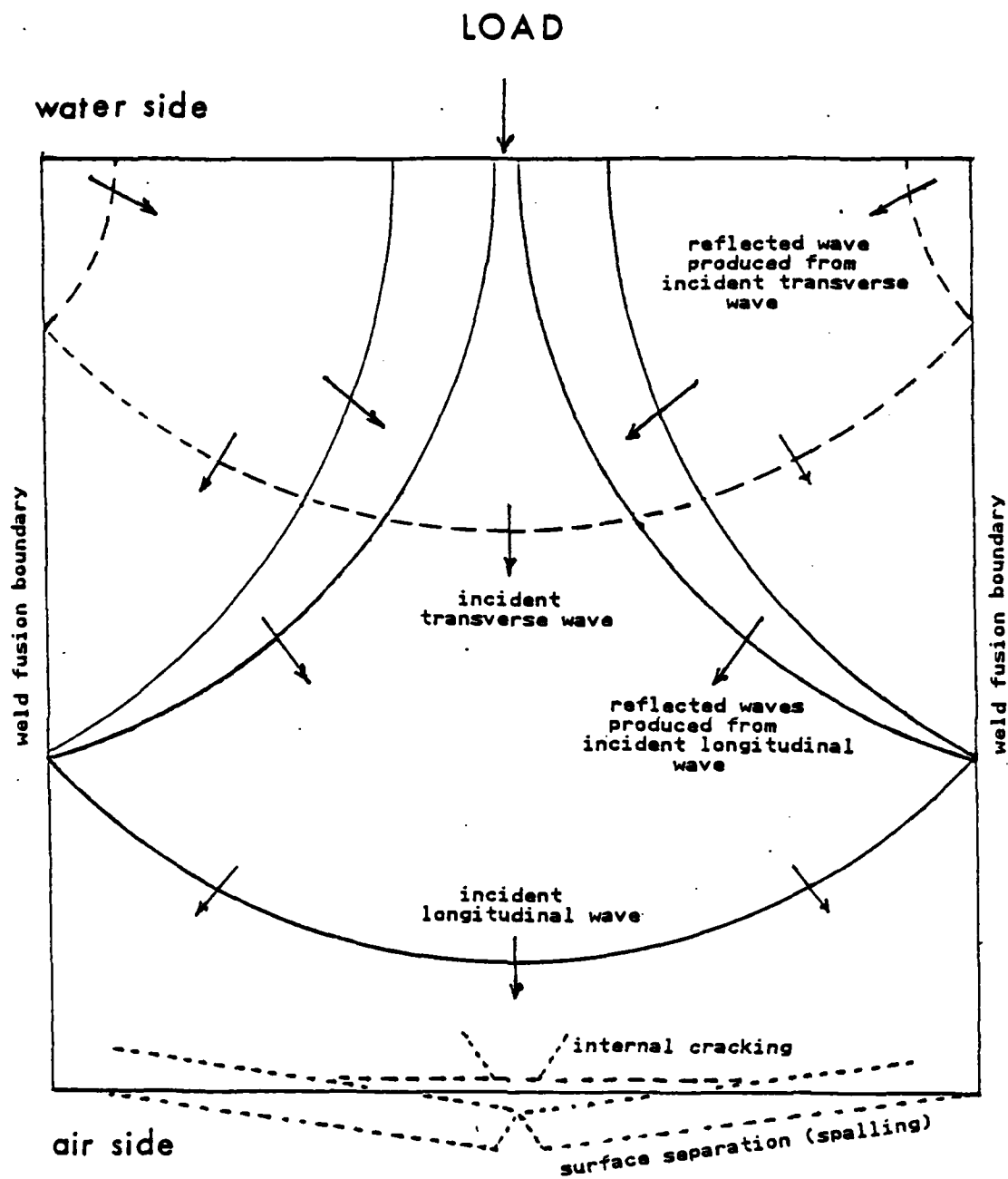
Figure 4.45   (Top) Incident and Reflected Waves in
Flat Plate.   (Bottom) Depiction
of Spalling.

91

V. CONCLUSIONS AND RECOMMENDATIONS

The static pressure deflection test of the panel machined for this purpose proved to be a source of very good strain and deflection data quantitatively representing the plate and stiffener behavior up to and into the elastic tripping region. Additionally, the progressive behavior of this plate-stiffener combination when loaded hydrostatically was found to be well defined, qualitatively predictable, and sensitive to tripping. As a consequence of this test, it was also determined that more than four plate thicknesses deflection would be required to initiate static inelastic tripping.

The dynamic response test, though complicated by the rapidly changing nature of the variables and the complex relationship between stress, strain, and strain-rate, provided strain histories and shock front arrival times clearly depicting the initial interaction between the shock front and the test panel. Accordingly, the shock front arrival times measured at twelve different plate locations were precise enough to indicate (through calculation) that the test chamber was not parallel to the shock front emenating from the eight pound TNT charge, but was inclined 22 degrees on the cable junction box side. It was also determined from post undex measurements of plate deflection that even at an extreme deformation of seven plate thicknesses there was not a total collapse of the narrow-flanged T-stiffener. Additionally it has become obvious that the geometry of the test panel machined "cavity" and its constraints determined both the location and the amount of plate fracturing which took place.

In summary, narrow-flanged T-stiffener tripping has been observed demonstrating both the static elastic and dynamic

92

inelastic behaviors. Also the underlying cause of the fracturing observed in the undex test plate has been attributed to the design geometry of the test panel.

It is recommended that if there is to be a further pursuit of dynamic data, the test panel warrants redesign so as to eliminate the cavity walls surrounding the stiffened plate, thus removing boundaries which may cause shock wave pressure amplification. It is not apparent how much effect the amplified corner pressures had on the plate deformation and strain histories, but to ensure strain histories representative of only the shock front and plate interaction, the follow-on undex test panels should be of the design shown in Figure 5.1 . Additionally, to avoid test chamber tilt from the cabling , the cabling connection box should be mounted directly beneath the test air-back chamber as shown in Figure 5.2, and the cabling allowed to lie on the bay bottom directly beneath the connection box.

As a by-product of this investigation (shock wave effects on welds), spalling of a weld repair should be of interest for any future studies evaluating the physical and metalurgical effects of an underwater explosion shock wave front on a metal panel containing multiple welds or weld repairs (e.g., spalling noted in the dynamic test plate). The importance of this is self-evident since the hull integrity of every Naval vessel is dependent upon the reliability of the welds bonding the plating together.

─WATER SIDE─
TOP VIEW

SIDE VIEW

END VIEW

air side
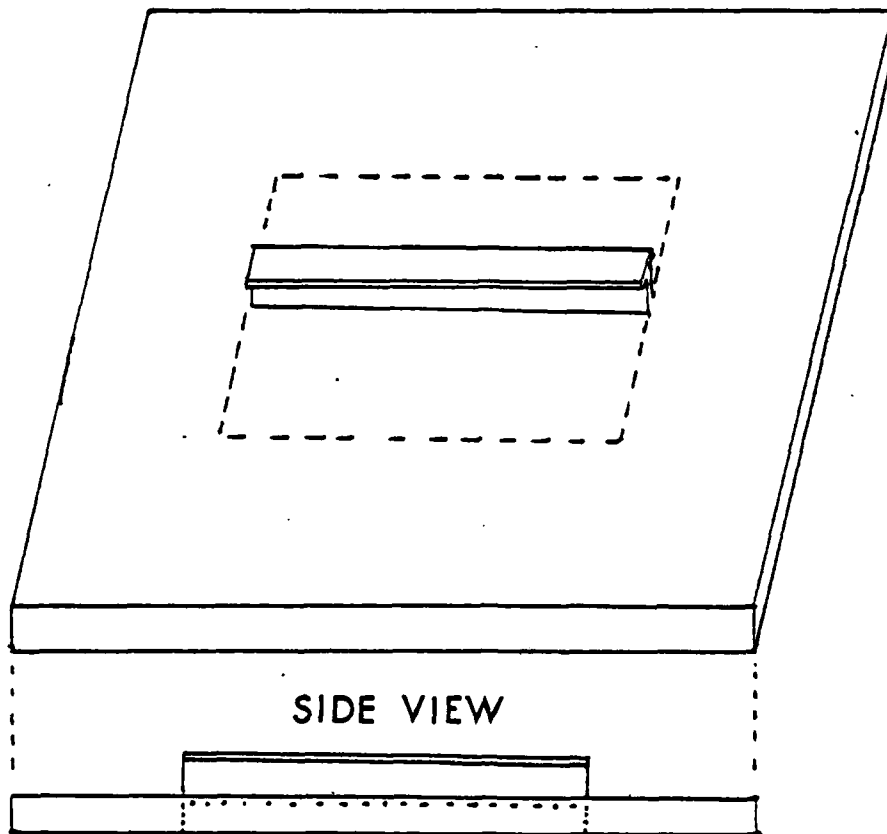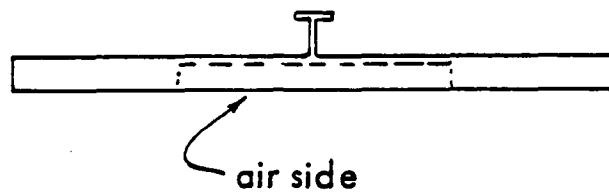
Figure 5.1   Redesigned Dynamic Test Panel
To Avoid Amplified Corner Pressures.
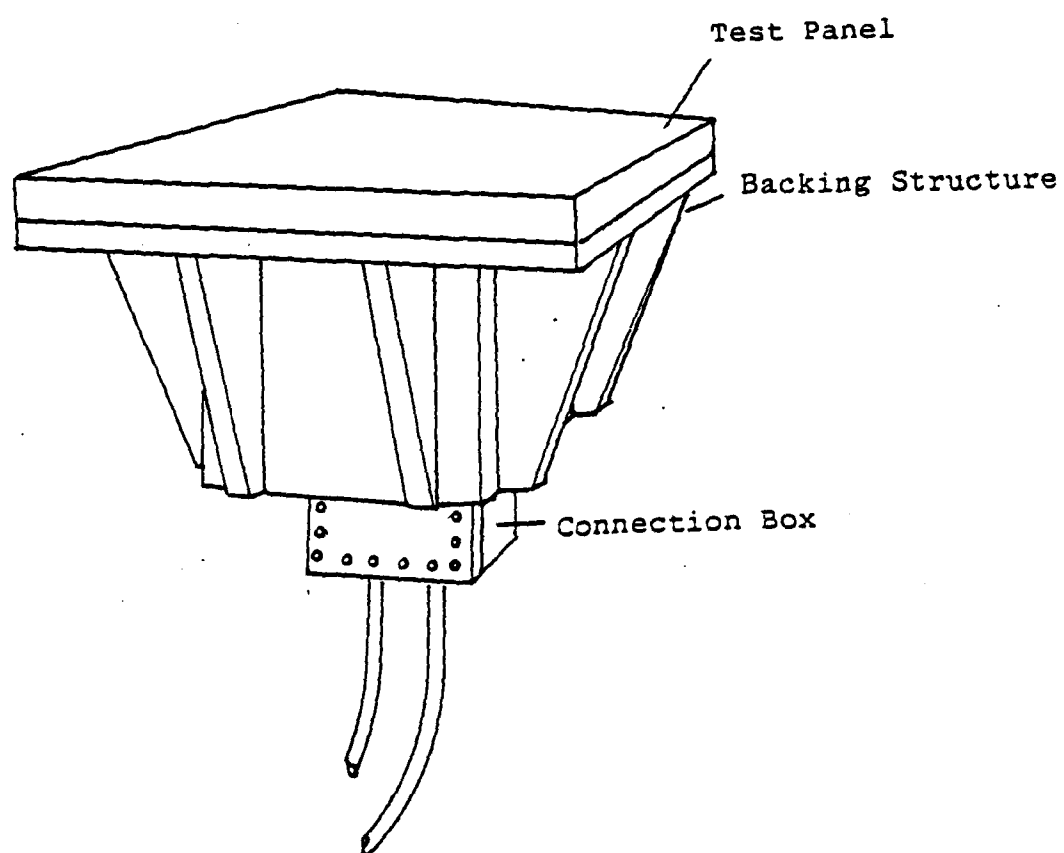
Figure 5.2   Air-Back Chamber Showing Connection
Box New Position.
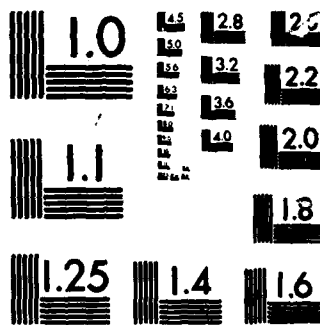
MICROCOP CHART

LIST OF REFERENCES

1. Faulkner,D.,_The Collapse Strength and Design of Submarines_, paper presented at the Symposium on Naval Submarines, London, May 1983.

2. Evans,J.H.,_Ship Structural Design Concepts_, Cornell Maritime Press, 1975.

3. Evans,J.H. and Adamchak,J.C.,_Ocean Engineering Structures_, vol.1, The MIT Press, 1969.

4. Thompson,J.M.T. and Hunt,G.W., _Collapse_, Cambridge University Press, 1982.

5. Mansour,A.E.,_Gross Panel Strength Under Combined Loading_, Project SR-225, Department of The Navy, Naval Ship Engineering Center, 1977.

6. Flax,A.H,"Aero and Hydro-Elasticity,"_Structural Mechanics_, Pergamon Press, 1960.

7. Gerard,G.,_Introduction to Structural Stability Theory_, McGraw-Hill Book Company, 1962.

8. Bleich,F.,_Buckling Strength of Metal Structures_, McGraw-Hill Book Company, 1952.

9. Kennard,E.H., _Tripping of T-shaped Stiffening Rings on Cylinders Under External Pressure_, Report 1079, NS 731-038, 1959.

10. Weertman,J.,"Dislocation Mechanics at High Strain Rates,"_Metallurgical Effects At High Strain Rates_, Plenum Press, 1973.

11. Jones,N., Dumas,J.W., Giannotti,J.G., and Grossit,K.E., "The Dynamic Plastic Behavior of Shells",_Dynamic Response of Structures_, Pergamon Press, 1972.

12. Rinehart,J.S. and Pearson,J.,_Behavior of Metals Under Impulsive Loads_, The American Society for Metals, 1954.

13. Rinehart,J.S. and Pearson,J.,_Explosive Working of Metals_, Pergamon Press, 1963.

14. Rentz,T.R., _An Experimental Investigation into the Dynamic Response of a Stiffened Flat Plate Loaded Impulsively by an Underwater Shockwave_, Master's Thesis, Naval Postgraduate School, Monterey, California, June 1984.

15. King,N.R., _Underwater Shock-Induced Responses of Stiffened Flat Plates: An Investigation into the Predictive Capabilities of the USA-STAGS Code_, Master's Thesis, Naval Postgraduate School, Monterey, California, December 1984.

16. Langan,J.R., _An Investigation into the Comparisons of the Underwater Shock Effects on a Stiffened Flat Plate to the Predictive Nature of a Computer Model_, Master's Thesis, Naval Postgraduate School, Monterey, California, March 1985.

17. Cole,R.H., _Underwater Explosions_, Princeton University, Princeton, New Jersey, 1948.

18. Gilot,A. and Clifton,R.J., "Pressure-Shear Waves in 6061-T6 Aluminum and Alpha-Titanium", _J. Mech. Phys. Solids_, no. 3, p 263-284, 1985.

19. Carden,A.E., Williams,P.E. and Karpp,R.R., "Comparison of the Flow Curves of 6061 Aluminum Alloy", _Shock Waves and High-Strain-Rate Phenomena in Metal_, Plenum Press, 1981.

20. Nicholas,T.,"Tensile Testing of Materials at High Rates of Strain", _Experimental Mechanics_, p177-185, May 1981.

21. American Society of Tool and Manufacturing Engineers, _High-Veloctiy Forming of Metals_, Prentice-Hall, 1964.

BIBLIOGRAPHY

Cottrel,A.H., "Deformation of Solids at High Rates of Strain," The Properties of Materials at High Rates of Strain, Institution of Mechanical Engineers, pp. 1-12, 1957.

David W. Taylor Naval Ship Research Center Report 79/064, Design Equations for Tripping of Stiffeners Under Inplane and Lateral Loads, by J. C. Adamchak, October 1979.

Johnson,J.N. and Barker,L.M., "Dislocation Dynamics and Steady Plastic Wave Profiles in 6061-T6 Aluminum," J. of Applied Physics, vol.40, no.11, pp. 4321-4334, October 1969.

Kirkwood,J.G., Shock and Detonation Waves, Gordon and Breach Science Publishers, New York, NY, 1967.

Muckle,W., The Design of Aluminum Alloy Ship Structures, Cornell Maritime Press, Cambridge, Maryland, 1963.

Naval Construction Research Establishment, Great Britain, R/611, Compressive Strength of Welded Steel Ship Grillages, by C. S. Smith, May 1975.

Richardson,J.M. and Kirkwood,J.G., Underwater Explosion Research, Volume III, The Damage Process, "Buckling Instability of Thin Cylindrical Shells," Office of Naval Research-Department of the Navy, pp. 423-459, February 28, 1950.

Smith,C.S., "Bending, Buckling and Vibration of Orthotropic Plate-Beam Structures," J. of Ship Research, vol.12, no.5, pp. 249-268, Dec.1968.

Smith,C.S. and Dow, R.S., "Effects of Localized Imperfections on Compressive Strength of Long Rectangular Plates," J. of Construction Steel Research, pp. 51-76, 1984.

Wittrick,W.H., "General Sinusoidal Stiffness Matrices for Buckling and Vibration Analyses of Thin Flat-Walled Structures, International Journal of Mechanical Sciences vol. 10, no. 12, pp. 949-966, Dec. 1968.

INITIAL DISTRIBUTION LIST

		No. Copies
1.	Defense Technical Information Center Cameron Station Alexandria, Virginia 22304-6145	2
2.	Library, Code 0142 Naval Postgraduate School Monterey, CA 93943	2
3.	Professor Y.S. Shin, Code 69Sg Department of Mechanical Engineering Naval Postgraduate School Monterey, CA 93943	5
4.	Professor R.E. Newton, Code 69Ne Department of Mechanical Engineering Naval Postgraduate School Monterey, CA 93943	1
5.	Department Chairman, Code 69 Department of Mechanical Engineering Naval Postgraduate School Monterey, California 93943	1
6.	Dr. N.T. Tsai Defense Nuclear Agency SPSS Washington, D.C. 20305-1000	3
7.	Dr. E. Sevin Defense Nuclear Agency Washington, D.C. 20305-1000	1
8.	Dr. M.L. Baron Weidlinger Associates 333 Seventh Avenue New York, N.Y. 10001	1
9.	Dr. R. Daddazio Weidlinger Associates 333 Seventh Avenue New York, N.Y. 10001	1
10.	Dr. Andrew P. Misovec Weidlinger Associates 333 Seventh Avenue New York, N.Y. 10001	1
11.	Dr. B. Whang, Code 1750.2 Hull Group Head, Submarine Protection Div. David Taylor Naval Ship Research and Development Center Bethesda, MD 20084	1
12.	Dr. Huang, Code R14 Naval Surface Weapon Center White Oaks, Silver Spring, MD 20910	1

13. Professor T.L. Geers   1
     Campus Box 427
     Department of Mechanical Engineering
     University of Colorado
     Boulder, Colorado 80309

14. Dr. J.A. DeRuntz   1
     Lockheed Research Laboratory
     3251 Hanover Street
     Palo Alto, CA 94304

15. Jim Kondo   1
     West Coast Shock Test Facility
     Code 290
     Department of Navy
     Supervisor of Shipbuilding, Conversion,
     and Repair
     San Francisco, CA 94135

16. Lt. H.L. Budweg, USN   2
     95810 N.B. Rogue
     Gold Beach, OR 97444

17. R.H. Budweg, SR   1
     P.O. Box 417
     Sumner, WA 98390

18. R.H. Budweg, JR   1
     P.O. Box 65
     Hunters, WA 99137

19. S.A. White   1
     9048 16th Ave, NO. 202
     Kenosha, WI 53140

END

DTIC

6 - 86